Odor guided behavior and its modulation in the fruit fly *Drosophila melanogaster*

A dissertation submitted to the Faculty of Biology and Pharmacy Department of the Friedrich-Schiller-University Jena

For the degree of

Doctorate in Phylosphy (Ph.D.)

by

Abu Farhan

Born on 2 Dec 1983, Ballia, India

Assessed by

1. Prof. Dr. Bill Hansson, MPI for chemical ecology, Jena
2. Prof. Dr. Andre Fiala, Georg-August University, Göttingen
3. Prof. Dr. David G. Heckel, MPI for chemical ecology, Jena

Date of public defense: 18 Dec 2013

Dedicated to my sweet sister

“Late Zeba Arif”

The Fly

Little Fly,
Thy summer's play
My thoughtless hand
Has brushed away.

Am not I
A fly like thee?
Or art not thou
A man like me?

For I dance
And drink, and sing,
Till some blind hand
Shall brush my wing.

If thought is life
And strength and breath,
And the want
Of thought is death;

Then am I
A happy fly,
If I live,
Or if I die.

William Blake (1757-1827)

Table of contents

Introduction

This thesis dissects the basis of odor-guided behavior, with an emphasis on modulatory mechanisms. I show olfactory modulations at different levels. First of all a food odorant's attractiveness can be abolished when it is mixed with a signature odor of harmful microbes. Secondly, I show that the feeding state of a fly modulates its physiological and behavioral olfactory response. E.g. starved flies are much more sensitive to ethyl acetate than fed flies (as deduced from single sensillum recordings) and are much more attracted to this compound. Finally, I show that an odorant's valence depends on its concentration and find a representation of the concentration-dependent valence at the level of the lateral horn, i.e. a higher brain center dedicated to the processing of olfactory information.

1.1 Odor-guided behavior in *Drosophila*

From an evolutionary point of view, olfaction is one of the most ancient senses. It is a chemical sense that transforms information carried in air-borne chemicals into brain activity, which finally governs odor-guided behavior. Odor-guided behavior is highly dependent on the chemical signal in the environment and allows most animals to search, detect and localize e.g. food or oviposition sites, or mating partners. Olfaction furthermore allows animals to detect danger like spoiled food, toxic substances and predators. Despite their small size, insects have olfactory systems of surprising sensitivity. Barrows (1907) first described the attraction of *Drosophila* to pure volatile chemicals and to the complex odors from fruits. Thorpe (1939) noted that adult flies are innately repelled by peppermint odor. Innate odor responses are fundamental behaviors that can be described as primitive reactions that animals can perform without any previous experience (Gong, 2012). Moreover, innate behaviors are hardwired, i.e. confronted with a specific stimulus, the animal responds promptly and in a stereotypic and predictable fashion (Tinbergen, 1951). However, beside its innate valence, an odorant's valence can be affected by learning. Learned olfactory behavior involves higher computation and includes flexible parallel processing traces (Davis, 2011; Séjourné et al., 2011). Studies have been done on olfactory learning in several animals and it has been proposed that complex sensory memory formation in insects occurs in the mushroom body calyx (MBc) exclusively (Giurfa, 2007). Apart from whether an odorant valence is learned or not, the animal's response to the odorant can be affected by other factors like

e.g. the animal's age (Devaud, 2003), feeding state (Root, 2011), pre-experience (Thorpe, 1939) and the concentration of the odorant (Semmelhack, 2009). This stage dependency will be the main topic of my thesis.

1.2. Organization of the olfactory system in *Drosophila*

Odorants are detected by two main peripheral parts of the olfactory circuit of *Drosophila*: the 3rd antennal segment and the maxillary palps. Both are equipped with small sensory bristles called sensilla that house the olfactory sensory neurons (OSNs). The OSNs are equipped with one of 62 olfactory receptors and are found in stereotyped combinations of 1 to 4 OSNs in three morphologically different sensillum types basiconic (long & cylindrical), coeloconic (small) and trichoid (long & thin) sensilla (de Bruyne et al., 2001; Singh, 1984). While basiconic and trichoid sensilla house OSNs expressing 47 odorant and 3 gustatory receptors (Robertson et al., 2003) the neurons housed in coeloconic sensilla mainly express a different kind of receptors, the so-called olfactory ionotropic receptors (Yao et al., 2005; Benton et al., 2008). A fourth class, the so-called intermediate sensillum, has been described with the properties of both trichoid and basiconic sensilla (Shanbhag et al., 1999). How can the fly that is equipped with only 62 different olfactory receptor types process the much higher number of different odorants (e.g. a single banana produces more than 700 different molecules)? Single odorants can activate either one or several OSN types. On the other hand each OSN type can be activated by either one or several odorants. This so-called olfactory code allows processing of the identity of an almost infinite number of odorants with a restricted number of receptors. The axons of the OSNs project to the first olfactory processing center the antennal lobe (AL), which in *Drosophila* contains ~46-50 spherical functional units called glomeruli (Stocker, 1994; Laissue et al., 1999; Voshall et al., 2000; Gao et al., 2000). The insect brain therefore retains a topographical map of the receptor activation such that the quality of an odor may be encoded by different spatial patterns of activity in the antennal lobe. Within the AL, the OSNs activate second order neurons, the so-called projection neurons (PNs) (Hildebrand and Shepherd, 1997). PNs innervate higher brain centers, the mushroom body (MB) and the lateral horn (LH) (Stocker et al., 1997**;** Wilson et al., 2005**;** Wong et al., 2002). The majority (five-sixths) of the OSNs sends axons that branch and innervates both the ipsilateral and contralateral antennal lobes; the remaining sixth of the neurons project only ipsilaterally (Stocker et al., 1990).

Local interneurons (LNs), which are of both excitatory (eLNs) and inhibitory (iLNs) types, provide extensive lateral connections within the antennal lobe and have been shown to play an important role in processing and modulating olfactory information (Wilson, 2008; Seki 2010; Chou 2010).

1.3. *Drosophila* as a model system to study odor-guided behavior

Drosophila is a widely used animal for studying the genetic control of complex behavior (Siddiqi O., 1987; Carlson, 1996). The fly can detect a variety of odorants with great sensitivity and discrimination. A distinct advantage of studying odor-guided behavior in *Drosophila* is that it has a relatively simple nervous system but is capable of functions similar to those of higher animals. The *Drosophila* olfactory system has about 1200 receptor neurons, compared to 10^7 in humans (Shier et al., 2004). It is also a good system for studying the underlying mechanism of olfactory behavior since the olfactory circuit of the fruit fly is structurally and functionally analogous to the mammalian one. The odor information is processed in the fly's antennal lobe in a manner similar to the vertebrate's olfactory bulb.

Perhaps, the greatest advantage of studying olfaction in *Drosophila* is the suitability of the system for genetic manipulation. Genetic manipulation can easily be performed in *Drosophila* due to the availability of many genetic tools and neuronal markers. Therefore, *Drosophila* has emerged as a favorite model system to study odor-guided behavior.

2. Processing and modulation of olfactory information in *Drosophila*

In the following chapters I will provide short introductions into the different parts of my thesis dealing with

2.1. A conserved dedicated olfactory circuit for detecting harmful microbes in *Drosophila*. (*Cell*) Stensmyr et al. 2012

2.2 The CCHamide 1 receptor modulates sensory perception and olfactory behavior in starved *Drosophila.* (*Scientific Reports*) Farhan et al. *In press*

2.3 Decoding odor attraction and intensity in the *Drosophila* brain. Strutz et al. *under review in Neuron*

2.1 A conserved dedicated olfactory circuit for detecting harmful microbes in *Drosophila*

In the environment thousands of chemicals are present and during evolution many of them have become ecologically relevant signals that evoke innate responses in insects. This so called innate behavior is hard wired (Tinbergen, 1951). When the right stimulus is known, stereotyped behaviors can easily be triggered. For example, chemicals like ethyl acetate and 2,3 butanedione are signature odors of fermented fruits and are extremely attractive to fruit flies (Baumberger, 1917). In addition, flies have been shown to innately avoid benzaldehyde, an odorant present in almond and wood (Knaden et al., 2012). While the reasoning behind this strong avoidance is not fully understood, we identified another *Drosophila* repellent and unraveled its ecological relevance. This study represents the first part of my thesis (Stensmyr et al., 2012). Trans-1,10-dimethyl-trans-9-decalol, (or better known as geosmin) is highly aversive to *Drosophila* and abolishes the attractiveness of the otherwise highly attractive blend of vinegar. We could show that geosmin is produced by a group of microbes, particularly by *Penicillium* fungal molds (Mattheis and Roberts, 1992) and *Streptomyces* soil bacteria (Gerber and Lechevalier 1965) that sometimes grow on rotten fruits and that are toxic for flies. While geosmin itself is not toxic it presents a signature odorant for spoiled food (Stensmyr, 2012). We furthermore show that *Drosophila* has one type of sensory neurons expressing an odorant receptor that is extremely sensitive and fully dedicated to detect this compound.

2.2. The CCHamide 1 receptor modulates sensory perception and olfactory behavior in starved *Drosophila*

'If the yeasty aroma of freshly baked bread awakens your hunger then in another way round hunger could also make you more aroma sensitive.'

Modulation and plasticity are key functions of all organisms for adapting to a changing environment and stress. Examples for modulations in olfactory systems are blood-feeding insects, which after a blood meal switch their olfactory preference from host odors to odors specific for oviposition sites (Davis, 1984; Siju; 2010; Denotter; 1991, Klowden; 1978, 1979, 1994; Takken, 2001). Further studies revealed an accompanying modulation at the peripheral level of odor detection, i.e. at the level of olfactory sensory neurons (Davis, 1984; Qiu, 2006; Bowen, 1988, 1990; Siju, 2010). Similarly in the African cotton leaf worm *Spodoptera littoralis*, the sensitivity of sensory neurons detecting feeding-related flower odors is down-regulated upon mating, while the sensitivity of neurons detecting oviposition-related green leaf odors is up-regulated (Saveer et al., 2012)

In *Drosophila* it has frequently been observed that wide ranges of behavior including food responses are modulated by the animal's physiological state. For example, feeding behavior is altered with mating status (Carvalho, 2006). Mated females consume substantially larger meals than age-matched virgins. While main emphasis has been laid on the central modulation for such behavior, few studies have focused on the peripheral neural modulation (Martel, 2009).

Apart from the mating status starvation is known to increase the fly's responses to food odors. Even before this starvation-dependent modulation was investigated in detail (Root et al., 2011; Farhan et al. in press) many studies dealing with odor-guided behavior used starved flies for behavioral analyses (Chakraborty, 2009; Semmelhack, 2009; Stoekl et al.**;** 2010**,** Becher, 2010). Root et al. (2011) were the first to investigate the starvation-dependent modulation in detail and showed that starvation increases the behavioral response and physiological sensitivity of *Drosophila* to the attractive food blend of apple cider vinegar. They furthermore found that this starvation-induced modulation is mainly governed by an increased expression of the short neuropeptide F receptor in olfactory sensory neurons expressing the olfactory receptor OR42b. In the second part of my thesis I present evidence that the starvation effect is not restricted to food odorants. I could

show that starved flies exhibit increased behavioral responses to odorants as different as food attractants, repellents and even pheromones. By performing single sensillum recordings I furthermore show that the increased behavioral sensitivity is accompanied by an increased physiological sensitivity. Some of the investigated olfactory sensory neurons do not express the short neuropeptide F receptor. I, therefore, performed microarray analyses in starved and fed flies and identified several more genes that become up-regulated upon starvation. By silencing some of the candidate genes in behaving flies I could unravel the important role of CCHamide in governing the starvation effect (Farhan et al. in press).

2.3. Decoding odor attraction and intensity in the *Drosophila* brain

After peripheral detection of an odor by OSNs, the first processing of this olfactory information takes place in the antennal lobe, from where the information is sent to the higher brain centers like the mushroom bodies and the lateral horn. There, second order synapses are situated that govern further processing with the mushroom bodies, being mainly involved in processing learned olfactory associations (Heisenberg, 1985; 2009), while the lateral horn is thought of being responsible for governing innate olfactory responses. This comparatively straight olfactory network allows us to decipher neural correlates of behavior. Some odorants have shown to be processed via a so-called *labeled line*, in which the odorant is transferred without further processing towards higher brain centers. The pheromone circuitry for example is composed of the activation of a single specific receptor, a single glomerulus and a specific region in the higher brain (Ruta et al., 2010; Sandeep, 2008). Comparable situations were found in the neuronal circuitry of CO_2, which governs strong avoidance behaviors in flies (Sachse, 2007; Suh, 2004) and in the processing of geosmin, a signature odorant for spoiled food (Stensmyr et al, 2012). This straight transfer of detected information without much processing, probably ensures hard-wired and ultimate innate behavioral responses and by that guarantees a fast stereotypic behavior that possibly saves the animal's life, time and energy. However contrary to the few odorants detected by *labeled lines*, most odorants are detected by more than one receptor and thus subjected to a more complex processing at the antennal lobe level as well as at higher brain centers before they provoke a proper innate behavior. The entire populations of projection neurons within the antennal lobe are assumed to collect an optimized code within the antennal lobe and to transfer this information to the

mushroom bodies and the lateral horn. This code contains all possible features, such as odor intensity, valence and identity (Sachse and Galizia, 2006, Knaden et al. 2012). Valence or intensity can be described as odor features or modalities, which can be shared across odors, whereas identity is a unique feature of an odor and accounts together with the other features for the quality/percept of the odor. We could show that these odor modalities are decoded by a group of inhibitory projection neurons (iPNs). iPNs extract positive valence information as well as odor-intensity information from distinct parts of the AL and integrate this information into restricted odor response domains in the lateral horn. Loss of inhibitory function in iPNs severely diminished general attraction behavior and disturbed odor-intensity discrimination. Moreover, a segregated group of third order neurons projecting to the ventrolateral protocerebrum revealed response dynamics exclusively correlated to repulsive odors. These findings suggest segregated regions within the lateral horn that govern olfactory-guided behavior based on odorant identity and concentration.

In summary, this thesis describes different mechanisms of olfactory processing in *Drosophila* and consolidates several fundamental modulatory strategies at different processing levels, which govern innate olfactory behavior.

Chapter I

A conserved dedicated olfactory circuit for detecting harmful microbes in *Drosophila*

Marcus C. Stensmyr*, Hany K.M. Dweck*, Abu Farhan*, Irene Ibba*, Antonia Strutz, Latha Mukunda, Jeanine Linz, Veit Grabe, Kathrin Steck, Sofia Lavista-Llanos, Dieter Wicher, Silke Sachse, Markus Knaden, Paul G. Becher, Yoichi Seki, and Bill S. Hansson

**These authors contributed equally to the work.*

Cell, published December 7, 2012

The bacterial product Geosmin activates a highly conserved and segregated olfactory pathway, crucial for detection and avoidance of toxic microbes.

Electrophysiology and further experiments revealed that geosmin interacts with the olfactory receptor OR56a exclusively, which is moreover tuned exclusively to the odor. In the brain, calcium imaging showed the exclusive activation of the OR56a-cognate DA2 glomerulus in the AL, on the OSN and PN level. PNs are as specificly tuned as their unique presynaptic sensory partners, as shown with patch-clamp recordings. The dedicated pathway confers innate avoidance and overrides attraction as shown for oviposition and feeding behavior. Electrophysiological screening of *Drosophila* siblings indicates that the geosmin detection system is a highly conserved feature in the genus *Drosophila*.

Built on an idea conceived by all authors.

designed & performed experiments: M.C. Stensmyr, H.K.M. Dweck, A. Farhan, I. Ibba, A. Strutz, L. Mukunda, J. Linz, V. Grabe, K. Steck, S. Lavista-Llanos, D. Wicher, S. Sachse, M. Knaden, P.G. Becher, Y. Seki, and B.S. Hansson

wrote the manuscript: M.C. Stensmyr, H. K.M. Dweck, A. Farhan, I. Ibba, A., B.S. Hansson

Chapter II

The CCHamide 1 receptor modulates sensory perception and olfactory behavior in starved *Drosophila*

Abu Farhan, Jyotasana Gulati, Ewald Große-Wilde, Heiko Vogel, Bill S. Hansson * and Markus Knaden*

**These authors contributed equally to the work.*

Scientific Reports, Accepted September 4, 2013

The olfactory response of the vinegar fly *Drosophila melanogaster* to food odor is modulated by starvation. Here we show that this modulation is not restricted to food odors and their detecting sensory neurons but rather increases the behavioral response to odors as different as food odors, repellents and pheromones. The increased behavioral responsiveness is paralleled by an increased physiological sensitivity of sensory neurons regardless whether they express olfactory or ionotropic receptors and regardless whether they are housed in basiconic, coeloconic, or trichoid sensilla. Silencing several genes that become up-regulated under starvation confirmed the involvement of the short neuropeptide f receptor in the starvation effect. In addition it revealed that the CCHamide-1 receptor is another important factor governing starvation-induced olfactory modifications.

Built on an idea conceived by all authors.

designed experiments analyzed obtained data: A. Farhan, M. Knaden

behavioral and electrophysiological experiments: A. Farhan

microarray experiment and analysis: A. Farhan, J. Gulati, G.W. Ewald, H. Vogel

wrote the manuscript: A. Farhan, M. Knaden, B.S. Hansson

Chapter III

Decoding Odor Attraction and Intensity in the *Drosophila* brain

Antonia Strutz, Jan Soelter, Amelie Baschwitz, Abu Farhan, Veit Grabe, Jürgen Rybak, Michael Schmucker, Markus Knaden, Bill S. Hansson & Silke Sachse

Submitted to Nature Neuroscience

Morphological, functional and behavioral properties of the inhibitory projection neuron (iPN) population are characterized. The data provide striking evidence that iPNs constitute a parallel second-order processing stream to the higher brain, which decodes odor attraction and intensity in the lateral horn. The inhibitory integration of these odor modalities into separated functional odor response domains in the lateral horn ultimately configures odor-based decision making of the fly.

Built on an idea conceived by all authors.

designed experiments analyzed obtained data: A. Strutz, S.Sachse

behavioral experiments: A. Farhan, M. Knaden

immunostainings: A. Baschwitz, J. Jybak, A.Strutz

OSN imaging experiments: V. Grabe

programmed NNMF algorithm: J. Soelter

analyzed Calcium imaging data: A. Strutz, J.Soelter

wrote the manuscript: A. Strutz, S. Sachse, B.S. Hansson

Chapter I

A conserved dedicated olfactory circuit for detecting harmful microbes in *Drosophila*

Marcus C. Stensmyr*, Hany K.M. Dweck*, Abu Farhan*, Irene Ibba*, Antonia Strutz, Latha Mukunda, Jeanine Linz, Veit Grabe, Kathrin Steck, Sofia Lavista-Llanos, Dieter Wicher, Silke Sachse, Markus Knaden, Paul G. Becher, Yoichi Seki, and Bill S. Hansson

**These authors contributed equally to the work.*

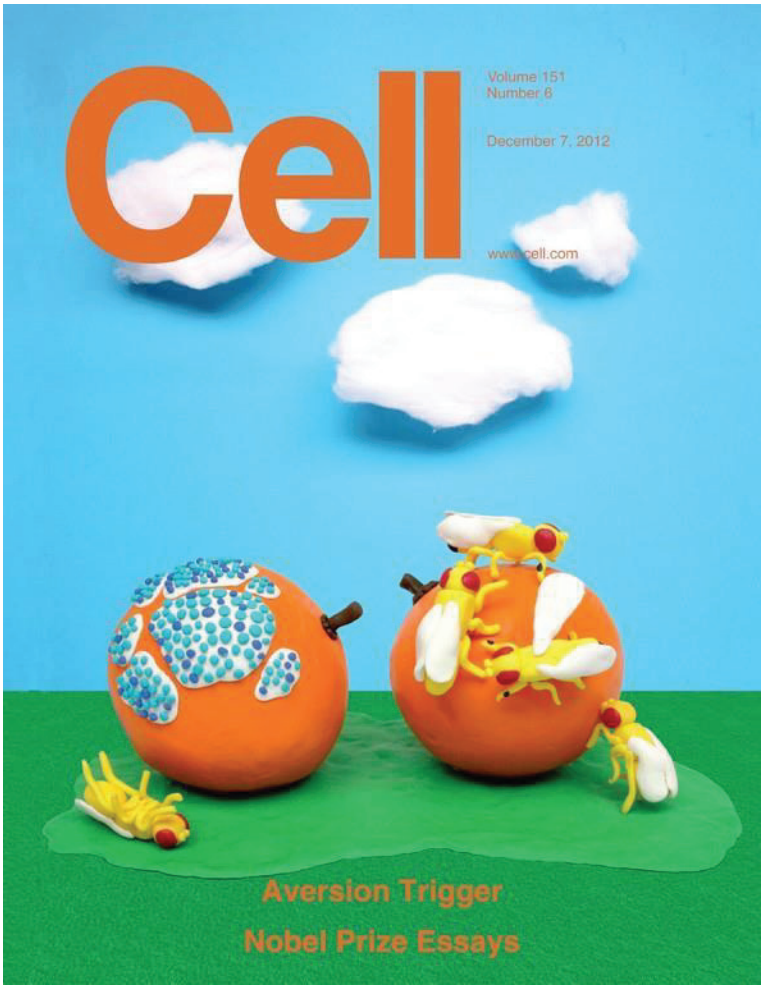

Cell

A Conserved Dedicated Olfactory Circuit for Detecting Harmful Microbes in *Drosophila*

Marcus C. Stensmyr,[1,3,*] Hany K.M. Dweck,[1,3] Abu Farhan,[1,3] Irene Ibba,[1,3] Antonia Strutz,[1] Latha Mukunda,[1] Jeanine Linz,[1] Veit Grabe,[1] Kathrin Steck,[1,4] Sofia Lavista-Llanos,[1] Dieter Wicher,[1] Silke Sachse,[1] Markus Knaden,[1] Paul G. Becher,[2] Yoichi Seki,[1,5] and Bill S. Hansson[1,*]

[1]Department of Evolutionary Neuroethology, Max Planck Institute for Chemical Ecology, Hans-Knöll-Strasse 8, 07745 Jena, Germany
[2]Division of Chemical Ecology, Swedish University of Agricultural Sciences, Box 102, 23053 Alnarp, Sweden
[3]These authors contributed equally to this work
[4]Present address: Behavior and Metabolism Laboratory, Centro Champalimaud Programa de Neurociências, Av. Brasília, Doca de Pedrouços, 1400-038 Lisbon, Portugal
[5]Present address: Laboratory of Cellular Neurobiology, School of Life Science, Tokyo University of Pharmacy and Life Sciences, 1432-1 Horinouchi, Hachioji, Tokyo 192-0392, Japan
*Correspondence: mstensmyr@ice.mpg.de (M.C.S.), hansson@ice.mpg.de (B.S.H.)
http://dx.doi.org/10.1016/j.cell.2012.09.046

SUMMARY

Flies, like all animals, need to find suitable and safe food. Because the principal food source for *Drosophila melanogaster* is yeast growing on fermenting fruit, flies need to distinguish fruit with safe yeast from yeast covered with toxic microbes. We identify a functionally segregated olfactory circuit in flies that is activated exclusively by geosmin. This microbial odorant constitutes an ecologically relevant stimulus that alerts flies to the presence of harmful microbes. Geosmin activates only a single class of sensory neurons expressing the olfactory receptor Or56a. These neurons target the DA2 glomerulus and connect to projection neurons that respond exclusively to geosmin. Activation of DA2 is sufficient and necessary for aversion, overrides input from other olfactory pathways, and inhibits positive chemotaxis, oviposition, and feeding. The geosmin detection system is a conserved feature in the genus *Drosophila* that provides flies with a sensitive, specific means of identifying unsuitable feeding and breeding sites.

INTRODUCTION

Animals respond with innate behaviors to certain stimuli in their environment. Innate behaviors, in contrast to learned behaviors, are hardwired; i.e., confronted with a specific stimulus, the animal will respond with a stereotyped behavior (Tinbergen, 1951). Many innate behaviors are triggered by odors. Prime examples are pheromones (Karlson and Lüscher, 1959), which have been particularly well studied in insects. In the vinegar fly *Drosophila melanogaster*, the male-produced pheromone *cis*-vaccenyl acetate (cVA) activates a single class of olfactory sensory neurons (OSN), which provides input to a single glomerulus (Kurtovic et al., 2007; van der Goes van Naters and Carlson, 2007) and a sexually dimorphic and functionally segregated circuit within the olfactory system (Datta et al., 2008; Ruta et al., 2010). In insects, odors associated with food or oviposition substrates can also elicit innate behaviors. The smell of vinegar confers obligate attraction in flies (Stökl et al., 2010). Although the vinegar odor activates a number of OSN classes, only a single glomerulus is sufficient and necessary for positive chemotaxis (Semmelhack and Wang, 2009). Pathways underlying hardwired attraction have thus been well characterized. Olfactory circuits mediating odorant-induced innate avoidance are, however, poorly understood. From an evolutionary perspective, being able to detect and respond quickly to harmful features in the environment should be an essential task for the olfactory system. In the fly, CO_2 elicits innate avoidance, which, like the attraction pathways, is mediated via a single glomerular circuit devoted exclusively to this stimulus (Suh et al., 2004). No dedicated avoidance circuit for an odorant sensu stricto (i.e., a volatile organic compound) has, however, been found in the fly or in any other insect. So far, all identified aversive odorants have activated multiple glomeruli (Knaden et al., 2012), and their identification depends on decoding of complex combinatorial glomerular activation patterns.

A volatile compound of interest in this context is geosmin (trans-1,10-dimethyl-trans-9-decalol) (Figure 1A). This substance is produced by a select number of fungi (Mattheis and Roberts, 1992), bacteria (Gerber and Lechevalier, 1965), and cyanobacteria (Jüttner and Watson, 2007) and to the human nose has a distinct and immediately recognizable earthy odor. A recent study found that addition of a small amount of geosmin reduced the attraction of flies to vinegar volatiles (Becher et al., 2010). Given its capacity to modulate innate attraction, this microbial volatile must be a very potent repellent and, as such, is possibly a candidate stimulus for a dedicated pathway for innate avoidance.

Cell

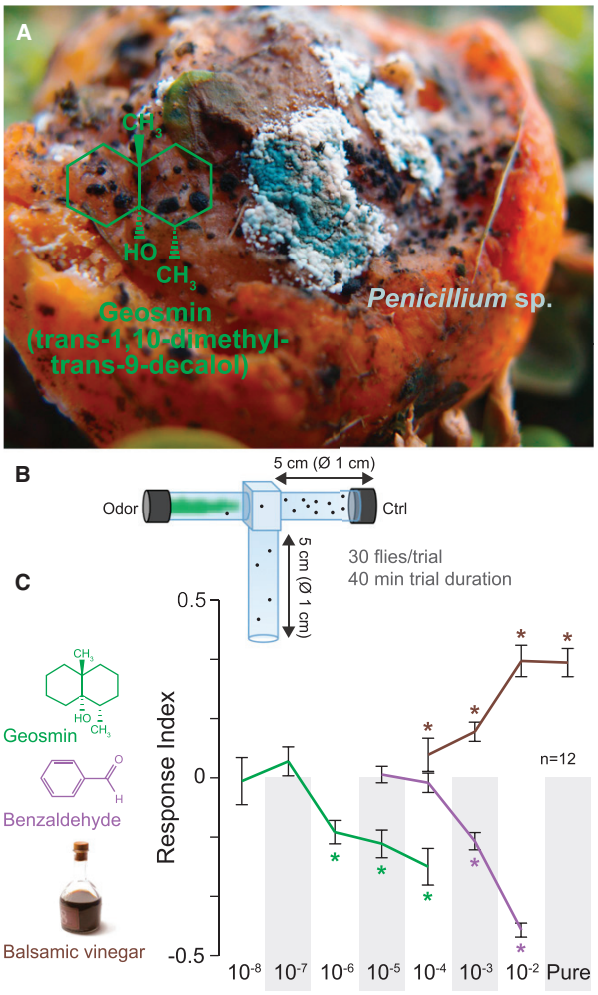

Figure 1. Geosmin—the Odor of Mold—Is Repellent to the Vinegar Fly

(A) Geosmin has a peculiar structure (left), which is distinct from odor ligands identified for *D. melanogaster*. Although a very common compound in nature, geosmin is produced only by a specific subset of microorganisms, including *Penicillium* sp. molds, shown here growing on an orange. Photo, MCS.

(B) Schematic drawing of the T-maze assay.

(C) Response indices of WT flies to geosmin, benzaldehyde, and balsamic vinegar in a T-maze assay. Deviation of the response index against zero was tested with a Student's t test ($p < 0.05$). Error bars represent SEM.

Here, we examine the functional significance of geosmin to the fly and show that geosmin activates only a single class of OSNs; these neurons express an odorant receptor that is exclusively tuned to this compound. Furthermore, we show that the geosmin-activated circuit constitutes a functionally segregated pathway, transferring the message arising from the periphery unaltered to central processing centers. We also demonstrate that this circuit alone is sufficient and necessary to trigger the avoidance behavior. Moreover, we show that, upon activation, the geosmin circuit overrides input from other circuits and inhibits positive chemotaxis. Additionally, we show that the peripheral part of the geosmin detection system is highly conserved across the genus *Drosophila*. Finally, we clearly demonstrate the ecological significance of this pathway, which is to detect toxic microbes.

RESULTS AND DISCUSSION

A Single Class of Olfactory Sensory Neurons Detects Geosmin

We first set out to determine the behavioral significance of geosmin by using a T-maze (Figure 1B). In this two-choice olfactory assay, geosmin on its own elicited avoidance at very low concentrations (10^{-6}) (Figure 1C). For comparison, benzaldehyde—a well-known repellant to flies—in the same assay required a 1,000-fold higher dose than geosmin to trigger repulsion (Figure 1C). The actual fold difference in flies' behavioral sensitivity toward these two compounds is greater once volatility is factored in. The vapor pressure of geosmin is 1,000-fold lower than for benzaldehyde (0.001 mmHg versus 1.27 mmHg at 25°C). Thus, at a given dose and temperature, the number of geosmin molecules in vapor phase is substantially lower than for benzaldehyde. Geosmin is accordingly not only repellent but is also repellent when present in exceedingly low amounts.

Flies are evidently equipped with a sensitive detection system for geosmin. To identify the population of OSNs that is activated by geosmin, we next turned to electrophysiology. Specifically, we performed single-sensillum recording (SSR) measurements, a method that allowed us to assess odor-induced OSN activity extracellularly. We aimed to obtain SSR measurements from all antennal olfactory sensillum types while stimulating the contacted OSNs with geosmin. The ~450 olfactory sensilla of the fly antennae (Shanbhag et al., 1999) can be divided into 17 functional types, which in total house 46 functionally distinct OSN classes (de Bruyne et al., 2001; Hallem et al., 2004; Couto et al., 2005; Yao et al., 2005; van der Goes van Naters and Carlson, 2007; Benton et al., 2009). In addition to these well-classified sensilla, morphological data indicate that the antennae also contain one more type, the so-called intermediate sensilla; these sensilla house an unknown number of functional OSN classes (Shanbhag et al., 1999). The second olfactory organ of the fly, the maxillary palp, houses an additional three types for a total of six distinct OSN classes (de Bruyne et al., 1999). By performing a considerable number of SSR measurements ($n > 1000$) using diagnostic odors and by comparing the response properties of contacted OSNs with previously published ligand affinities, we were able to locate and record from all sensillum types present on the antennae (including two types of intermediate sensilla), as well as from the three types found on the maxillary palps (Figure 2A).

Response to geosmin came from just a single class of antennal OSNs, namely, the ab4B OSNs (Figures 2B and 2C). These neurons express the odorant receptors (OR) *Or56a* and *Or33a* (Couto et al., 2005; Fishilevich and Vosshall, 2005), of which only the former is functional in the *Canton-S* strain we used here (Kreher et al., 2008). Although ab4B OSNs have been measured from previously (e.g., de Bruyne et al., 2001), geosmin is the first ligand reported for this neuron class. To confirm that

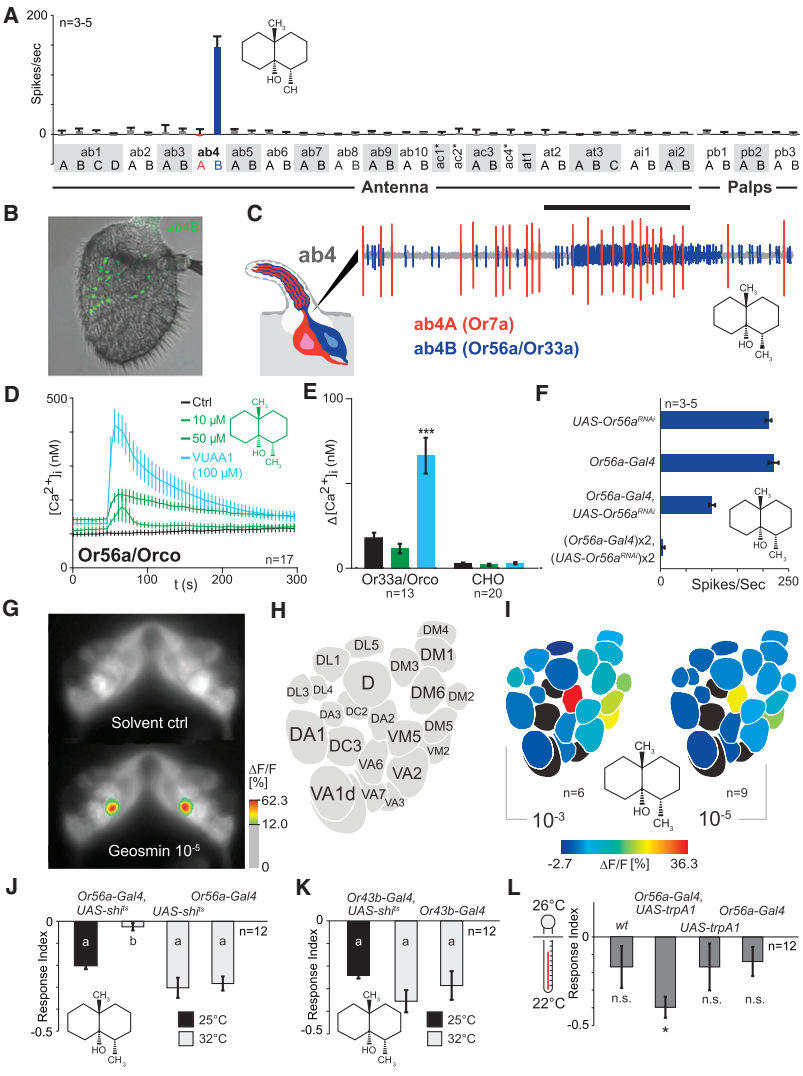

Figure 2. Geosmin Activates a Single Class of Antennal Olfactory Sensory Neurons

(A) SSR measurements from all olfactory sensilla with geosmin (10^{-3}) as a stimulus. ab, antennal basiconic sensilla (s.); ac, antennal coeloconic s.; at, antennal trichoid s.; ai, antennal intermediate s.; pb, palp basiconic s. Stars denote that activity from individual OSNs was not separated. Error bars represent SEM.

(B) Distribution of ab4B neurons on the antenna as visualized by the expression of GFP from the *Or56a* promoter.

(C) Representative SSR traces from an ab4 sensillum. The smaller amplitude spiking neuron, i.e., ab4B responds to geosmin (10^{-3}). The duration of the stimulus delivery (0.5 s) is marked by the black bar.

(D) The free intracellular Ca^{2+} concentration $[Ca^{2+}]_i$ in CHO cells expressing Or56a and Orco increases after the application of geosmin and VUAA1 (100 μM), but not of saline (control). Error bars represent SEM.

(E) Mean increase in free intracellular Ca^{2+} concentration $[Ca^{2+}]_i$ in CHO cells expressing Orco and Or33a or nontransfected CHO cells after the application of saline (control), geosmin (50 μM), and VUAA1 (100 μM). Star denotes response significantly different from control (Student's t test, $p < 0.05$). Color scale as in (D). Error bars represent SEM.

(F) Quantification of responses to geosmin (10^{-3}) from ab4B OSNs of flies expressing RNAi against Or56a in the ab4B OSNs and the corresponding parental lines. Error bars represent SEM.

(G) False color-coded images showing solvent-induced (top) and geosmin-induced (bottom) calcium-dependent fluorescence changes in the AL of a fly expressing the activity reporter GCaMP3.0 from the *Orco* promoter.

(H) Glomerular atlas of the AL.

(I) Odor-induced activity plotted on schematic ALs (average % Δ*F*/*F*).

(J) RI to geosmin (10^{-5}) of flies expressing *Shibire*^{ts} from the *Or56a* promoter and corresponding parental lines in a T-maze assay. Significant differences are denoted by letters (analysis of variance [ANOVA] followed by Tukey's test; $p < 0.05$). Error bars represent SEM.

(K) RIs to geosmin (10^{-5}) of flies expressing *Shibire*^{ts} from the *Or43b* promoter and the corresponding parental lines in a T-maze assay. No significant differences (ANOVA followed by Tukey's test; $p > 0.05$). Error bars represent SEM.

(L) RIs of flies expressing *dTRPA1* from the *Or56a* promoter, the corresponding parental lines, and WT in a T-maze assay confronted with a choice between 22 and 26°C. Deviation of the RI against zero was tested with a Student's t test ($p < 0.05$). Error bars represent SEM.

See also Figure S1.

Or56a is indeed the geosmin receptor, we next expressed this protein in Chinese hamster ovary (CHO) cells that stably expressed the OR coreceptor *Orco* (Larsson et al., 2004). Because insect ORs are Ca^{2+}-permeable ionotropic receptors, OR activation can be monitored by measuring the free intracellular Ca^{2+} concentration $[Ca^{2+}]_i$. The application of geosmin transiently increased $[Ca^{2+}]_i$ in a concentration-dependent manner (Figure 2D). The cells responding to geosmin were seen to respond to the Orco agonist VUAA1 (Jones et al., 2011), although there was no response to control application of saline (Figure 2D and Figure S1A available online). We then expressed *Or33a* in the same CHO cell line. Although the cells responded to VUAA1, we found no responses to geosmin (Figure 2E). CHO cells not expressing *Orco* or either of the two tuning ORs produced no Ca^{2+} signals in response to the application of geosmin or VUAA1 (Figure 2E). Loss of function of *Or56a* should render ab4B OSNs insensitive to geosmin. We next used SSR to examine the function of ab4B OSNs expressing a *UAS*-RNA interference (RNAi) construct against *Or56a*. The expression of *UAS-Or56a*^{RNAi} reduced the response to geosmin in a dose-dependent manner (Figures 2F and S1B). In flies carrying one copy each of *Or56a-Gal4* and *UAS-Or56a*^{RNAi}, the response to

geosmin was reduced by ~50% compared to the response displayed by the parental lineages. With two copies of each, the response was essentially abolished (~98% reduction) (Figure 2F). Thus, we conclude that *Or56a* alone underlies the ability of the ab4B cells to detect geosmin.

To further verify that geosmin is detected only by a single class of OSNs, we next employed functional imaging to examine the activity pattern in the antennal lobe (AL) evoked by geosmin (Figures 2G and S1C). We used the *Gal4-UAS* system to express the Ca^{2+}-sensitive reporter gene GCaMP3.0 (Tian et al., 2009) from the *Orco* promoter, thereby labeling all OSNs except those relying on ionotropic receptors (Benton et al., 2009) for odorant detection. Activated glomeruli were then identified by comparing the activation pattern with the map of the fly AL (Couto et al., 2005; Fishilevich and Vosshall, 2005) (Figure 2H). We stimulated flies with diagnostic odors to assist glomerular identification (data not shown) and with geosmin at 10^{-3} and 10^{-5} dilutions (Figures 2G and 2I). At 10^{-5}, geosmin elicited repeatable signals from only a single locus in the AL—the DA2 glomerulus, which receives input from ab4B neurons (Couto et al., 2005; Fishilevich and Vosshall, 2005). We note that DA2 is also situated in the same lateral part of the AL that has previously been implicated in handling aversive odors (Knaden et al., 2012). In a number of recordings, we also noted activity from VM2; however, these signals were not consistently reproducible. In the SSR screen, we never observed any activity in response to geosmin from OSNs innervating VM2; these OSNs are housed in the ab8 sensillum (Figure 2A). Hence, the activity noted from VM2 most likely does not reflect actual peripheral input but, rather, may stem from intrinsic AL processes. We therefore conclude that geosmin is indeed detected by a single class of OSNs. It should be stressed that the level of specificity shown here toward a nonpheromonal odor is most unusual, if not unique, among the olfactory systems investigated to date.

Activation of the ab4B Neurons Is Necessary and Sufficient for the Aversive Behavior

If the behavior triggered by geosmin is solely derived from the activity of ab4B neurons, silencing this OSN subpopulation should also abolish the aversive behavior. To silence these neurons, we expressed the temperature-sensitive mutant dynamin *Shibire^{ts}* (Kitamoto, 2001) from the *Or56a* promoter. At the restrictive temperature (32°C), flies carrying this construct displayed no aversive behavior toward geosmin (Figure 2J). The same flies, tested at a permissive temperature (25°C), showed a strong aversion to geosmin. Parental lines tested at the nonpermissive temperature showed a somewhat increased repellency, which was likely caused by the increased volatility of geosmin at the higher temperature. Silencing the ab4B neurons had no effect on flies' behavior in response to benzaldehyde (Figure S1D). In line with the SSR experiments, silencing input to VM2—via the expression of *Shibire^{ts}* from the *Or43b* promoter—did not affect flies' behavior in response to geosmin (Figure 2K). The ab4B OSNs are evidently necessary for the aversive behavior.

We next asked whether selectively activating these neurons is sufficient to cause aversion. We expressed the temperature-sensitive cation channel *dTRPA1* in the ab4B neurons, a procedure that allowed us to conditionally activate these OSNs at temperatures >26°C (Hamada et al., 2008). As a control, we first examined the temperature preference (26°C versus 22°C) of wild-type (WT) flies in a T-maze assay. WT flies showed a tendency toward aversion against the higher temperature (Figure 2L). Having established baseline behavior in the assay, we next asked whether flies bearing the *Or56a-Gal4*, *UAS-dTRPA1* construct displayed a stronger aversion toward the higher temperature. In fact, flies expressing *dTRPA1* in ab4B OSNs showed significant avoidance toward the warm side, whereas parental control flies showed moderate (but insignificant) aversion (Figure 2L). Thus, specifically activating these neurons induces aversion in flies. In summary, these experiments demonstrate that the aversive behavior caused by geosmin is mediated solely through a single class of OSNs.

The ab4B Neurons Respond Exclusively to Geosmin

As seen, geosmin is detected by a single class of OSNs, ab4B. We next asked whether or not these neurons are exclusively tuned to geosmin. We again used SSR but now screened with 103 structurally diverse odorants (tested at 10^{-2} dilution) (Figure S2A). The larger spiking neuron in the ab4 sensillum responded to a range of compounds (Figure S2B). Interestingly, we note that the most potent ligands for these OSNs are all known repellants. The functional significance, if any, of having two neurons both responding to aversive odorants that are cocompartmentalized is unclear. The ab4B neurons, in contrast, displayed a striking degree of selectivity, as none of the screened odorants—apart from geosmin—elicited any increased spike firing (Figure 3A). Showing specificity in the context of the olfactory system is, however, difficult, as there are thousands of volatile chemicals in nature. Our tested set thus represents only a fraction of the volatile chemicals potentially present in the natural habitat of *D. melanogaster*.

To address this issue and to more firmly examine the specificity of these neurons, we next expanded our SSR investigation by using a gas chromatograph (GC) for stimulus delivery. GC-linked SSR enables the screening of headspace collections from complex odor sources and, consequently, enables the probing of large numbers of volatiles. We first sampled odors from a wide range of sources present in the natural habitat of *D. melanogaster* in native Africa as well as in the "Diaspora." We collected odors from 14 sources, including avoided ones, such as feces (from African mammals) and rotting meat, as well as attractive ones, such as fruits and vinegar. The total number of volatiles present in these samples is difficult to firmly establish, but the number of distinguishable flame ionization detection (FID) peaks amounts to ~2,900 in total. The actual number of compounds present is, however, likely considerably higher. The headspace of many fruits typically contains >400 volatiles (e.g., Petro-Turza, 1987); hence, in our samples, many more compounds were presumably present but only in amounts below the FID limit. These compounds were nevertheless effectively screened, as insects, including *Drosophila*, are capable of detecting compounds present well below the FID limit.

Having collected and verified the odor samples, we then proceeded to perform GC-SSR measurements from ab4B neurons.

Cell

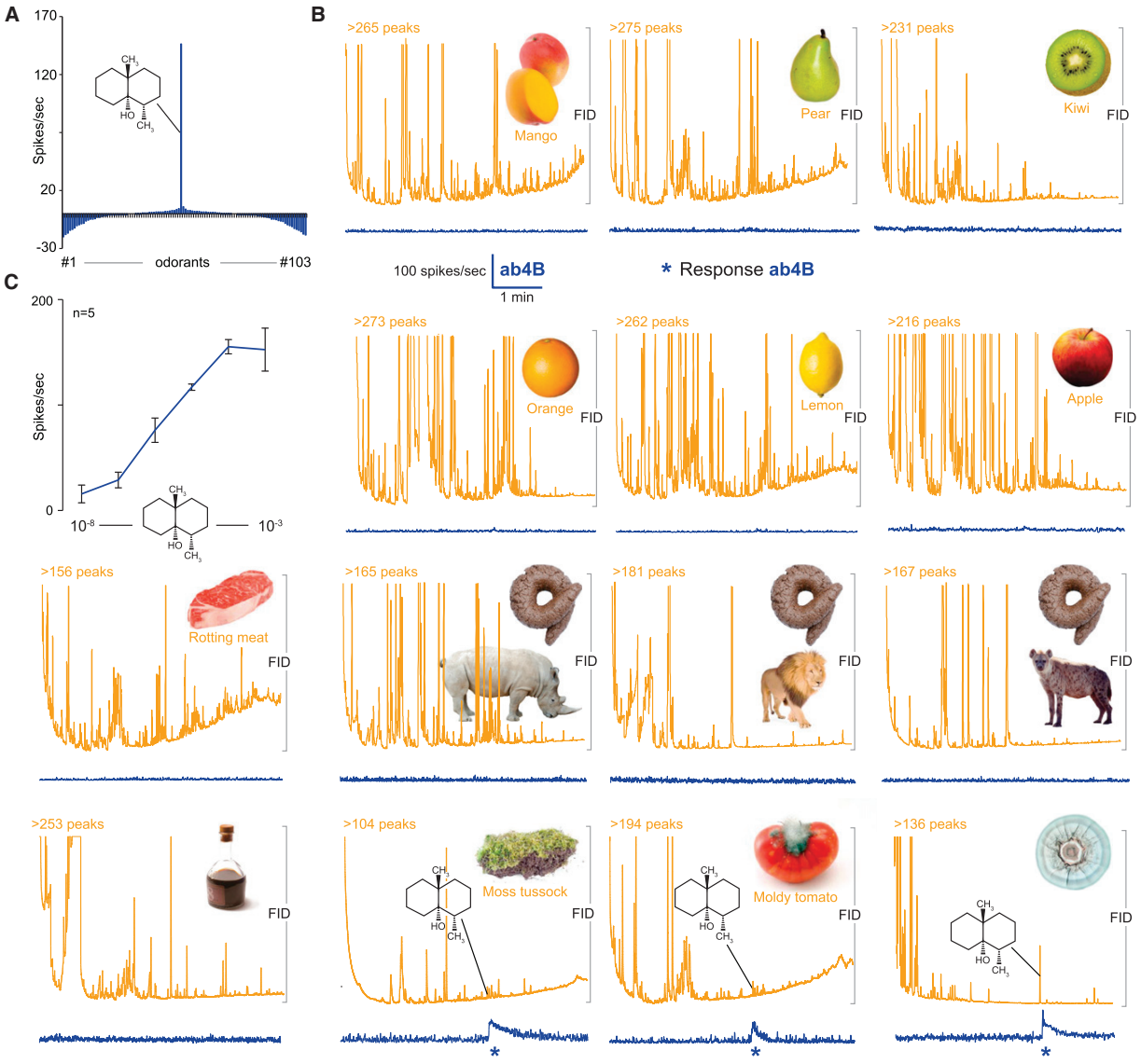

Figure 3. The ab4B Neurons Respond Exclusively to Geosmin

(A) Tuning curve for the ab4B neuron type based on a screen of 103 synthetic substances (10^{-2} dilution). Error bars represent SEM.

(B) Gas-chromatography-linked SSR measurements from ab4B neurons. The orange trace represents the FID, photos depict the screened odor sources, and the blue trace depicts the simultaneously recorded neural activity of ab4B neurons. Stars denote response. n = 1–3.

(C) Dose response curve from ab4B neurons toward geosmin. Error bars represent SEM.

See also Figure S2.

Out of the 14 odor samples we screened, only three evoked responses (Figure 3B), namely the headspace of a moldy tomato, a moss tussock, and isolated cultures of the common soil bacterium *Streptomyces coelicolor*. In each of the active samples, only a single FID peak elicited a response. We next used GC-linked mass spectroscopy (GC-MS) combined with synthetic standards to identify the functionally relevant peaks in these three samples; in all cases, these turned out to be geosmin. Thus, the ab4B neurons are indeed extremely specific, and it is reasonable to conclude that the sole function of these neurons is to detect geosmin.

How sensitive are the ab4B neurons toward geosmin? Our T-maze experiments (Figure 1C) had already shown that the flies respond behaviorally at very low concentrations. Indeed, the ab4B neurons respond to geosmin at 10^{-8} dilution (corresponding to 100 pg of substance in the stimulus pipette)

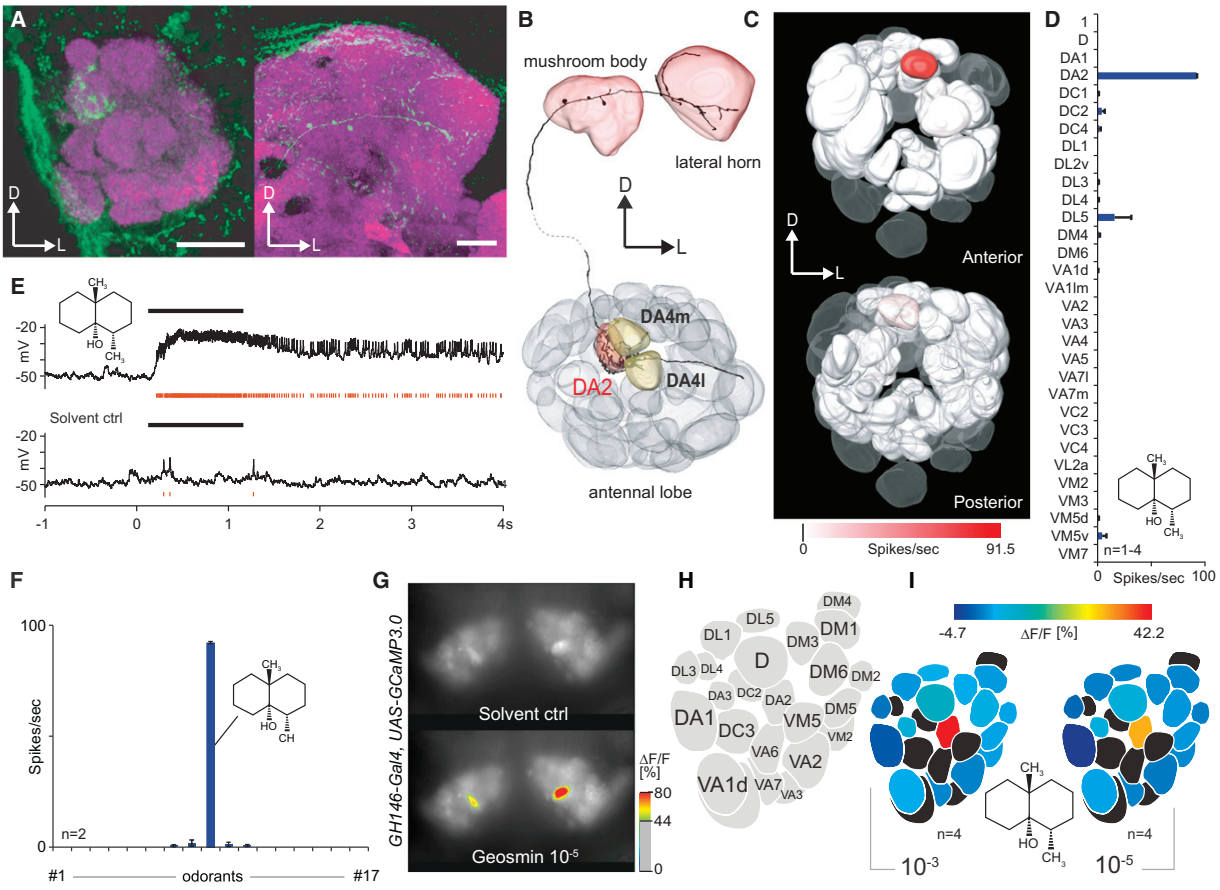

Figure 4. Geosmin Activates a Functionally Segregated Pathway

(A) A PN innervating the DA2 glomerulus (left) and sending its axon to the calyx of the mushroom body and terminating in the lateral horn (right). PN, green; nc82, magenta. D denotes dorsal, and L denotes lateral.

(B) Reconstruction of the neuron in (A).

(C) Glomeruli from which PN recordings were obtained (in solid), with the response to geosmin (10^{-3}) false color coded. Transparent glomeruli were not investigated.

(D) The net change in spike frequency in response to geosmin (10^{-3}) stimulation from PNs innervating 31 glomeruli. Error bars represent SEM.

(E) Example spike trace from a DA2 PN responding to geosmin (10^{-3}). Black bar marks the 1 s odor stimulus. Red trace represents extracted spikes.

(F) Tuning curve for DA2 PNs based on 17 synthetic substances (10^{-2} dilution, except geosmin, which was used at 10^{-3}). Error bars represent SEM.

(G) False color-coded images showing solvent-induced (top) and geosmin-induced (bottom) calcium-dependent fluorescence changes in AL PNs of a fly bearing the *GH146-Gal4*, *UAS-GCaMP3.0* constructs.

(H) Glomerular atlas of the AL.

(I) Odor-induced activity plotted on schematic ALs (average % Δ*F*/*F*).

See also Figure S3.

(Figure 3C), which is in good agreement with the dilution of geosmin (1.74×10^{-7}) causing reduced upwind flight attraction to vinegar headspace when vaporized in the wind tunnel (Becher et al., 2010).

Geosmin Triggers a Segregated Pathway through the Antennal Lobe to Higher Brain Centers

How is the specific tuning in flies to geosmin seen in the peripheral sensory neurons transferred to higher brain centers? In *Drosophila*, the OSNs form synapses with projection neurons (PNs) and local interneurons within the AL. Most PNs innervate only a single glomerulus (Figures 4A and 4B), whereas local interneurons typically show broad innervation throughout the AL. The PNs send their axons to the mushroom body and lateral horn (Figures 4A and 4B) (Vosshall and Stocker, 2007). PNs tend to respond to a somewhat broader range of odors than do their corresponding OSNs (Wilson et al., 2004; Bhandawat et al., 2007). For instance, the PNs connected to OSNs that respond only to geranyl acetate respond to additional odors as well. However, PNs connected to OSNs that respond to the sex

Cell

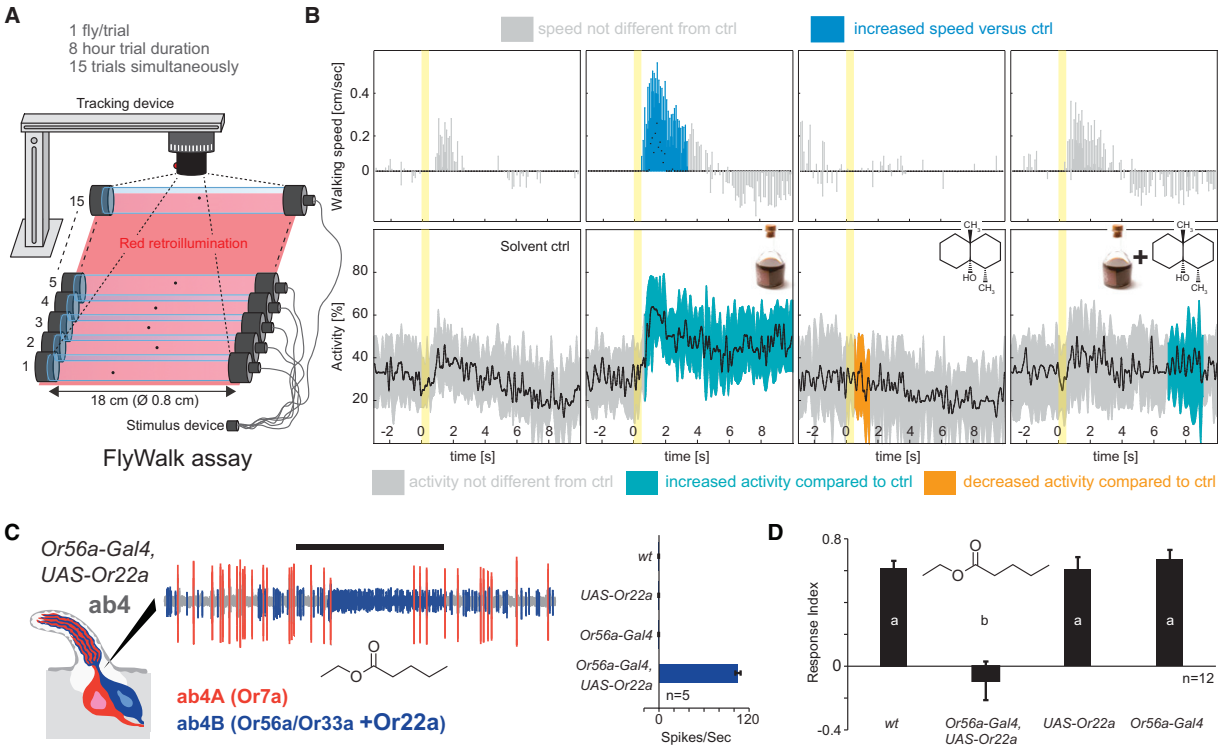

Figure 5. Activation of the Geosmin Pathway Reduces Attraction

(A) Schematic drawing of the Flywalk assay used in (B). For details, see Steck et al. (2012).

(B) Quantified behavior from individual flies stimulated with balsamic vinegar, geosmin (10^{-3}), and a mix of the two in the Flywalk assay. Top graphs, box plot representations of odor-induced changes in upwind speed of flies (n = 30); black line represents median upwind speed; box, interquartile range; whiskers, 90th and 10th percentiles. Lower graphs, undirected activity of flies (n = 30); black line, median activity; shaded area, interquartile range. Yellow area marks the 500 ms odor stimulus. Statistical analysis per Steck et al. (2012).

(C) Left, representative SSR trace from an ab4 sensillum, stimulated with ethyl butyrate (10^{-5}) in which the B neuron expresses Or22a. Right, quantification of mean responses to ethyl butyrate from control ab4B OSNs and ab4B OSNs misexpressing Or22a.

(D) Response indices of flies expressing Or22a in the ab4B OSNs, corresponding parental lines and WT flies to ethyl butyrate (10^{-5}) in a T-maze assay. Significant differences are denoted by letters (ANOVA followed by Tukey's test; $p < 0.05$). Error bars represent SEM.

See also Figure S4.

pheromone cVA do not show a broad response pattern and are just as specific as their cognate OSNs (Schlief and Wilson, 2007). We thus asked: how specific is the response of PNs that respond to geosmin?

We carried out whole-cell patch-clamp recordings from a large number of randomly selected uniglomerular PNs, stimulating with 17 chemicals, including geosmin (Figure S3). We obtained recordings and fills from 66 PNs (from 66 individual flies), which covered 31 different glomeruli. Geosmin elicited significant responses only from two PNs, both of which innervated the DA2 glomerulus (Figures 4A–4E). Although not all glomeruli were covered, this result strongly suggests that geosmin information does not diffuse broadly across the AL to other glomeruli. Moreover, DA2 PNs appear to be as selective as the input OSNs because these PNs responded exclusively to geosmin and not to any of the other screened compounds (Figures 4F and S3). To further examine the specificity of the AL output, we next imaged flies carrying the *GH146-Gal4* and *UAS-GCaMP3.0* constructs in which ~1/2 of the PNs express the GCaMP3.0 activity reporter (Stocker et al., 1997; Jefferis et al., 2001). Stimulation with geosmin again exclusively activated the DA2 glomerulus (Figures 4G–4I). Thus, we conclude that, like the labeled line pheromone pathway, the geosmin circuit forms a dedicated functionally segregated pathway, at least to the point of the calyx and lateral horn. The fate of the signal past this point remains to be elucidated.

The Geosmin Circuitry Can Modulate and Override Innate Attraction

As mentioned before, the addition of geosmin to vinegar significantly reduced positive chemotaxis in flies' response to this innately attractive odor. To verify that geosmin indeed has the capacity to reduce flies' attraction to vinegar, we next repeated the wind tunnel experiments with an alternative bioassay, the Flywalk (Steck et al., 2012) (Figure 5A). This assay enables high-resolution quantification of behavior from individual flies in

Cell

response to short pulses of an odor stimulus repeated during an extended period of time. Our Flywalk results parallel the findings from the wind tunnel (Figure 5B). Exposing flies to pulses of balsamic vinegar induced bursts of positive chemotaxis, which were significantly reduced when geosmin was added to the vinegar volatiles. Geosmin alone induced a "freezing" behavior, i.e., a decrease of the flies' activity, which, in this assay, reflects aversion (Steck et al., 2012). The ability of geosmin to reduce the attractiveness of vinegar is robust and can be repeated with both the trap assay (Larsson et al., 2004) (Figures S4A and S4B) and the T-maze (Figure S4C).

In light of the physiology findings, the cause of the reduced attractiveness of the geosmin-vinegar mix should stem from activation of the DA2 pathway. This circuit should consequently have the capacity to override and modulate an innate behavior. To test this notion, we used the *Or56a-Gal4* line to drive the expression of an additional odorant receptor (*Or22a* targeting glomerulus DM2) in ab4B OSNs (Figure 5C), enabling us to manipulate the activity of the DA2 circuit in the absence of geosmin and thereby to separate the chemical from the actual effect. In flies expressing Or22a under the *Or56a* promoter, stimulation with ethyl butyrate, a potent ligand for Or22a that is highly attractive to flies (Figure 5D), should result in the activation of both DM2 and DA2, in turn reducing the flies' attraction to ethyl butyrate. Through SSR, we first verified that the misexpression of Or22a conferred sensitivity toward ethyl butyrate in ab4B neurons (Figure 5C). Having established physiological function, we then tested the flies' behavioral response toward ethyl butyrate by using a T-maze. The parental control lines showed the expected strong positive response of WT flies toward this fruit ester. On the other hand, flies additionally expressing Or22a in the ab4B OSNs showed no attraction toward ethyl butyrate (Figure 5D). Thus, activating DA2 and the associated pathway can modulate and override innate attractive behavior.

Geosmin Is Used by the Fly to Detect Toxic Molds and Bacteria

We next asked what the possible evolutionary and ecological reason might be for the strong and hard-wired chemosensory avoidance of geosmin. Because geosmin itself is nontoxic to invertebrates as well as mammals (Young et al., 1996), the function of the circuit is not just to alert *D. melanogaster* to the presence of this compound. With some exceptions, the majority of volatiles flies detect are widely produced in nature and, thus, are difficult to firmly associate with a specific source. Geosmin—although very abundant in nature—is solely produced by a narrow range of microbes, in particular *Penicillium* fungal molds (Mattheis and Roberts, 1992) and *Streptomyces* soil bacteria (Gerber and Lechevalier, 1965). Has the system for detecting geosmin evolved to identify these specific microorganisms? We first examined whether flies could survive on these types of microbes. We transferred newly eclosed flies to vials with a yeast-containing medium or to vials additionally containing cultures of either *Streptomyces coelicolor* or *Penicillium expansum*. Flies were unable to survive in the presence of either of these microbes (Figure 6A), presumably due to the accumulation of toxins. Many fungal molds, including *P. expansum*, produce a range of toxic secondary metabolites, several of which have been shown to have strong insecticidal activity (Castillo et al., 1999). Many geosmin-producing microbes are not only toxic but are also known to outcompete or even kill the yeasts flies graze on (Arndt et al., 1999). Thus, for the fly, being able to detect and avoid fruit colonized by harmful molds and bacteria should be an essential skill.

Because many geosmin-producing microbes are detrimental to flies, we suspected that substrates colonized by this type of microbe are avoided for oviposition. Thus, we next looked for an olfactory-based oviposition preference in flies by using a two-choice assay (Figure 6B) in which flies were given the option of laying eggs on plates containing either standard *Drosophila* yeast medium or on plates additionally inoculated with *S. coelicolor*. Indeed, flies avoided laying eggs on plates containing *S. coelicolor* (Figure 6C). Is the avoidance of the bacterial plates mediated via geosmin? To address this question, we subsequently repeated the oviposition experiments. We inoculated one of the plates with a gene-targeted *S. coelicolor* strain (J3001), which carries a deletion in a key gene involved in the geosmin synthesis pathway (Gust et al., 2003). The J3001 strain is thus identical to WT *S. coelicolor* except for its inability to produce geosmin, the lack of which we also confirmed via GC-MS and GC-SSR (Figure 6D). Abolishing the production of geosmin completely eliminated the avoidance in response to *S. coelicolor* (Figure 6C). In the absence of geosmin, flies readily oviposited on the harmful media. Eggs deposited onto *S. coelicolor* did not develop into adult flies (data not shown), and survival on the J3001 strain did not differ from survival on WT *S. coelicolor* (log rank test; $p = 0.22$). In a pure olfactory choice assay, the trap assay (Figure S4A), flies also discriminated between the two strains, preferring J3001 over WT (Figure S5).

We next wondered whether the reluctance to oviposit in the presence of (WT) *S. coelicolor* is dependent on the DA2 circuit. To address this question, we examined the oviposition preference of flies carrying the previously used *Or56a-Gal4*, *UAS-Shibire^{ts}* construct. At permissive temperatures, these flies strongly avoided plates containing *S. coelicolor*, whereas at restrictive temperatures, there was no avoidance, and the flies even showed a slight preference for the bacterial substrate (Figure 6E). In line with our hypothesis, the presence of geosmin alone should also prevent egg laying, which it did. Plates containing geosmin (10^{-3}) were avoided as an oviposition substrate (Figure 6F). One could speculate that the presence of any strongly repellent odor would also prevent oviposition from occurring. However, benzaldehyde did not inhibit oviposition from occurring at 10^{-4} and 10^{-2} dilutions and barely did so even when tested as a pure substance (Figure 6F).

Are flies also hesitant to consume food contaminated with this type of microbe? We next examined feeding preference by using a capillary feeder assay (Figure 6G) (Ja et al., 2007); here, flies could choose between two 5% sucrose solutions, one of which was based on a wash from WT *S. coelicolor* colonies. Indeed, flies clearly preferred the pure sucrose solution (Figure 6H). We then repeated these experiments, replacing the WT *S. coelicolor* with the J3001 strain. The solution

Cell

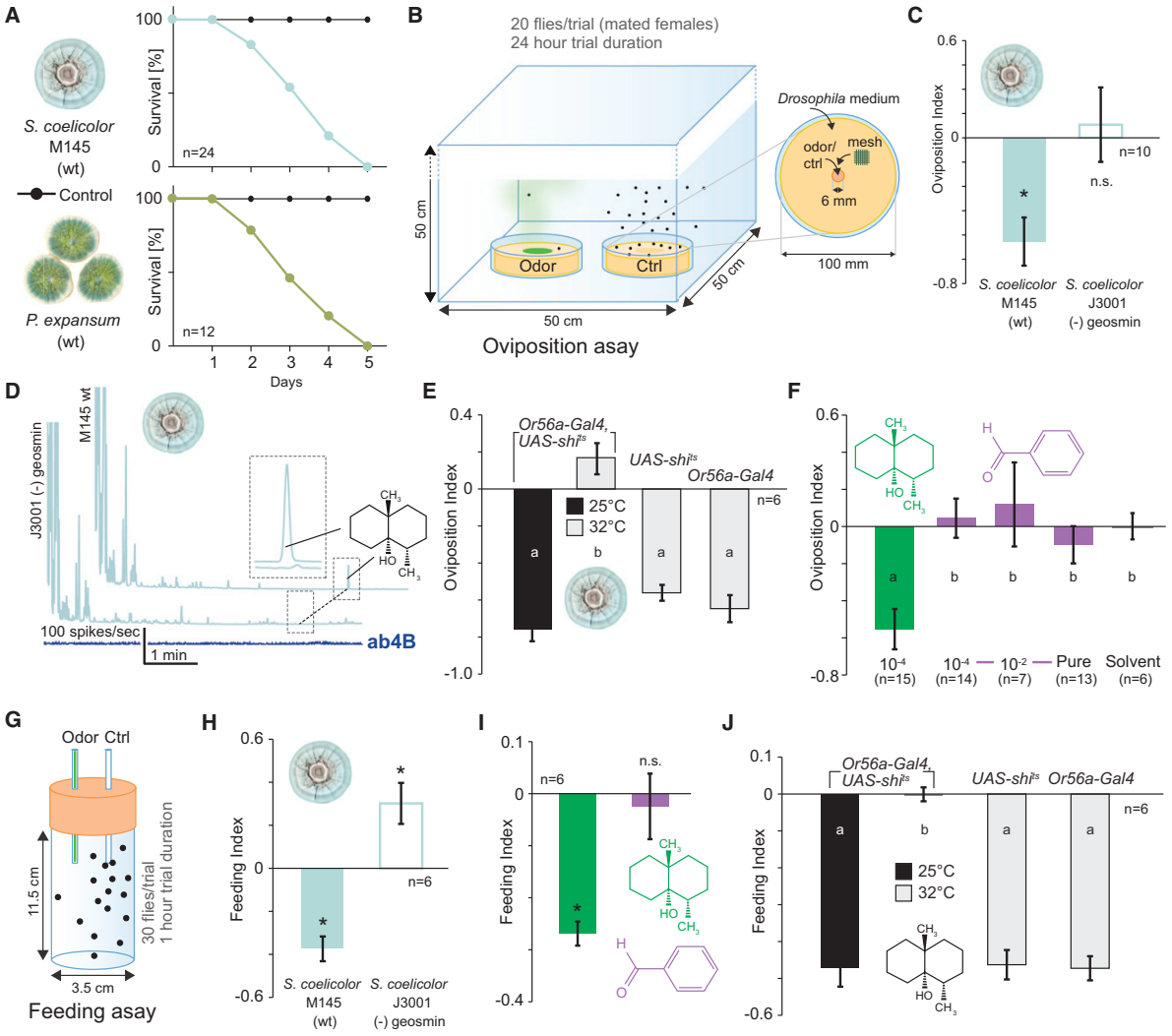

Figure 6. Geosmin Is Used by Flies to Detect Toxic Molds and Bacteria

(A) Survival rate of newly eclosed flies transferred to vials containing pure agar medium or medium with 1-week-old cultures of either of two geosmin-producing microbes.

(B) Schematic drawing of the oviposition choice assay used in (C), (E), and (F).

(C) Oviposition indices (OI) to WT (M145) and J3001 *S. coelicolor* of WT flies. The J3001 only differs from WT by its inability to produce geosmin. Deviation of the oviposition index against zero was tested with a Student's t test ($p < 0.05$). Error bars represent SEM.

(D) GC-MS and GC-SSR analysis of headspace from J3001 and M145. Pale blue represents flame ionization detection traces. The dark blue trace shows activity from an ab4B OSN being stimulated with J3001 headspace (no response).

(E) OIs to WT *S. coelicolor* of flies expressing *Shibire^{ts}* in the ab4B OSNs and corresponding parental lines at permissive (25°C) and restrictive (32°C) temperatures. Significant differences are denoted by letters (ANOVA followed by Tukey's test; $p < 0.05$). Error bars represent SEM.

(F) OIs to geosmin and benzaldehyde of WT flies. Significant differences are denoted by letters (ANOVA followed by Tukey's test; $p < 0.05$). Error bars represent SEM.

(G) Schematic drawing of the capillary feeding assay (modified from Ja et al. [2007]) used in (H)–(J).

(H) Feeding indices (FI) to 5% sucrose solutions containing traces of WT (M145) or J3001 *S. coelicolor* of WT flies. Deviation of the feeding index against zero was tested with a Student's t test ($p < 0.05$). Error bars represent SEM.

(I) FIs to 5% sucrose solutions containing geosmin (0.1%) or benzaldehyde (0.1%) of WT flies. Deviation of the feeding index against zero was tested with a Student's t test ($p < 0.05$). Error bars represent SEM.

(J) FIs to 5% sucrose solutions containing traces of WT (M145) *S. coelicolor* of flies expressing *Shibire^{ts}* from the *Or56a* promoter and corresponding parental lines at permissive (25°C) and restrictive (32°C) temperatures. Significant differences are denoted by letters (ANOVA followed by Tukey's test; $p < 0.05$). Error bars represent SEM.

See also Figure S5.

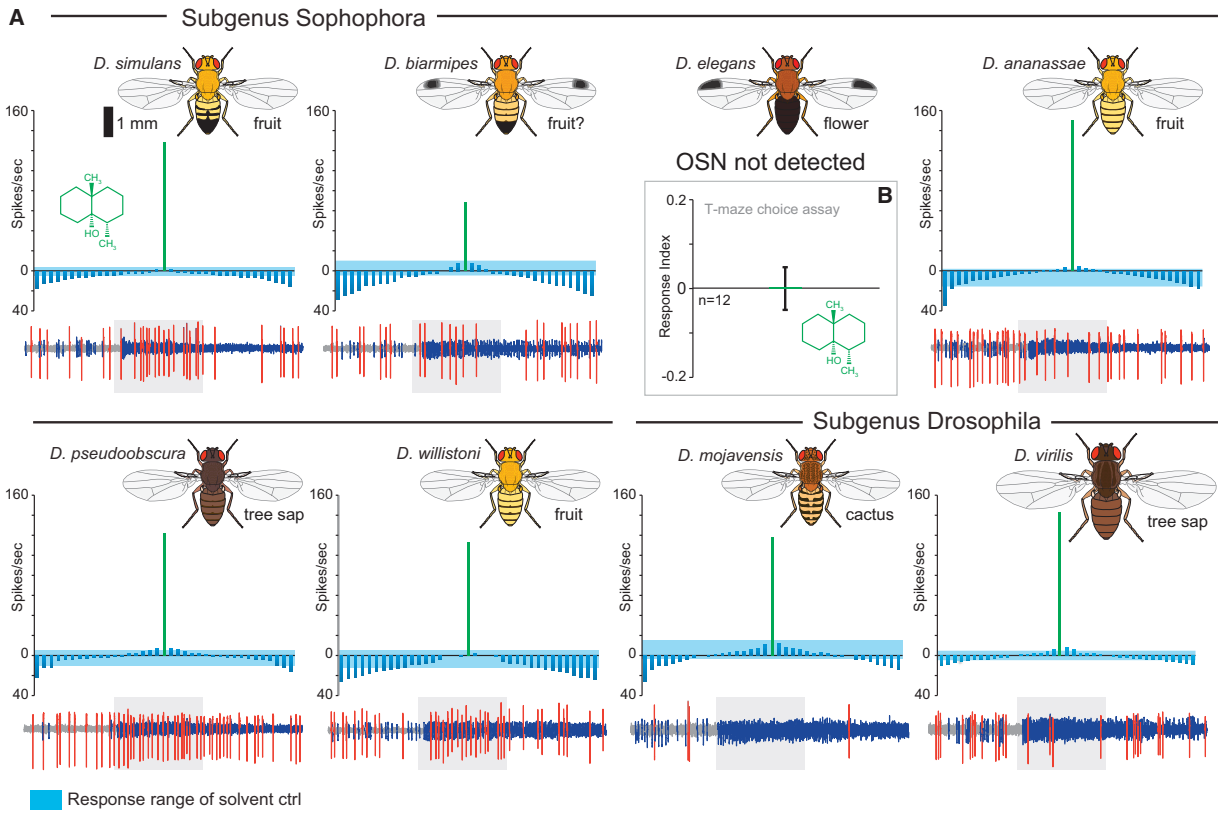

Figure 7. Responses to Geosmin in Drosophilids Are Deeply Conserved

(A) Tuning curves for neurons with similar response properties to the ab4B neurons of *D. melanogaster* from select members of the genus *Drosophila* (n = 3 for all species). The tuning curves are based on a screen with 37 compounds, tested at 10^{-2}. Below curves are representative SSR traces showing responses to geosmin (10^{-3}), with the gray box indicating the 0.5 s stimulus delivery period. The natural breeding substrates are indicated underneath the schematic drawings of the species. Error bars represent SEM.

(B) Response index to geosmin (10^{-5}) of *D. elegans* in a T-maze assay. Deviation of the response index against zero was tested with a Student's t test (not significant). Error bars represent SEM.

See also Figure S6.

containing J3001 did not reduce feeding but was slightly preferred over the sucrose-only solution (Figure 6H), suggesting that the aversion is due to the presence of geosmin. In line with this observation, adding geosmin (0.1%) also reduced feeding (Figure 6I). The addition of another aversive odor, benzaldehyde (0.1%), had no effect on feeding (Figure 6I). We next wondered whether the feeding aversion is due to olfactory input to the DA2 pathway. Indeed, the reduced feeding stems not from geosmin having an aversive taste but from the activation of ab4B OSNs because silencing input to this pathway—via *Shibire*^{ts}—also fully abolished the geosmin-induced feeding aversion (Figure 6J). Thus, geosmin also functions as an antifeedant, operating via the olfactory system.

Taken together, these findings strongly suggest that the ecological significance of geosmin is to alert flies to the presence of toxic molds and bacteria. The geosmin circuit performs a critical task, providing flies with a reliable and sensitive means of identifying unsuitable hosts.

The Geosmin Detection System Is Conserved across the Genus *Drosophila*

To shed light on the origin and evolution of the geosmin detection system circuit, we next turned to a comparative approach. We tested eight drosophilid species—chosen based on genome availability and phylogenetic and ecological considerations—for their capacity to detect geosmin (Figure S6A). We set out to identify neurons able to detect geosmin via SSR, stimulating with a set of 37 chemically diverse odorants (at 10^{-2} dilution) (Figure S3D). We located OSNs tuned to geosmin in all the screened species except *D. elegans* (Figure 7A). Electroantennogram recordings from this species also showed no response to geosmin (data not shown) and neither does this species respond behaviorally to geosmin in a T-maze assay (Figure 7B). As in *D. melanogaster*, in each of the species responding to geosmin, detection was noted only from a single class of OSNs, which also responded exclusively to geosmin (Figure 7A). The geosmin OSNs we found in the other species may well

Cell

serve the same function that they serve in *D. melanogaster*. The lack of a geosmin detection system in *D. elegans* may be a consequence of the low susceptibility to mold growth of this species' breeding substrate, namely, fresh flowers (Yoshida et al., 2000). Putatively functional orthologs of *Or56a* are also present across the species in which we have complete OR repertoires (Guo and Kim, 2007). We also located intact orthologs of *Or56a* in draft genome assemblies from an additional eight drosophilids (Figure S6B), including *D. biarmipes* and *D. elegans*. The function (if any) of the *Or56a* ortholog in the latter remains unknown. Analysis of selection pressure also showed that the *Or56a* genes are under overall purifying selection (Figure S6C). The response properties of the second neuron residing in these sensilla are much less conserved (Figure S6D). These neurons also do not express orthologous receptors across the examined species. In *D. melanogaster*, the ab4A neurons express Or7a (Hallem et al., 2004), orthologs of which are, however, found only in the subgenus *Sophophora* (Guo and Kim, 2007). Yet, also in species in which we can assume that Or7a underlies the response property, we did note variation in ligand affinity. The function of the ab4A OSNs hence likely reflects species-specific requirements. The striking specificity toward geosmin seen in the olfactory system of *D. melanogaster* is accordingly a basal feature of the genus *Drosophila*, conserved for at least ~40 million years (Russo et al., 1995).

Conclusions

The manner in which flies decode and rely upon geosmin has few, if any, direct parallels. Comparable circuits are essentially found only within the subset of the olfactory nervous system that relays pheromone information. However, also within this context, it is exceedingly rare for animals to rely on just a single chemical to identify a critical resource. Almost all pheromones characterized to date have been complex blends processed by multiple neuronal pathways. Moreover, the specificity toward geosmin shown here surpasses many pheromone-tuned neurons; if presented with enough odorants or with odorants in sufficient concentration, these neurons will also display responses to other substances (Hansson and Stensmyr, 2011).

The closest match to the geosmin pathway is found outside of the regular olfactory system, namely in the detection and processing machinery for the atmospheric trace gas CO_2. Although CO_2 is a fundamentally different chemical from geosmin, the similarity in which these two stimuli are decoded is striking. In flies, the CO_2 circuit forms a functionally segregated pathway that mediates innate avoidance. Input to the CO_2 circuit is likewise fed by sensory neurons exclusively tuned to a single stimulus (Suh et al., 2004). Although organized similarly, the ecological significance of these two circuits seems to differ. Geosmin is used by flies as a universal warning sign for the presence of toxic compounds that are comorbid with geosmin. The evolutionary significance of this circuit is clear: it provides flies with a sensitive and specific means to identify unsuitable hosts. The ecological meaning of CO_2 for *D. melanogaster* is, however, unclear. In fact, it is puzzling why flies would be repelled by CO_2 at all. *D. melanogaster* is highly adapted toward breeding (and feeding) on substrates with high ethanol content. Because CO_2 is a ubiquitous byproduct of alcoholic fermentation, it would make an ideal cue for flies to follow when searching for suitable hosts. Elucidating the role of CO_2 from the point of view of flies and using assays that better reflect the natural setting should be a focus of future studies.

Circuits analogous to the geosmin pathway are a likely feature in the olfactory systems of most, if not all, insects. Although these circuits are probably similar mechanistically and functionally (i.e., selective with regards to input, mediating innate aversion, and abolishing attraction), the identity of the eliciting stimulus will differ, reflecting the demands raised by the taxon-specific ecology.

EXPERIMENTAL PROCEDURES

Fly Stocks

All experiments with WT *D. melanogaster* were carried out with the Canton-S strain. Species other than *D. melanogaster* were obtained from the *Drosophila* species stock center (https://stockcenter.ucsd.edu/info/welcome.php). Transgenic lines were obtained from the Bloomington *Drosophila* stock center (http://flystocks.bio.indiana.edu/), except for *UAS-Or22a*, which was donated by L. Vosshall (The Rockefeller University, New York) and *UAS-Or56-a^{RNAi}*, which was obtained from the Vienna RNAi stock center (http://www.vdrc.at).

Stimuli and Chemical Analysis

All synthetic odorants tested were acquired from commercial sources (Sigma, http://www.sigma-aldrich.com and Bedoukian, http://www.bedoukian.com) and were of the highest purity available. (±)-Geosmin (of >97% purity) was obtained from Sigma. Stimuli preparation and delivery followed Stökl et al. (2010). The headspace collection of volatiles was carried out according to standard procedures. *S. coelicolor* M145 and J3001 strains were gifts from K. Flärdh (Lund University, Sweden) and K. Chater (John Innes Centre, UK), respectively. *P. expansum* was obtained from Centraalbureau voor Schimmelcultures (http://www.cbs.knaw.nl). Microorganisms were kept on strain-specific media (HiMedia, http://www.himedialabs.com), following standard protocols. Mammalian fecal samples were provided by the Leipzig Zoo. For GC stimulation, 1 μl of the odor sample was injected onto a DB5 column (Agilent Technologies, http://www.agilent.com), fitted in an Agilent 6890 GC, equipped with a four-arm effluent splitter (Gerstel, www.gerstel.com), and operated as previously described (Stökl et al., 2010) except for the temperature increase, which was set at 15°C min^{-1}. GC-separated components were introduced into a humidified airstream (200 ml min^{-1}) directed toward the antennae of a mounted fly. Signals from OSNs and FID were recorded simultaneously. GC-MS analysis was performed as previously described (Stökl et al., 2010).

Behavioral Assays

T-maze experiments were conducted as shown in Figure 1B, with flies starved for 4 hr prior to experiments with water provided ad libitum. The response index (RI) was calculated as (O-C)/T, where O is the number of flies in the baited arm, C is the number of flies in the control arm, and T is the total number of flies used in the trial. The resulting index ranges from −1 (complete avoidance) to 1 (complete attraction). Trap assay experiments (Figure S4A) were performed as described in Stökl et al. (2010) with RI calculated as above. The Flywalk experiments followed protocols outlined in Steck et al. (2012) (Figure 5A). Survival was measured for individual flies (males and females, except for tests with J3001, in which only females were examined), which were kept for 5 days (at 23°C) in glass tubes (16 × 100 mm) with metal caps containing 1-week-old cultures of *S. coelicolor* or *P. expansum* grown on yeast-containing media (HiMedia). Oviposition experiments were carried out as shown in Figure 6B. Oviposition index was calculated as (O-C)/(O+C), where O is the number of eggs on a baited plate, and C is the number of

eggs on a control plate. Feeding experiments were conducted as described in Figure 6G. A feeding index was calculated as (O-C)/(O+C), where O is the amount of food consumed from odorous solutions, and C is the amount from control sucrose-only solutions.

Physiology and Morphology

Electroantennogram (EAG) recordings were performed following standard procedures (e.g., Stökl et al., 2010). For SSR measurements, the recording electrode and the reference electrode (inserted into the eye) were positioned under a microscope (Olympus BX51W1; http://www.olympus.com). The recording electrode was positioned by using a motorized, piezo-translator-equipped micromanipulator (Märzhauser DC-3K/PM-10; http://www.marzhauser.com/de/). The signal was amplified (Syntech UN-06, http://www.syntech.nl), digitally converted (Syntech IDAC-4), and finally visualized and analyzed by using Syntech AutoSpike v3.2. CHO cells stably expressing dOrco (Trenzyme, http://www.trenzyme.com) were transiently transfected with dOr56a/pcDNA3.1(−) or dOr33a/pcDNA3.1(−) by using a Roti-Fect transfection kit (Carl Roth, http://www.carlroth.com) as described (Sargsyan et al., 2011). Ca^{2+} imaging of CHO cells was performed as described (Wicher et al., 2008). The functional imaging of odor-induced glomerular activity was conducted as outlined in Stökl et al. (2010). Patch-clamp recording was performed as previously described (Seki et al., 2010), except that in vivo preparation was used, and odor stimuli were given. Preparation followed Stökl et al. (2010), with the exception that the neurolemma was removed to allow the recording electrode access to the cell bodies of the PNs. Spike analysis, immunohistochemistry, laser scanning microscopy, and 3D reconstructions were performed as previously described (Seki et al., 2010).

Statistics and Bioinformatics

Estimates of the selection pressure were done by maximum likelihood as implemented in PAML (Yang, 1997). Additional orthologs of *Or56a* were identified via TBLASTN searches of draft genomes (courtesy of modENCODE/Baylor College of Medicine), downloaded from http://www.ncbi.nlm.nih.gov/bioproject/63477.

SUPPLEMENTAL INFORMATION

Supplemental Information includes six figures and can be found with this article online at http://dx.doi.org/10.1016/j.cell.2012.09.046.

ACKNOWLEDGMENTS

This work was supported by the Max Planck Society, the German Federal Ministry of Education and Research (A.S., V.G., and S.S.), and the Swedish research council Formas (P.G.B.). We wish to thank S. Caron and F. Maderspacher for valuable comments on the manuscript, E. Wheeler for editorial assistance, and R. Stieber, K. Weniger, and S. Kaltofen for technical support. We thank I. Urru for assisting with odor collections, S. Koczsan and J. Rybak for morphological analysis, and M. Thoma for providing help with the Flywalk experiments.

Received: June 7, 2012
Revised: August 28, 2012
Accepted: September 24, 2012
Published: December 6, 2012

REFERENCES

Arndt, C., Cruz, M.C., Cardenas, M.E., and Heitman, J. (1999). Secretion of FK506/FK520 and rapamycin by *Streptomyces* inhibits the growth of competing *Saccharomyces cerevisiae* and *Cryptococcus neoformans*. Microbiology *145*, 1989–2000.

Becher, P.G., Bengtsson, M., Hansson, B.S., and Witzgall, P. (2010). Flying the fly: long-range flight behavior of *Drosophila melanogaster* to attractive odors. J. Chem. Ecol. *36*, 599–607.

Benton, R., Vannice, K.S., Gomez-Diaz, C., and Vosshall, L.B. (2009). Variant ionotropic glutamate receptors as chemosensory receptors in *Drosophila*. Cell *136*, 149–162.

Bhandawat, V., Olsen, S.R., Gouwens, N.W., Schlief, M.L., and Wilson, R.I. (2007). Sensory processing in the *Drosophila* antennal lobe increases reliability and separability of ensemble odor representations. Nat. Neurosci. *10*, 1474–1482.

Castillo, M.-A., Moya, P., Cantín, A., Miranda, M.A., Primo, J., Hernández, E., and Primo-Yúfera, E. (1999). Insecticidal, anti-juvenile hormone, and fungicidal activities of organic extracts from different Penicillium species and their isolated active components. J. Agric. Food Chem. *47*, 2120–2124.

Couto, A., Alenius, M., and Dickson, B.J. (2005). Molecular, anatomical, and functional organization of the *Drosophila* olfactory system. Curr. Biol. *15*, 1535–1547.

Datta, S.R., Vasconcelos, M.L., Ruta, V., Luo, S., Wong, A., Demir, E., Flores, J., Balonze, K., Dickson, B.J., and Axel, R. (2008). The *Drosophila* pheromone cVA activates a sexually dimorphic neural circuit. Nature *452*, 473–477.

de Bruyne, M., Clyne, P.J., and Carlson, J.R. (1999). Odor coding in a model olfactory organ: the Drosophila maxillary palp. J. Neurosci. *19*, 4520–4532.

de Bruyne, M., Foster, K., and Carlson, J.R. (2001). Odor coding in the Drosophila antenna. Neuron *30*, 537–552.

Fishilevich, E., and Vosshall, L.B. (2005). Genetic and functional subdivision of the *Drosophila* antennal lobe. Curr. Biol. *15*, 1548–1553.

Gerber, N.N., and Lechevalier, H.A. (1965). Geosmin, an earthly-smelling substance isolated from actinomycetes. Appl. Microbiol. *13*, 935–938.

Guo, S., and Kim, J. (2007). Molecular evolution of *Drosophila* odorant receptor genes. Mol. Biol. Evol. *24*, 1198–1207.

Gust, B., Challis, G.L., Fowler, K., Kieser, T., and Chater, K.F. (2003). PCR-targeted *Streptomyces* gene replacement identifies a protein domain needed for biosynthesis of the sesquiterpene soil odor geosmin. Proc. Natl. Acad. Sci. USA *100*, 1541–1546.

Hallem, E.A., Ho, M.G., and Carlson, J.R. (2004). The molecular basis of odor coding in the *Drosophila* antenna. Cell *117*, 965–979.

Hamada, F.N., Rosenzweig, M., Kang, K., Pulver, S.R., Ghezzi, A., Jegla, T.J., and Garrity, P.A. (2008). An internal thermal sensor controlling temperature preference in Drosophila. Nature *454*, 217–220.

Hansson, B.S., and Stensmyr, M.C. (2011). Evolution of insect olfaction. Neuron *72*, 698–711.

Ja, W.W., Carvalho, G.B., Mak, E.M., de la Rosa, N.N., Fang, A.Y., Liong, J.C., Brummel, T., and Benzer, S. (2007). Prandiology of Drosophila and the CAFE assay. Proc. Natl. Acad. Sci. USA *104*, 8253–8256.

Jefferis, G.S.X.E., Marin, E.C., Stocker, R.F., and Luo, L. (2001). Target neuron prespecification in the olfactory map of *Drosophila*. Nature *414*, 204–208.

Jones, P.L., Pask, G.M., Rinker, D.C., and Zwiebel, L.J. (2011). Functional agonism of insect odorant receptor ion channels. Proc. Natl. Acad. Sci. USA *108*, 8821–8825.

Jüttner, F., and Watson, S.B. (2007). Biochemical and ecological control of geosmin and 2-methylisoborneol in source waters. Appl. Environ. Microbiol. *73*, 4395–4406.

Karlson, P., and Lüscher, M. (1959). Pheromones': a new term for a class of biologically active substances. Nature *183*, 55–56.

Kitamoto, T. (2001). Conditional modification of behavior in *Drosophila* by targeted expression of a temperature-sensitive shibire allele in defined neurons. J. Neurobiol. *47*, 81–92.

Knaden, M., Strutz, A., Ahsan, J., Sachse, S., and Hansson, B.S. (2012). Spatial representation of odorant valence in an insect brain. Cell Rep. *1*, 392–399.

Kreher, S.A., Mathew, D., Kim, J., and Carlson, J.R. (2008). Translation of sensory input into behavioral output via an olfactory system. Neuron *59*, 110–124.

Kurtovic, A., Widmer, A., and Dickson, B.J. (2007). A single class of olfactory neurons mediates behavioural responses to a *Drosophila* sex pheromone. Nature *446*, 542–546.

Larsson, M.C., Domingos, A.I., Jones, W.D., Chiappe, M.E., Amrein, H., and Vosshall, L.B. (2004). Or83b encodes a broadly expressed odorant receptor essential for *Drosophila* olfaction. Neuron *43*, 703–714.

Mattheis, J.P., and Roberts, R.G. (1992). Identification of geosmin as a volatile metabolite of *Penicillium expansum*. Appl. Environ. Microbiol. *58*, 3170–3172.

Petro-Turza, M. (1987). Flavor of tomato and tomato products. Food Rev. Int. *2*, 309–351.

Russo, C.A.M., Takezaki, N., and Nei, M. (1995). Molecular phylogeny and divergence times of drosophilid species. Mol. Biol. Evol. *12*, 391–404.

Ruta, V., Datta, S.R., Vasconcelos, M.L., Freeland, J., Looger, L.L., and Axel, R. (2010). A dimorphic pheromone circuit in *Drosophila* from sensory input to descending output. Nature *468*, 686–690.

Sargsyan, V., Getahun, M.N., Lavista Llanos, S., Olsson, S., Hansson, B., and Wicher, D. (2011). Phosphorylation via PKC regulates the function of the Drosophila odorant co-receptor. Front. Cell. Neurosci. Published online June 16, 2011. http://dx.doi.org/10.3389/fncel.2011.00005.

Schlief, M.L., and Wilson, R.I. (2007). Olfactory processing and behavior downstream from highly selective receptor neurons. Nat. Neurosci. *10*, 623–630.

Seki, Y., Rybak, J., Wicher, D., Sachse, S., and Hansson, B.S. (2010). Physiological and morphological characterization of local interneurons in the *Drosophila* antennal lobe. J. Neurophysiol. *104*, 1007–1019.

Semmelhack, J.L., and Wang, J.W. (2009). Select *Drosophila* glomeruli mediate innate olfactory attraction and aversion. Nature *459*, 218–223.

Shanbhag, S., Mueller, B., and Steinbrecht, R. (1999). Atlas of olfactory organ of *Drosophila melanogaster* 1. Types, external organization, innervation and distribution of olfactory sensilla. Int. J. Insect Morphol. Embryol. *28*, 377–397.

Steck, K., Veit, D., Grandy, R., Badia, S.B., Mathews, Z., Verschure, P., Hansson, B.S., and Knaden, M. (2012). A high-throughput behavioral paradigm for *Drosophila* olfaction - The Flywalk. Sci. Rep. *2*, 361.

Stocker, R.F., Heimbeck, G., Gendre, N., and de Belle, J.S. (1997). Neuroblast ablation in *Drosophila* P[GAL4] lines reveals origins of olfactory interneurons. J. Neurobiol. *32*, 443–456.

Stökl, J., Strutz, A., Dafni, A., Svatos, A., Doubsky, J., Knaden, M., Sachse, S., Hansson, B.S., and Stensmyr, M.C. (2010). A deceptive pollination system targeting drosophilids through olfactory mimicry of yeast. Curr. Biol. *20*, 1846–1852.

Suh, G.S., Wong, A.M., Hergarden, A.C., Wang, J.W., Simon, A.F., Benzer, S., Axel, R., and Anderson, D.J. (2004). A single population of olfactory sensory neurons mediates an innate avoidance behaviour in *Drosophila*. Nature *431*, 854–859.

Tian, L., Hires, S.A., Mao, T., Huber, D., Chiappe, M.E., Chalasani, S.H., Petreanu, L., Akerboom, J., McKinney, S.A., Schreiter, E.R., et al. (2009). Imaging neural activity in worms, flies and mice with improved GCaMP calcium indicators. Nat. Methods *6*, 875–881.

Tinbergen, N. (1951). The Study of Instinct (Oxford: Clarendon Press).

van der Goes van Naters, W., and Carlson, J.R. (2007). Receptors and neurons for fly odors in *Drosophila*. Curr. Biol. *17*, 606–612.

Vosshall, L.B., and Stocker, R.F. (2007). Molecular architecture of smell and taste in *Drosophila*. Annu. Rev. Neurosci. *30*, 505–533.

Wicher, D., Schäfer, R., Bauernfeind, R., Stensmyr, M.C., Heller, R., Heinemann, S.H., and Hansson, B.S. (2008). *Drosophila* odorant receptors are both ligand-gated and cyclic-nucleotide-activated cation channels. Nature *452*, 1007–1011.

Wilson, R.I., Turner, G.C., and Laurent, G. (2004). Transformation of olfactory representations in the *Drosophila* antennal lobe. Science *303*, 366–370.

Yang, Z.H. (1997). PAML: a program package for phylogenetic analysis by maximum likelihood. Comput. Appl. Biosci. *13*, 555–556.

Yao, C.A., Ignell, R., and Carlson, J.R. (2005). Chemosensory coding by neurons in the coeloconic sensilla of the *Drosophila* antenna. J. Neurosci. *25*, 8359–8367.

Yoshida, T., Chen, H.W., Toda, M.J., Kimura, M.T., and Davis, A.J. (2000). New host plants and host plant use for *Drosophila elegans* Bock and Wheeler, 1972. Drosoph. Inf. Serv. *83*, 18–21.

Young, W.F., Horth, H., Crane, R., Ogden, T., and Arnott, M. (1996). Taste and odour threshold concentrations of potential potable water contaminants. Water Res. *30*, 331–340.

Cell

Supplemental Information

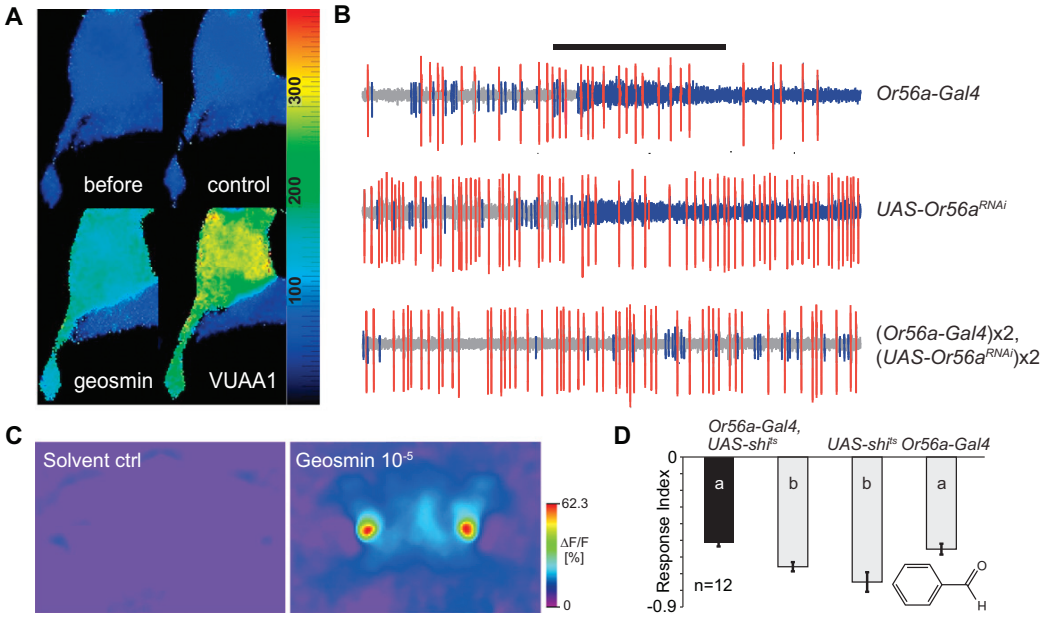

Figure S1. Molecular Function of Or56a, Related to Figure 2

(A) Color coded $[Ca^{2+}]_i$ (scaling bar, nM) in a CHO cell expressing *Or56a* and *Orco* before and 10 s after application of saline (control), geosmin (50 μM) and VUAA1 (100 μM).

(B) Representative SSR traces from control ab4 sensilla (top two traces) and from an ab4 sensillum with reduced levels of Or56a (bottom trace). Expression of RNAi directed against Or56a in ab4B OSNs (blue spikes) abolishes the response to geosmin (10^{-3}). Duration of the stimulus delivery (0.5 s) is marked by the black bar.

(C) Raw images from the same recording as in Figure 2G.

(D) Silencing ab4B neurons, via *Shibire^{ts}*, does not abolish aversion toward benzaldehyde (10^{-2} dilution). Significant differences are denoted by letters (ANOVA followed by Tukey's test; $p < 0.05$). Error bars represent SEM.

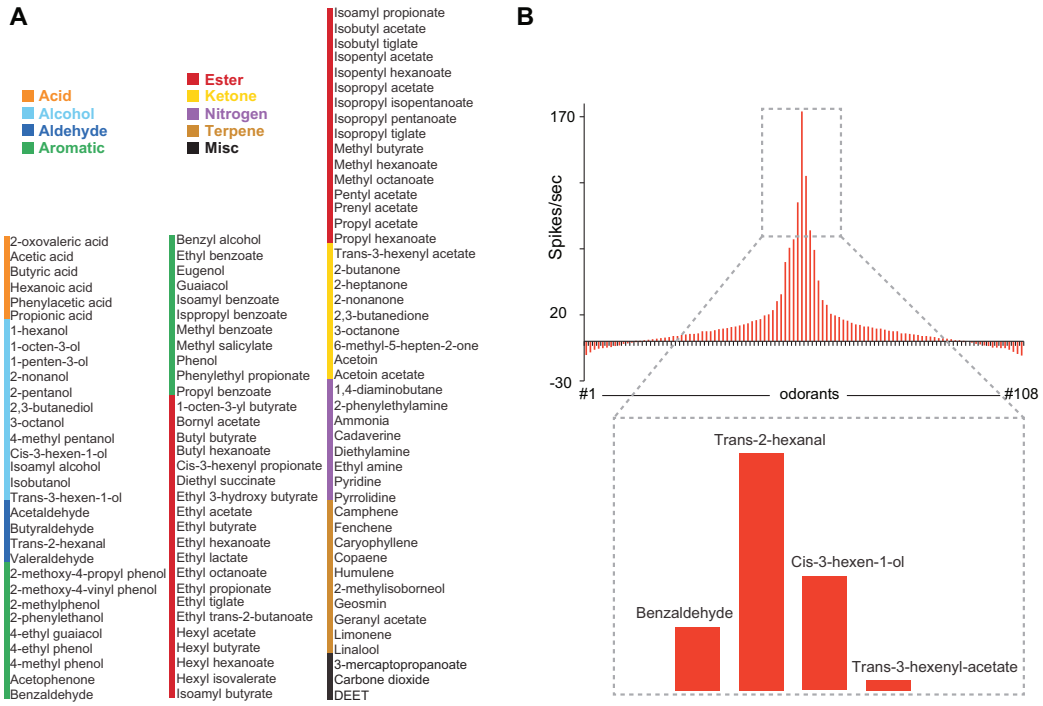

Figure S2. Screened Synthetic Volatiles and Properties of the ab4A Neuron, Related to Figure 3

(A) Screened odorants.

(B) Tuning curve for the ab4A neuron type based on a screen of 103 synthetic substances.

Cell

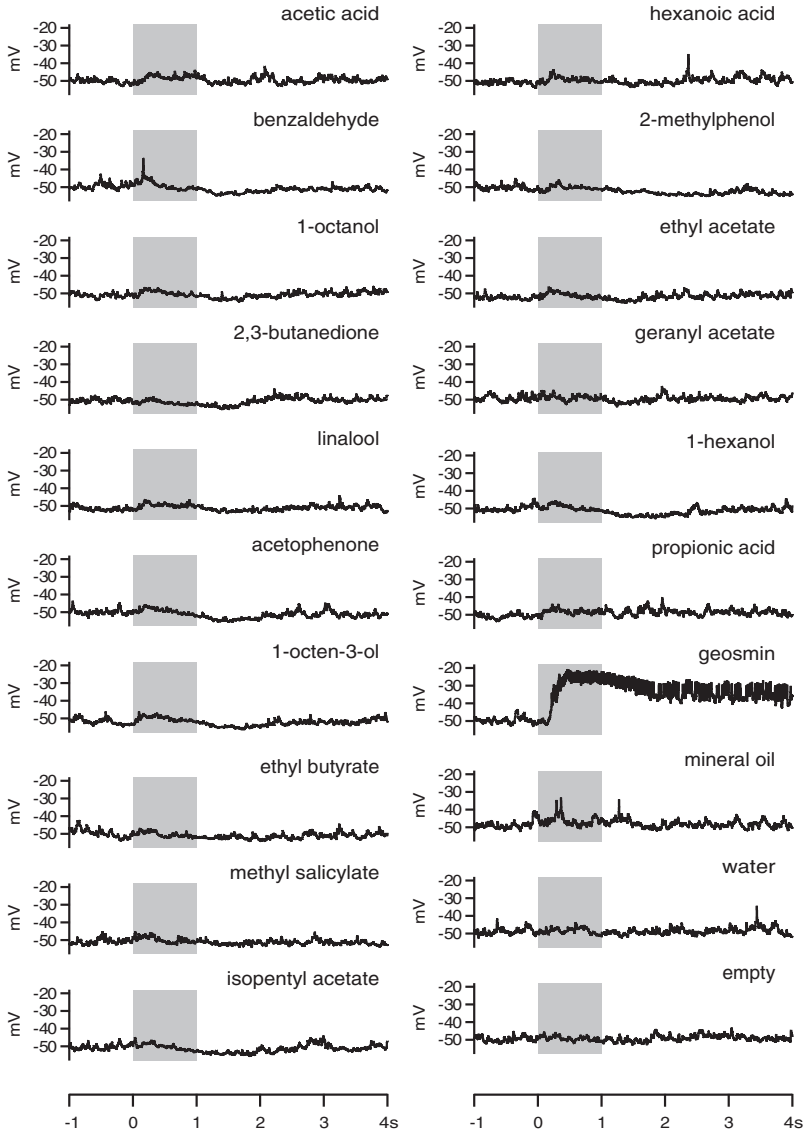

Figure S3. Spike Traces from a DA2 Projection Neuron, Related to Figure 4

Spike traces from a DA2 PN following odor stimulation. Only geosmin elicits any response.

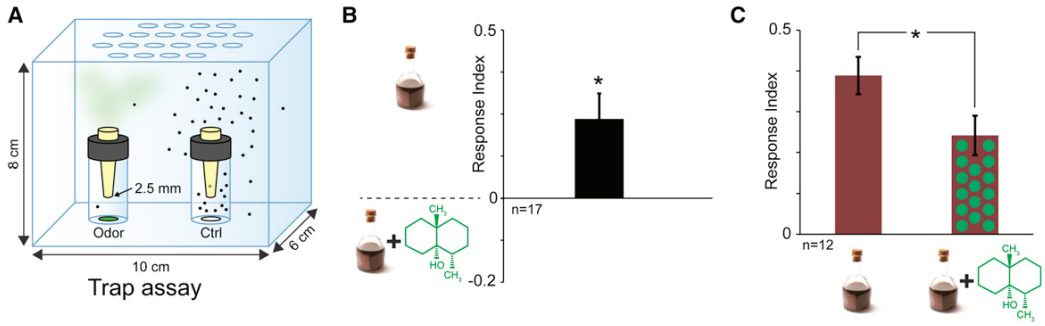

Figure S4. T-Maze and Trap Assay Choice Experiments with a Vinegar and Geosmin Mix, Related to Figure 5

(A) Schematic drawing of the trap assay (Larsson et al., 2004) used in panel (B). For each trial, ~50 flies were placed inside the test boxes. Number of flies in and outside traps was then counted after 24 hr (for further details, see Stökl et al. [2010] and Knaden et al. [2012]).

(B) Response index of wt flies given a choice between balsamic vinegar and balsamic vinegar additionally containing 10^{-3} geosmin in the trap assay. Deviation of the response index against zero was tested with a Student's t test ($p < 0.05$). Error bar represent SEM.

(C) Response indices of wt flies to balsamic vinegar and balsamic vinegar containing geosmin (10^{-3}) in the T-maze assay. Star denotes significant difference (Student's t test $p < 0.05$). Error bars represent SEM.

Cell

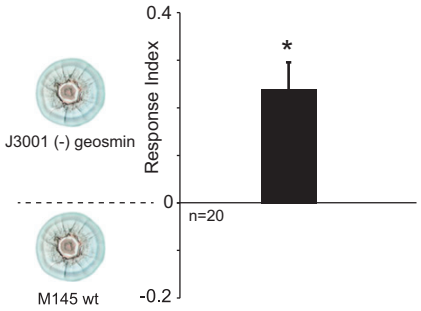

Figure S5. Trap Assay Two-Choice Experiment with WT and Mutant *S. coelicolor*, Related to Figure 6

Response index of flies given a choice between wt (M145) *S. coelicolor* and the J3001 strain in the olfactory choice trap assay (Figure S4A). Star denotes significant difference (Student's t test $p < 0.05$). Error bar represent SEM.

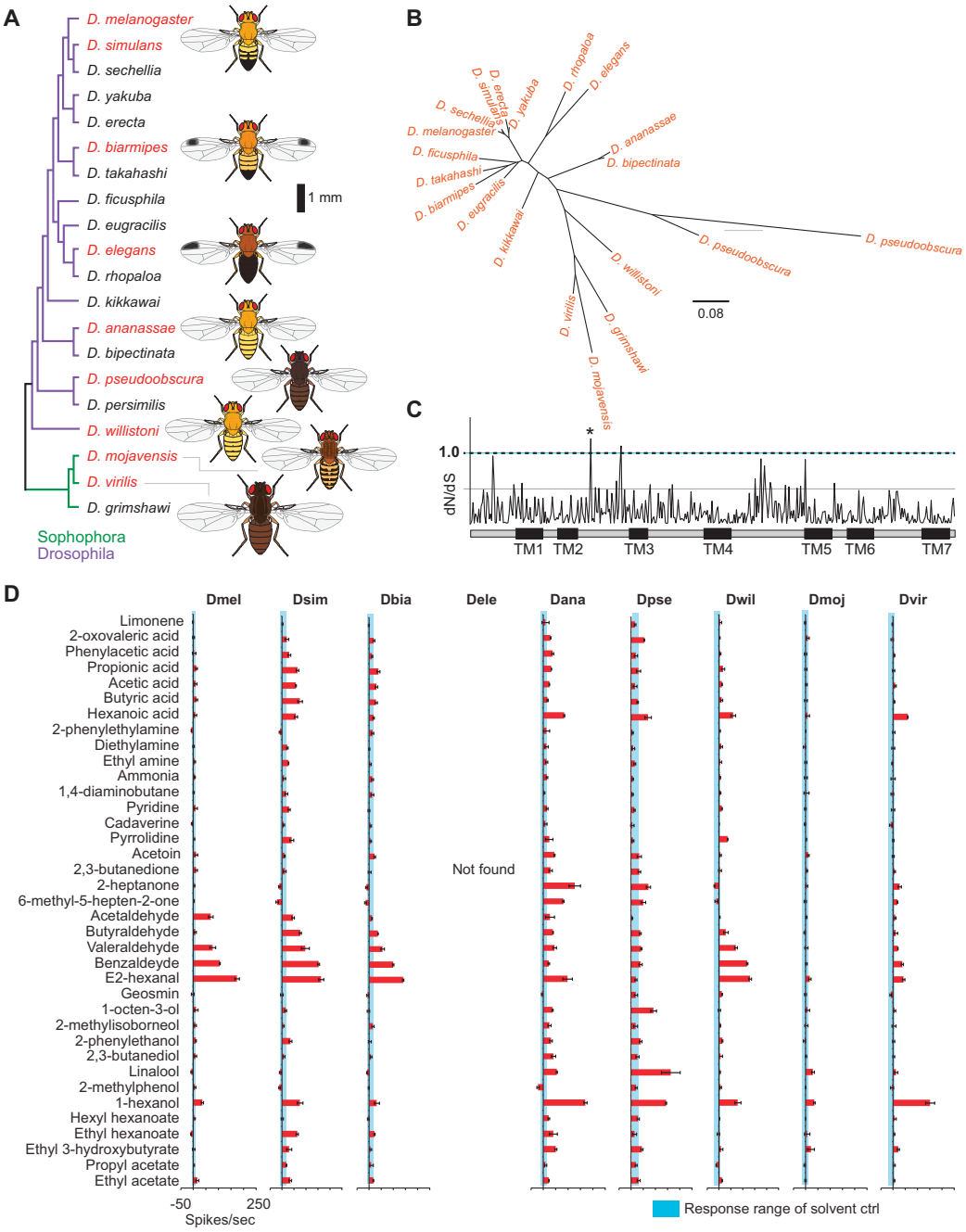

Figure S6. Molecular and Physiological Properties of the ab4 Type Sensillum across Related Drosophilids, Related to Figure 7

(A) Phylogenetic relationship of the examined species.

(B) Phylogenetic tree of *Or56a* orthologs from 19 species. The tree was constructed with RAxML from a Muscle alignment. Scale bar represents number of substitutions per site.

(C) Estimation of the selection pressure acting upon *Or56a*. Plot shows dN/dS ratios (obtained through PAML, model M8) for all codons, here plotted on the sequence of *D. melanogaster*. TM1-7 indicates putative locations of transmembrane domains (estimated with HMMTOP/TMHMM). Star denotes site under significant positive selection (Bayes Empirical Bayes).

(D) Response profile of neurons (n = 3) paired with the geosmin responsive neurons shown in Figure 6. Error bars represent SEM.

Chapter II

The CCHamide 1 receptor modulates sensory perception and olfactory behavior in starved *Drosophila*

Abu Farhan, Jyotasana Gulati, Ewald Große-Wilde, Heiko Vogel, Bill S. Hansson * and Markus Knaden*

**These authors contributed equally to the work.*

Scientific Reports, Accepted September 4, 2013

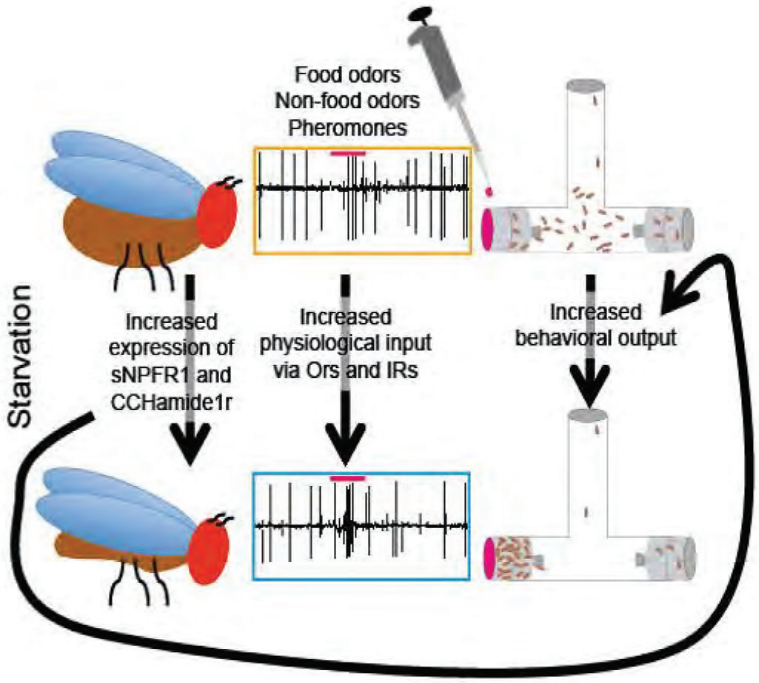

SCIENTIFIC REPORTS

Chapter II

OPEN

SUBJECT AREAS:
OLFACTORY SYSTEM
NEUROSCIENCE
OLFACTORY RECEPTORS

Received
9 July 2013

Accepted
4 September 2013

Published
26 September 2013

Correspondence and requests for materials should be addressed to M.K. (mknaden@ice.mpg.de) or B.S.H. (hansson@ice.mpg.de)

* These authors contributed equally to this work.

The CCHamide 1 receptor modulates sensory perception and olfactory behavior in starved *Drosophila*

Abu Farhan[1], Jyotasana Gulati[2], Ewald Groβe-Wilde[1], Heiko Vogel[3], Bill S. Hansson[1]* & Markus Knaden[1]*

[1]Department of Evolutionary Neuroethology, Max Planck Institute for Chemical Ecology, [2]Department of Molecular Ecology, Max Planck Institute for Chemical Ecology, [3]Department of Entomology, Max Planck Institute for Chemical Ecology, Hans-Knöll-Str. 8, 07749 Jena, Germany.

The olfactory response of the vinegar fly *Drosophila melanogaster* to food odor is modulated by starvation. Here we show that this modulation is not restricted to food odors and their detecting sensory neurons but rather increases the behavioral response to odors as different as food odors, repellents and pheromones. The increased behavioral responsiveness is paralleled by an increased physiological sensitivity of sensory neurons regardless whether they express olfactory or ionotropic receptors and regardless whether they are housed in basiconic, coeloconic, or trichoid sensilla. Silencing several genes that become up-regulated under starvation confirmed the involvement of the short neuropeptide f receptor in the starvation effect. In addition it revealed that the CCHamide-1 receptor is another important factor governing starvation-induced olfactory modifications.

Modulation and plasticity are key features of all organisms for adapting to e.g. a changing environment, stress, and food availability. Examples are blood-feeding insects, which after a blood meal switch their olfactory preference from host odors to odors specific for oviposition sites[1–3]. Accompanying this behavioral switch, receptors sensitive to lactic acid, a host-attractant substance, become desensitized[1], while receptors sensitive to odors specific for oviposition sites become more sensitive[1]. Similarly in the African cotton leaf worm *Spodoptera littoralis*, the sensitivity of sensory neurons detecting feeding-related flower odors is down regulated upon mating, while the sensitivity of neurons detecting oviposition-related green leaf odors is up regulated[4]. We used the olfactory circuit of a well-established model, *Drosophila*[5–8], to investigate whether feeding status modulates the flies' physiological and behavioral responses to odors. The main peripheral part of the olfactory circuit of *Drosophila* is housed in sensilla on the third antennal segment, where volatiles are detected via ca. 1200 olfactory sensory neurons (OSN). The OSNs are equipped with one of 62 olfactory receptor types and are found in stereotyped combinations of one-to-four OSNs in three morphological types of sensilla[8]. Root and coworkers showed that starvation increases the behavioral response and physiological sensitivity of *Drosophila* to the attractive food blend of apple cider and that this starvation-induced modulation is mainly governed by increased expression of the sNPF receptor in OSNs expressing the olfactory receptor OR42b[9]. Here, we illustrate that the starvation effect is neither restricted to these OSNs nor to food odors. It rather occurs in different OSN types, which express different olfactory receptors or even an ionotropic receptor. We furthermore confirm the role of the short neuropeptide f receptor (sNPF) and additionally establish the role of the CCHamide-1 receptor (CCHamide1r) in governing the starvation-induced modulation of fly olfactory responses.

Starvation affects the behavior towards stimuli as distinct as food odorants, repellents and a pheromone. Hence, starved flies found to be tuned not only to locate potential food sources from long distance, but also to evaluate the food quality and the presence of conspecifics efficiently.

Results

Starvation-induced changes in behavior. We tested female flies in a T-maze paradigm (Fig. 1A) with the food odorants ethyl acetate and phenyl acetaldehyde. The odorants were attractive to fed flies only at medium concentrations and became repellent at high concentrations. However, starved flies were more strongly attracted than fed flies to all concentrations and were not repelled by high concentrations (Fig. 1B + C). We found an increased behavioral response to ethyl acetate already after few hours of starvation, but the effect increased with prolonged starvation time (Fig. S1). Contrary to these two odorants, 2,3-butanedione, another

SCIENTIFIC REPORTS SREP-13-03157-T.3d 12/9/13 14:23:35

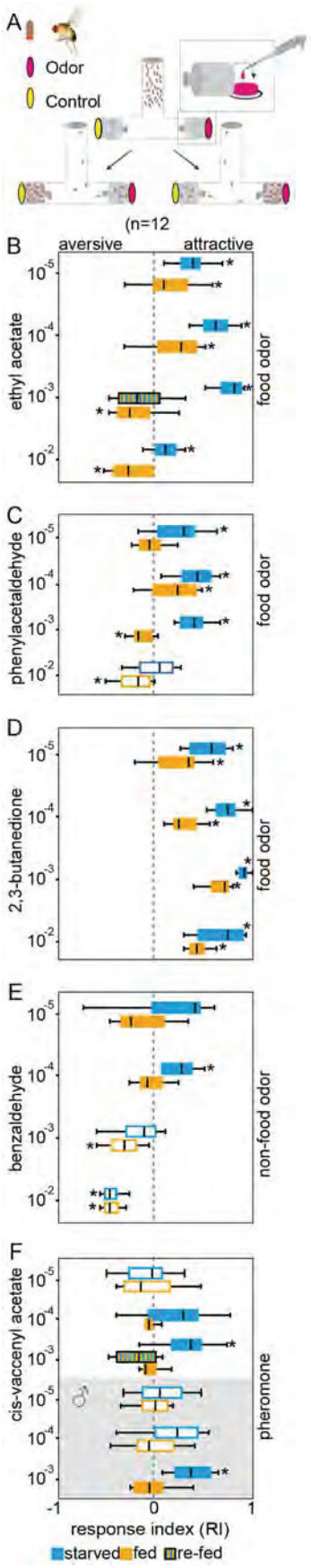

Figure 1 | Behavioral responses of starved and fed flies. A. T-maze paradigm. 30 female flies were introduced into the center arm. Traps at the end of the T-arms were filled with an odor (red) or with solvent only (yellow). After 40 min flies in each trap and flies that did not enter any trap were counted and the response index calculated as RI = (#flies in odor trap – #flies in solvent trap)/#total flies. B–F. Fly choice in the T-maze tested with different concentrations of 5 odors. Grey shaded area in F, experiment performed with male flies. Box plots give the median (black bold line), 2nd and 3rd quartiles (box), and minima and maxima (whiskers) of twelve replicates. Filled boxes represent experiments with significant differences between starved and fed flies (Mann-Whitney-U test, $p < 0.05$); asterisks depict experiments where the RI values differed significantly from 0 (i.e. the odor was attractive or repellent).

food-related odor, attracted fed flies in low as well as in high concentrations. However, again starved flies were significantly more attracted to all concentrations tested (Fig. 1D).

In order to test whether this increased behavioral responsiveness of starved flies was restricted to food odors only, we repeated the experiments with benzaldehyde, a well known repellent for *Drosophila*[10,11]. The fed flies did not respond to this odorant at low concentrations, while the starved flies became attracted to it. However, at high concentrations benzaldehyde repelled both starved and fed flies (Fig. 1E). Finally we tested cis-vaccenyl acetate (*c*VA), a pheromone that is involved in aggregation[12], aggression[13], and mating behavior[14]. While *c*VA was neutral to fed flies at all concentrations, it was attractive to starved flies at high concentrations (Fig. 1F). Since *c*VA regulates aggression and mating in male *Drosophila*, we additionally tested males. Like females, males became attracted to *c*VA only when they were starved before (Fig. 1F). To sum up, regardless which odors we tested we found an increased responsiveness in starved flies. Future studies will reveal whether this increased responsiveness of starved flies can also be observed towards odors that are sensed by sensory neurons expressing only one specific receptor type and are further processed via labeled lines like described for CO_2[15,16] and geosmin[17].

Starvation-induced changes in peripheral olfactory sensitivity. We next asked whether the increased behavioral responsiveness observed in starved flies comes along with a change in physiological sensitivity. We performed single sensillum recordings (Fig. 2A) from OSNs expressing the main target receptors of the same set of odors that was used in the behavioral experiments. All odors evoked stronger physiological responses in starved flies with the effects being most pronounced at low odor concentrations (Fig. 2B–F). In addition to increased spike rates after stimulation, we found increased spontaneous firing rates (Fig. 3A and B) and reduced response latencies in starved flies (Fig. 3C and Fig. S2). Again, the starvation effect was found not restricted to the detection of food odors (ethyl acetate and 2,3-butanedione both mainly targeting Or59b in the basiconic sensilla ab2, and phenyl acetaldehyde mainly targeting Ir84a in the coeloconic sensilla ac4, Fig. 2B–D). It also occurred in OSNs detecting non-food odors like benzaldehyde (Or7a in the basiconic sensilla ab4, Fig. 2E) and the pheromone *c*VA (Or67d in the trichoid sensilla at1, Fig. 2F). Therefore starvation affected all sensillum types and both receptor types – olfactory receptors (OR) as well as ionotropic receptors (IR). It should be pointed out here, that changes in the peripheral sensitivity might not necessarily be sufficient to explain the observed behavioral changes. It might well be, but was not the subject of this study, that also higher-order neurons involved in further processing the olfactory information and – hence – in governing the olfactory response might be affected as well.

Interestingly, when starved flies were exposed to sucrose, the starvation effect was abolished and one hour after feeding, both the behavior of the flies (Fig. 1B and F) and their sensitivity (Fig. 2B and F) resembled that of fed flies.

Genes involved in the starvation effect. To investigate the molecular basis of the starvation process, we compared gene expression at the

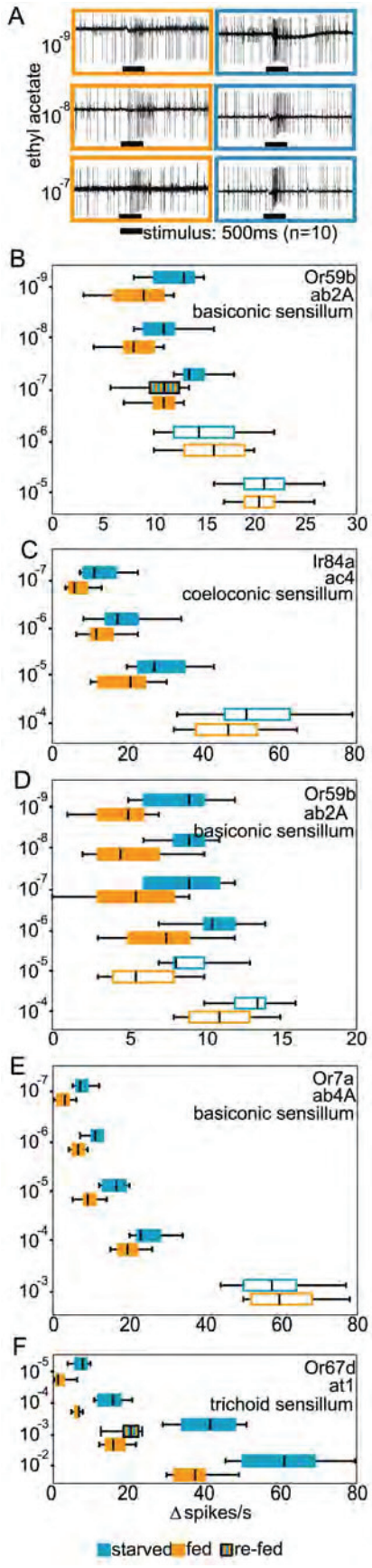

Figure 2 | Physiological responses of starved and fed flies. A. Example spike traces from an ab2 sensillum stimulated with different concentrations of ethyl acetate. B–F. OSN changes in spike frequencies. (spike frequency during 1 s after stimulus onset) minus (spontaneous spike frequency during 1 s before stimulus onset) when stimulated with different concentrations of the same odors as in B–F. Single sensillum recordings from starved and fed flies. Box plots summarize the results recorded from each 10 sensilla. OSN and sensillum types are given in the top right corner of each plot. Orange: fed flies; blue: starved flies; striped: re-fed flies. In all cases re-fed flies were significantly different from starved flies but not from fed flies.

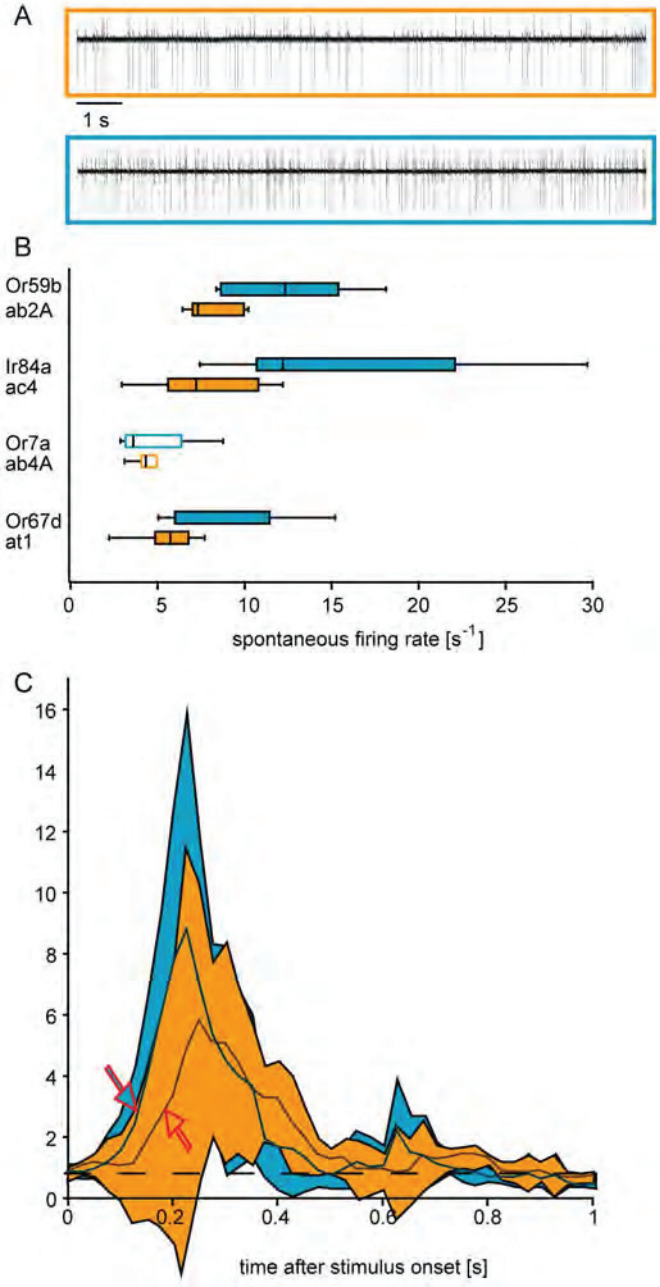

Figure 3 | Spontaneous firing rate and response latencies of OSNs in starved and fed flies. A. Examples of spontaneous spike traces from OSNs housed in sensillum ab2. B. Starvation-induced changes in spike frequencies of different OSNs. C. Mean normalized response profile of OSNs in 10 ab2A sensilla to 500 ms pulses of ethyl acetate (diluted 10^{-7} in paraffin oil). Average firing rate before the stimulus was set as 1. Firing rates after the stimulus were normalized accordingly. Arrows indicate where the response becomes significantly higher than before the stimulus (Wilcoxon signed ranks test, $N = 10$, $p < 0.05$, Lines, average response; shaded areas, standard deviation).

level of the antenna and the brain for fed and starved flies. After 28 hours of starvation, the expression of 209 genes in the antennae and of 999 genes in the brain was up regulated, while the expression of 47 genes in the antennae and 372 genes in the brain was down regulated (Table S1, FDR = 0.05). We found e.g. the expression of the short neuropeptide F 2.3times and that of the neuropeptide allatostatine 3.6times upregulated within the antenna, while the expression of CCHamide was 2.5times upregulated in the brain. We next focused on some of the genes that are known to be involved in the synthesis of these neuropeptides (allatostatine) or of the corresponding neuropeptide receptors (sNPFR1, CCHamide1r and AlstR).

We silenced these genes at the level of the OR-expressing OSNs by using UAS-*RNAi* and Orco-Gal4 driver lines. We then tested if the flies still exhibited a starvation-induced increased behavioral responsiveness despite the silenced target genes (Fig. 4A–C). When we tested the behavior of starved flies to ethyl acetate (mainly detected by OR59b) silencing allatostatine, its corresponding receptor, or the sNPF receptor did not affect the starvation effect. Only silencing the CCHamide1 receptor resulted in an abolished starvation effect, suggesting a major role of CCHamide1 or its corresponding receptor in starvation-induced modulation in OR59b-expressing OSNs (Fig. 2A). Although sNPFR1 has been reported to govern the starvation effect (Root et al. 2011), sNPF seems not to be expressed in OR59b[18]. Therefore, we did not expect that the silencing of the sNPF receptor would affect the starvation-induced increased response to an odorant sensed by this neuron. The picture changed when we tested starved flies with cis-vaccenyl acetate (Fig. 2B). This compound is mainly detected by OSNs carrying OR67d, the neurons that have been shown to express sNPF[18]. As expected, silencing the sNPF receptor abolished the starvation-induced increased response to cVA, which confirms the involvement of this receptor in the starvation-induced modulation as shown before[9]. Again silencing the CCHamide1 receptor reduced the starvation effect, emphasizing the important role of this receptor in governing starvation-induced modulation. As expected, silencing the sNPF or the CCHamide1 receptor in OR-expressing OSNs did not affect the flies' responses to phenylacetaldehyde (Fig. 4C), which is mainly detected by OSNs expressing ionotropic receptors[19]. Only when we used CCHamid1r-mutant flies (i.e. flies that lacked the receptor not only in the olfactory but also in the ionotropic receptors), the starvation effect towards the IR-detected odorant phenylacetaldehyde was abolished (Fig. 4C).

Discussion

Drosophila melanogaster uses olfaction to find and evaluate food sources[20]. Starved flies have been shown to be more attracted and more sensitive to the smell of cider vinegar[9]. Root and coworkers showed that the starvation-induced up-regulated neuropeptide receptor sNPFR1 in some of the OSNs activated to vinegar odor is responsible for the increased physiological and behavioral response to this odor.

Our finding that starved flies respond stronger to all tested odorants (Fig. 1) suggests that this starvation-induced modulation of olfaction is not restricted to food odors but is found also in the perception of odors that are significant in other contexts, like the repellent benzaldehyde or the pheromone cis-vaccenyl aldehyde. Following the finding of Root and coworkers that the expression of sNPFR1 is necessary and sufficient to explain the starvation-induced modulation, we expected that the behavioral response towards odorants that are mainly detected by neurons that do not express sNPF should not exhibit any starvation-induced modulation.

However, the behavioral response was up-regulated upon starvation not only for key ligands of the sNPF expressing neuron (cis-vaccenyl aldehyde targeting OR67d), but also for ligands of neurons which do not express sNPF (Carlsson et al. 2010; ethyl acetate and 2,3 butanedione, both targeting OR59b; benzaldehyde targeting OR7a; phenylacetaldehyde targeting IR84a). Hence, starved flies respond stronger to all odorants, regardless whether they are mainly detected by sNPFR1-expressing neurons or not. Therefore, beside the sNPF receptor, additional factors could be involved in the starvation-induced modulation. However most odorants are sensed by neurons expressing different receptor types (e.g. ethyl acetate is one of the main ligands of OR59b but is also detected by OSNs expressing 22a, 43b, and 47a[6]. Therefore, it cannot be ruled out that one of the

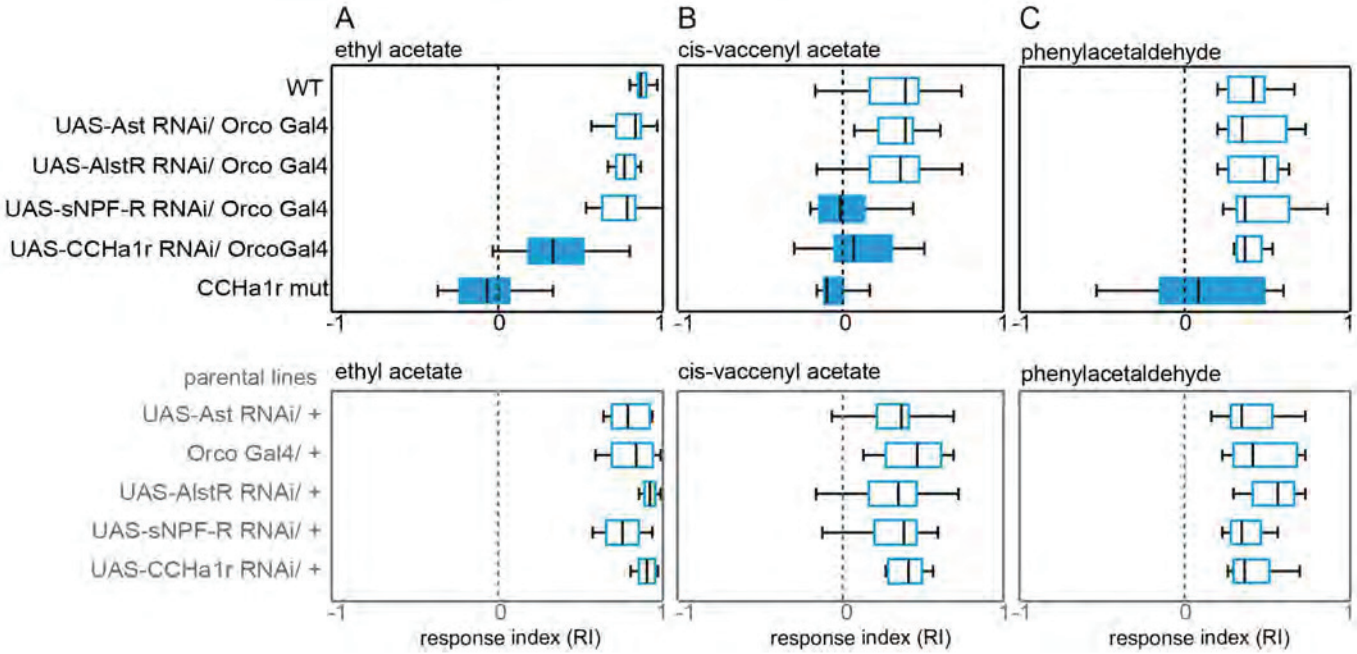

Figure 4 | Impact of neuropeptides and their corresponding receptors on the starvation-induced modulation. A–C. Upper panels, behavioral responses of starved flies with silenced genes for neuropeptides or corresponding receptors to ethyl acetate (A), cis-vaccenyl acetate (B), and phenylacetaldehyde (C). Lower panels, olfactory behavioral responses of parental lines. For T-maze paradigm and explanation of box plot representation see Fig. 1. Filled boxes represent experiments with significant differences between mutant and wild type flies (one way ANOVA followed by tukey test, $p < 0.05$).

neuron types activated by ethyl acetate expresses the sNPF receptor and hence, governs the up-regulated behavioral response.

By performing single sensillum recordings with the same set of odorants, that was used for the behavioral experiments, we found that starved flies exhibit an increased physiological response to low concentrated odorants (Fig. 2). Root and coworkers showed that in *Drosophila* the olfactory-driven activity of some OSNs and the corresponding projection neurons increases upon starvation[9], while Farhadian and coworkers did not find any starvation-induced sensitization when recording from OSN that expressed OR47a[21]. Our data are in accordance with Root and coworkers but are contradictory to those of Farhadian and coworkers. However, one should bear in mind that we found the strongest difference in OSN responses of fed and starved flies when we tested odorants at low concentrations that were by 2–3 orders of magnitude lower than the concentrations used by Farhadian[21]. Therefore, we cannot say whether the conflicting results are caused by the different OSN types both studies recorded from or are due to the starvation effect becoming significant only at very low stimulus concentrations.

Biogenic amines have been shown to regulate a wide range of behavior including foraging[22], circadian rhythms[23] and sexual interactions[24]. In *Drosophila* it has been shown that sNPFR is involved in up-regulation of olfactory sensitivity due to starvation[9]. However, only about 25% of the *Drosophila* OSNs seem to express the sNPF receptor[25]. By silencing several genes that are known to be involved in the synthesis of neuropeptides or neuropeptide receptors, we could confirm the involvement of the sNPF receptor (Fig. 4). However, our observations indicate that starvation-induced modulation is not restricted to the OSNs expressing this gene. In addition the CCHamide1 receptor is involved in this modulation also (Figure 4). This explains, why OSNs – regardless whether they express ionotropic or olfactory receptors and regardless in which sensillum type they are housed – become sensitized upon starvation. This rather globally working starvation effect might increase the efficiency of starved flies to localize and evaluate food sources.

Methods

Flies. We used flies of the following lines: CantonS, UAS-s-NPFR *RNAi*, UAS-AST *RNAi*, UAS-AST-R *RNAi*, UAS-CCHa1r *RNAi*, Or83b GAL4, Mi{ET1}CCHa1^{MB11962} (Bloomington).

Fly rearing and maintenance. Flies were maintained at 25°C, 70% relative humidity under 12L : 12D in standard food vials (25 mm × 95 mm) containing standard cornmeal. Newly hatched flies (0–12 hrs old) were transferred to an odor-reduced medium[26] and from now on were kept at 20°C. The flies were transferred to fresh medium every day in order to reduce pre-experimental olfactory experience. At the age of 4 days, female flies were collected and starved for 28 hours in a glass vial containing a moist bed of tissue paper (from now on referred to as "starved flies"). A second group of flies was kept under the same conditions but with access to 3% sucrose ("fed flies"). A third group of flies was starved for 27 hours and had access to 3% sucrose during the subsequent hour ("re-fed flies").

T-maze paradigm. Experiments were performed with a T-maze in which flies could enter either a trap that contained an odor or a control trap filled with solvent (Fig. 1A, for a detailed description see[17]). Thirty female flies (unless stated otherwise) were introduced to the maze and their position was scored after 40 minutes. We calculated the olfactory response index (RI) as described in legend of Fig. 1. The index could range from −1 (complete avoidance) to 1 (complete attraction). A value of 0 characterizes no response, i.e. the odor is not detected or is neutral. Each experiment was repeated 12 times and the RIs of starved and fed flies were compared with the Mann-Whitney-U test and tested against 0 (no response) by the Wilcoxon-rank-sum test.

Single sensillum recordings. We performed single sensillum recordings from basiconic, coeloconic, and trichoid sensilla as described by[7]. Odor stimulation was performed as described by[18] with slight modifications. A glass tube ended 15 mm from the antenna and supplied humidified air (9 ml/min). Odors were diluted in paraffin oil. In order to avoid cross-contamination, we used disposable pasture pipettes to add the odor stimuli (head space of 10 µl of the diluted odor on filter paper, duration 500 ms, controlled via Syntech CS55). All chemicals used in this study were delivered by Sigma-Aldrich (Stenheim, Germany) with the highest purity available (90–99%). Spike frequencies were analyzed for one second before and after the stimulation onset with the software Auto Spike v 3.2 (Syntech, Hilversum, The Netherlands). The response was calculated as spike frequency after stimulation – spike frequency before stimulation. The identification of different OSNs in a single sensillum was performed by spike sorting, i.e. based on differences in the spike amplitudes.

RNA extraction and microarray analysis. Both for starved and fed flies RNA extraction was done four times each with 100 Antennae and 50 brains from 50 flies using the Qiagen RNA extraction kit. RNA concentration was measured photometrically with a NanoDrop ND-1000 and RNA quality and integrity was controlled with the Agilent 2100 Bioanalyzer. RNA was labeled with cyanine 3-CTP dye using the Low RNA Input Linear Amplification kit according to manufacturer instructions (Agilent Technologies). Labelled amplified cRNA samples were analyzed on a Nanodrop spectrophotometer using the microarray function and used for microarray hybridization at 65°C for 17 hours. Slides were washed, treated in stabilization and drying solution, scanned with the Agilent Microarray Scanner, and data was extracted with Agilent Feature Extraction software version 9.1. The resulting gene expression profiles were analyzed using GeneSpring GX software (Silicon Genetics, Redwood City, CA). Raw intensities were normalized using the 75th percentile value and log2 and baseline transformed prior statistical analysis. We performed the implemented t-test for comparing two samples at a time and corrected the p-value for multiple testing. The microarray data with each probe name was deposited in the NCBI GEO database (accession number GSE48077).

1. Davis, E. E. Regulation of sensitivity in the peripheral chemoreceptor systems for host-seeking behavior by a hemolymph-borne factor in *Aedes aegypti*. *J. Insect Physiol.* **30**, 179–183 (1984).
2. Siju, K. P., Hill, S. R., Hansson, B. S. & Ignell, R. Influence of blood meal on the responsiveness of olfactory receptor neurons in antennal sensilla trichodea of the yellow fever mosquito, *Aedes aegypti*. *J. Insect Physiol.* **56**, 659–665 (2010).
3. Denotter, C. J., Tchicaya, T. & Schutte, A. M. Effects of age, sex and hunger on the antennal olfactory sensitivity of tsetse-flies. *Physiol. Entomol.* **16**, 173–182 (1991).
4. Saveer, A. M. *et al*. Floral to green: mating switches moth olfactory coding and preference. *P. Roy. Soc. B-Biol. Sci.* **279**, 2314–2322 (2012).
5. Vosshall, L. B., Wong, A. M. & Axel, R. An olfactory sensory map in the fly brain. *Cell* **102**, 147–159 (2000).
6. Hallem, E. A. & Carlson, J. R. Coding of odors by a receptor repertoire. *Cell* **125**, 143–160 (2006).
7. de Bruyne, M., Foster, K. & Carlson, J. R. Odor coding in the *Drosophila* antenna. *Neuron* **30**, 537–552 (2001).
8. Hansson, B. S., Knaden, M., Sachse, S., Stensmyr, M. C. & Wicher, D. Towards plant-odor-related olfactory neuroethology in *Drosophila*. *Chemoecology* **20**, 51–61 (2010).
9. Root, C. M., Ko, K. I., Jafari, A. & Wang, J. W. Presynaptic facilitation by neuropeptide signaling mediates odor-driven food search. *Cell* **145**, 133–144 (2011).
10. Kreher, S. A., Mathew, D., Kim, J. & Carlson, J. R. Translation of sensory input into behavioral output via an olfactory system. *Neuron* **59**, 110–124 (2008).
11. Knaden, M., Strutz, A., Ahsan, J., Sachse, S. & Hansson, B. S. Spatial Representation of odorant valence in an insect brain. *Cell Rep.* **1**, 392–399 (2012).
12. Bartelt, R. J., Schaner, A. M. & Jackson, L. L. Cis- vaccenyl acetate as an aggregation pheromone in *Drosophla melanogaster*. *J. Chem. Ecol.* **11**, 1747–1756 (1985).
13. Wang, L. M. & Anderson, D. J. Identification of an aggression-promoting pheromone and its receptor neurons in *Drosophila*. *Nature* **463**, 227–231 (2010).
14. Kurtovic, A., Widmer, A. & Dickson, B. J. A single class of olfactory neurons mediates behavioural responses to a *Drosophila* sex pheromone. *Nature* **446**, 542–546 (2007).
15. Suh, G. S. B. *et al*. A single population of olfactory sensory neurons mediates an innate avoidance behaviour in *Drosophila*. *Nature* **431**, 854–859 (2004).
16. Sachse, S. *et al*. Activity-dependent plasticity in an olfactory circuit. *Neuron* **56**, 838–850 (2007).
17. Stensmyr, M. C. *et al*. A conserved dedicated olfactory circuit for detecting harmful microbes in *Drosophila*. *Cell* **151**, 1345–1357 (2012).
18. Carlsson, M. A., Diesner, M., Schachtner, J. & Nassel, D. R. Multiple neuropeptides in the *Drosophila* antennal lobe suggest complex modulatory circuits. *J. Comp. Neurol.* **518**, 3359–3380 (2010).
19. Grosjean, Y. *et al*. An olfactory receptor for food-derived odours promotes male courtship in Drosophila. *Nature* **478**, 236–240 (2011).
20. Asahina, K., Pavlenkovich, V. & Vosshall, L. B. The survival advantage of olfaction in a competitive environment. *Curr. Biol.* **18**, 1153–1155 (2008).
21. Farhadian, S. F., Suarez-Farinas, M., Cho, C. E., Pellegrino, M. & Vosshall, L. B. Post-fasting olfactory, transcriptional, and feeding responses in *Drosophila*. *Physiol. Behav.* **105**, 544–553 (2012).
22. Rex, E. *et al*. Tyramine receptor (SER-2) isoforms are involved in the regulation of pharyngeal pumping and foraging behavior in *Caenorhabditis elegans*. *J. Neurochem.* **91**, 1104–1115 (2004).
23. Bloch, G., Hazan, E. & Rafaeli, A. Circadian rhythms and endocrine functions in adult insects. *J. Insect Physiol.* **59**, 56–69 (2013).
24. Loer, C. M. & Kenyon, C. J. Serotonin-deficient mutants and male mating-behavior in the nematode *Caenorhabditis elegans*. *J. Neurosci.* **13**, 5407–5417 (1993).

25. Carlsson, M. A., Diesner, M., Schachtner, J. & Nassel, D. R. Neuropeptides in the *Drosophila* antennal lobe. *J. Neurogenet.* **24**, 34–34 (2010).
26. Iyengar, A., Chakraborty, T. S., Goswami, S. P., Wu, C. F. & Siddiqi, O. Post-eclosion odor experience modifies olfactory receptor neuron coding in *Drosophila*. *P. Natl. Acad. Sci. USA* **107**, 9855–9860 (2010).

Acknowledgements

This study was financed by the Max Planck Society. We thank Sascha Bucks for the help with RNA extraction and microarray experiments.

Author contributions

Behavioral experiments were designed and analysed by A.F., B.S.H. and M.K. Behavioral experiments were conducted by A.F. Microarray analysis was conducted and analysed by A.F., J.G., E.G.W. and H.V. Manuscript was written by A.F., B.S.H. and M.K. All authors reviewed the manuscript.

Additional information

Supplementary information accompanies this paper at http://www.nature.com/scientificreports

Competing financial interests: The authors declare no competing financial interests.

How to cite this article: Farhan, A. *et al.* The CCHamide 1 receptor modulates sensory perception and olfactory behavior in starved *Drosophila*. *Sci. Rep.* **3**, 2765; DOI:10.1038/srep02765 (2013).

The CCHamide 1 receptor modulates sensory perception and olfactory behavior in starved *Drosophila*

Figure S1

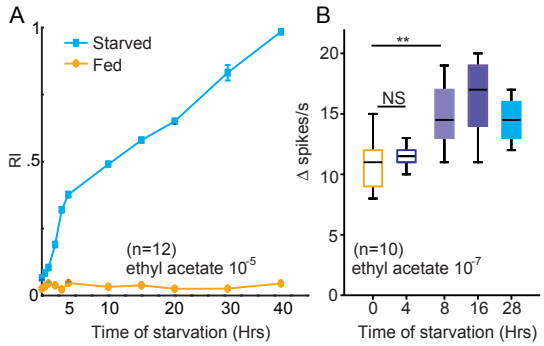

Figure S1.

3

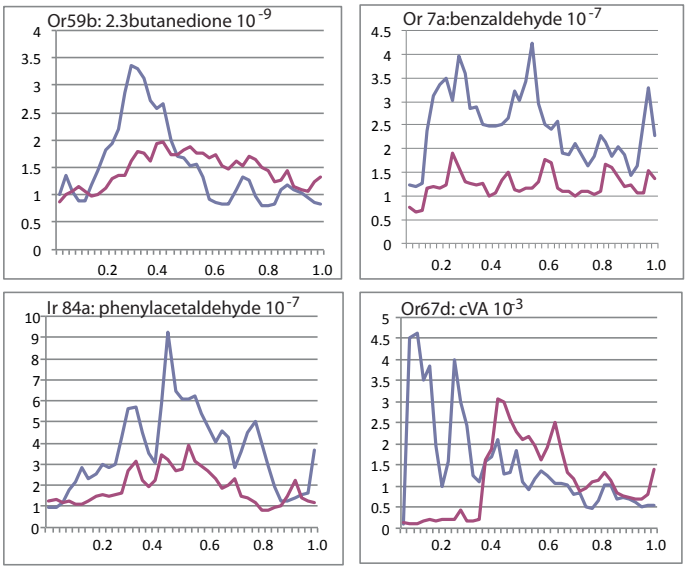

Figure S2.

Chapter III

Decoding Odor Attraction and Intensity in the *Drosophila* brain

Antonia Strutz, Jan Soelter, Amelie Baschwitz, Abu Farhan, Veit Grabe, Jürgen Rybak, Michael Schmucker, Markus Knaden, Bill S. Hansson & Silke Sachse

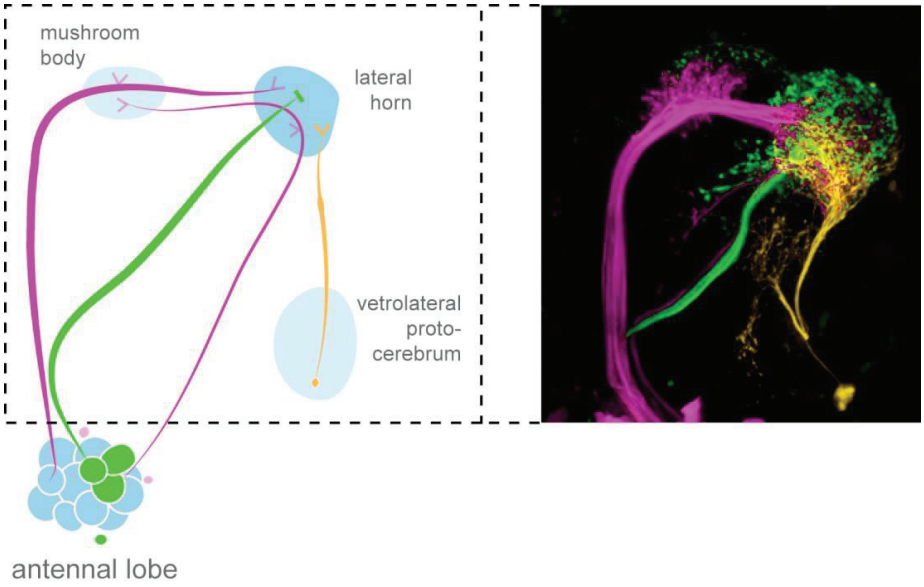

HIGHLIGHTS

- iPNs constitute an independent inhibitory processing pathway to the LH exclusively
- iPNs mediate odor attraction behavior and are necessary for odor-intensity discrimination
- the LH can be subdivided into odor response domains decoding distinct odor features
- iPNs decode odor features like positive hedonic valence and odor-intensity information

SUMMARY

To accurately reflect their sensory environment, animals create internal neural maps encoding the entire raw information of the external stimulus space. For optimal navigation, decision-relevant information has to be extracted from the primary neural code. We have characterized an olfactory processing stream, comprised of inhibitory projection neurons (iPNs) decoding positive valence as well as odor-intensity information from the topographic antennal lobe (AL) activity code into the lateral horn (LH). The iPN population is split into two neuronal subgroups conveying either of the features towards the LH exclusively. Selectively silencing inhibitory transmitter release of iPNs severely diminished general attraction behavior and disturbed odor-intensity discrimination. Functional imaging further disclosed an independent LH domain tuned to repulsive odors exclusively comprised of ventrolateral protocerebrum neurons. Our data demonstrate a spatial and functional arrangement of the LH, decoding olfactory information of opposite hedonic valence and intensity.
This study elucidates the LH role as the center for innate decisions by adding an inhibitory processing stream decoding decisive odor features.

INTRODUCTION

Sensory systems have to fulfill three essential tasks to provide animals with the capability to navigate their environment in a way optimizing survival and reproduction. First, the external world has to be translated into an internal representation in form of an accurate neural map. A common design principle of sensory systems is to generate a topographic map, which ideally encodes the stimulus' identity (identity coding) as well as characteristic features like intensity and spatiotemporal properties. Second, the neural map has to be readable and interpretable, i.e., the generated neural code must allow a fast and ultimate feature extraction of common attributes across stimuli. The extracted feature information must be re-integrated into downstream areas of the network to enable the animal to make appropriate behavioral decisions (Sachse and Galizia, 2006) (decoding relevant information). Third, the animal has to be able to adapt to environmental changes and to assign meaning to new stimuli important for its orientation and survival (sensory memory formation) (reviewed in Harris et al., 2001; Heisenberg, 2003; Pasternak and Greenlee, 2005).

Many studies have been dedicated to unravel primary translation into neuronal representations within various sensory systems (amongst others reviewed in Manni and Petrosini, 2004; Vosshall and Stocker, 2007; Sanes and Zipursky, 2010) and to elucidate neuronal plasticity and sensory memory formation in higher processing centers (Heisenberg, 2003; Pasternak and Greenlee, 2005). In contrast, feature extraction and integration of stimulus modalities towards a final behavioral output have been studied mainly in the visual system (Bausenwein et al., 1992; Livingstone and Hubel, 1988), while it remains an open question how the olfactory system accomplishes these crucial functions.

The olfactory system of the vinegar fly *Drosophila melanogaster* provides an excellent model for deciphering general olfactory processing mechanisms, since it displays remarkable similarities to the mammalian system, but is reduced in numerical complexity and is highly genetically tractable. Like other sensory systems, the olfactory system employs a topographic map to translate chemosensory space into neuronal activity patterns in the brain. This map emerges due to a strict convergence of all olfactory sensory neurons (OSN) expressing the same chemosensory receptor into one exclusive glomerulus in the primary olfactory neuropil, the antennal lobe (AL) (equivalent to the olfactory bulb in mammals) (Axel, 1995; Hildebrand and Shepherd, 1997; Stocker et al., 1990; Vosshall et al., 1999). Glomeruli represent the functional and morphological units of the AL and form specific microcircuits, where OSNs are connected to multiglomerular local interneurons (LNs) (granule cells in mammals) and to glomerulus-specific secondary output neurons, termed excitatory projection neurons (ePNs) in insects and mitral/ tufted cells in mammals (Couto et al., 2005; Fishilevich and Vosshall, 2005; Stocker et al., 1997).

The stringent spatial arrangement of OSNs and ePNs in the AL generates a topographic map with characteristic glomerular activity patterns for any odorant (Vosshall et al., 2000; Wang et al., 2003a). Uniglomerular ePNs produce acetylcholine (ACh) and convey the olfactory information to higher brain centers like the mushroom body calyx (MBc) and the lateral horn (LH) of the protocerebrum (Stocker et al., 1997). The MBc is involved in olfactory memory formation (Heisenberg, 2003), and thus enables contextualization of the odor space (Caron et al., 2013). By exclusion, the LH is believed to be involved in innate olfactory behavior (De Belle JS, 1994; Jefferis et al., 2007). Excitatory PNs retain the sensory information encoded in the AL and form, depending on the cognate glomerulus, stereotype axonal terminal fields in the LH (Marin et al., 2002; Tanaka et al., 2004; Wong et al., 2002). Regarding a topographic map in the LH, a compartmentalization was found only between fruit and pheromone odor information processing ePNs (Jefferis et al., 2007). The biological values of these two odor groups are consequently extracted from the identity-code in the AL and represented in the LH separately. Nevertheless, ePNs mainly transfer odor identity information, which can be contextualized within the MBc and integrated into the LH.

Like many other sensory networks, the olfactory circuit of the fly contains spatially distinct pathways to the higher brain (Galizia and Rössler, 2010). This tract, labeled by the enhancer trap line MZ699-

GAL4, projects from the AL to the LH exclusively and consists of ~45 presumably inhibitory PNs (iPNs) exhibiting multiglomerular AL innervations (Ito et al., 1997; Lai et al., 2008; Okada et al., 2009). As shown for the visual system, this parallel pathway might allow a dual processing of distinct odorant features along the ePN odor-identity pathway. The multiglomerular AL pattern of iPNs gives rise to the assumption that these potentially perform the necessary task of feature extraction from the glomerular code and re-integrate this information into the LH network to finally configure odorant-based decision-making.

We dissected the inhibitory olfactory processing pathway morphologically, functionally and behaviorally and revealed that iPNs indeed play a crucial role in olfactory coding. We demonstrate that multiglomerular GABAergic iPNs are subdivided into two spatially and functionally segregated groups; one extracting positive hedonic valence and one extracting intensity information from the AL. At the LH level, these iPNs remain separated and converge into discrete LH zones, constituting functional domains decoding the transferred odor features via feed-forward inhibition. Selective silencing of the inhibitory properties of iPNs abolished odor attraction behavior and severely impeded odor concentration discrimination. Our findings strongly support a model of two parallel processing streams towards the LH: one excitatory stream integrating odorant identity and a parallel inhibitory processing stream, extracting positive odorant valence and intensity. We furthermore substantiated the hypothesis of a feature-based, spatially segregated activity in the LH (Jefferis et al., 2007) by discovering an iPN-independent repulsion-selective (negative hedonic valence) LH domain formed by third-order neurons.

We have thus expanded the role of the LH as a center for integrating behaviorally relevant olfactory information towards innate decision-making with a second dimension of iPNs integrating attraction and intensity information in the higher brain.

RESULTS

iPNs receive cholinergic AL input and provide feed-forward inhibition to the LH

To unravel the role of iPNs within the olfactory circuitry, we first analyzed their morphological properties. Cell bodies of iPNs are exclusively located in the ventral cell cluster, leading to a clear separation from ePNs labeled by GH146-GAL4 (Marin et al., 2002; Stocker et al., 1990, 1997).

The complete ventral somata cluster consists of ~50 iPNs (Lai et al., 2008), which project via the medial antennocerebral tract (mACT) to the LH exclusively, thereby bypassing the mushroom body calyx (MBc) (Ito et al., 1997) (Figure 1A). In contrast, somata of ePNs are located anterodorsally and laterally of the AL and their axons project through the inner antennocerebral tract (iACT) to the MBc prior to terminating in the LH (Stocker et al., 1997). A very low number of ePNs project via the outer antennocerebral tract (oACT) to the LH prior to terminating in the MBc (Hildebrand and Shepherd, 1997; Lai et al., 2008). To analyze morphological features of both neuronal populations, we labeled iPNs and ePNs simultaneously *in vivo* (Figure 1A). Reporter expression is clearly separated within the complete brain, but olfactory neuropils show common innervations in the AL and the LH. Interestingly, only a small posterior-lateral LH area is dominated by ePN innervations (Figure 1A, Figure S1A). In GH146 positive (GH146+) PNs, immunolabeling reveal GABA production in all ~6 PNs of the ventral cell cluster (Wilson and Laurent, 2005), whereas ePNs in this line are exclusively cholinergic (Shang et al., 2007; Yasuyama et al., 2003). For the ~45 MZ699 positive (MZ699+) iPNs, GAD1 (glutamic acid decarboxylase) *in situ* hybridizations imply GABA synthesis (Okada et al., 2009), which we verified via immunostainings (Figure S1B). Hence, all iPNs do with high probability produce the inhibitory neurotransmitter GABA and therefore have a contrary effect on postsynaptic neurons compared to cholinergic ePNs (Figure 1B).

To determine the polarity of both PN populations, we expressed two reporter proteins enabling us to identify neuronal input and output sites. The construct UAS-Dα7:mcherry marks postsynaptic input sites by labeling ACh receptors (AChR) (Figure 1C, C') while UAS-Synaptotagmin:hemagglutinin (Syt:HA) labels presynaptic terminals (Figure 1D, D') (Robinson et al., 2002). Both neuronal populations reveal dense Dα7:mcherry fluorescence in the AL, indicating the AL as the cholinergic input region for both PN types (Figure 1C). Interestingly, the Dα7:mcherry signal intensity varies among different glomeruli, e.g. the pheromone glomerulus DA1 gives a highly enriched signal in ePNs as well as iPNs, most likely caused by dense dendritic innervations. In the LH, the AChR-reporter was detected only in third-order lateral horn neurons (LHNs), and exhibits high fluorescence intensity in GH146+ LHNs (Ruta et al., 2010) and lower intensity in MZ699+ LHNs (Figure 1C'). Nevertheless, both PN types reveal no Dα7::mcherry signal in the LH. Thus, iPNs and ePNs receive excitatory cholinergic input in the AL only, and are most probably directly driven by OSN input.

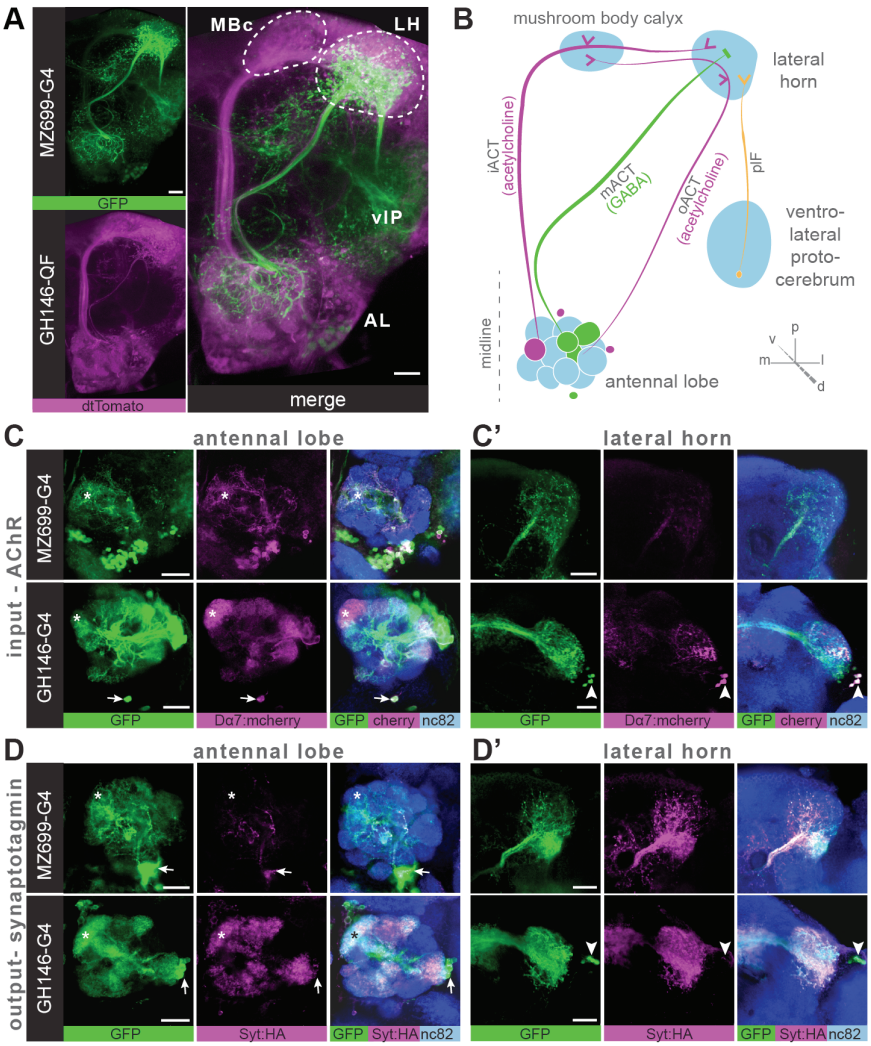

Figure 1. Characterization of ePN and iPN innervations and input and output sites

(A) Simultaneous labeling of MZ699-GAL4;G-CaMP and GH146-QF;dtTomato *in vivo* reveals separated projections to the LH. All iPNs labeled by MZ699 and iPNs labeled by GH146 bypass the MBc and innervate the LH exclusively. MZ699 labels a few LHNs projecting via the posterior lateral fascicle (plF) from the ventrolateral protocerebrum (vlP) to the LH. (B) Schematic drawing of the connectivity relay from the AL to higher brain centers (right hemisphere) involving the enhancer trap lines GH146 and MZ699. ePNs are indicated in magenta, iPNs in green, and LHNs in orange. (C) Whole mount and vibratome immunostainings in flies carrying UAS-Dα7:mcherry as a marker for AChRs and G-CaMP as a neuronal marker either in MZ699-GAL4 (upper lane) or GH146-GAL4 (lower lane), in the AL (C) and the LH (C'). Nc82 was employed as a neuronal background staining of the complete brain. The asterisk denotes the DA1 glomerulus and the arrowhead somata of ventral PNs at the AL and LHNs at the LH, respectively. (D) Analogous immunostainings in flies carrying UAS-Syt:HA as a marker for presynapses in MZ699-GAL4 (upper lane) or GH146-GAL4 (lower lane), in the AL (D) and the LH (D'). Scale bar, 20 µm.

Analysis of theoutput site reveals a dense distribution of presynaptic terminals for both PN lines in the LH (Figure 1D'). Syt:HA signals of ePNs in the AL verify AL-restricted synapto-pHluorin localization in GH146+ PNs (Ng et al., 2002) and therefore likely represent ACh-releasing sites in the AL (Wilson and Mainen, 2006)(Figure 1D). In contrast, presynaptic terminals of iPNs are almost absent in the AL, indicating a lack of feedback inhibition in the primary olfactory neuropil (Figure 1D). Weak signals could derive from transported Syt:HA molecules through main axonal iPN tracts. We verified these observations with the presynaptic reporter UAS-brp::mcherry in MZ699-GAL4 *in vivo* (data not shown).

Altogether our results show that ePNs receive cholinergic input in the AL and release the excitatory neurotransmitter ACh in both MBc and LH, but also in the AL (Figure 1A). In contrast, the morphologically well separated iPN population exhibits a unidirectional polarity, receiving excitatory input in the AL and releasing the inhibitory neurotransmitter GABA in the LH exclusively.

iPN dendrites collect sensory information from two-thirds of the AL glomeruli

Since both PN subtypes receive OSN input, we analyzed the precise glomerular distribution of neurite innervations to unravel iPN selectivity of information acquisition in the AL (Figure 2A). To allow glomerulus identification *in vivo*, we generated a transgenic fly with a constitutively fluorescent-labeled neuropil. This fly carries the construct elav-n-synaptobrevin:DsRed (END1-2), which enables expression of the presynaptically targeted fusion protein under control of the neuron-specific elav promotor (Figure 2B). To visualize the glomerular background, both enhancer trap lines were combined with the END1-2 construct (Figure S2A). Reliable validation of identified glomeruli was achieved by double labeling of the glomerular ensemble of both PN populations simultaneously. Reconstruction and assignment of all AL glomeruli (Figure 2C) provided a total number of 53 glomeruli, of which 75% are innervated by MZ699+ iPNs (40) and only 58% (31) are covered by GH146+ ePNs. Thus, GH146+ uniglomerular ePNs cover barely half of the AL. Other, GH146- ePNs are covered by distinct enhancer trap lines (Lai et al., 2008). Nevertheless, altogether 43% of all glomeruli are innervated by both lines. Moreover, compared to multiglomerular LNs, dendritic MZ699 innervation density is not homogeneously distributed. Certain glomeruli are densely innervated, in particular DM2, DM5, VM2, whereas others do not reveal any postsynaptic terminals, e.g. DL1, DL5. The glomeruli V, VC2, VC5, VM1 and the IR-glomerulus "arm" are not innervated by any of the lines (for a detailed tabulation see Figure S1) (Silbering et al., 2011). Interestingly, two densely iPN-innervated glomeruli (DM2, DM5) were previously classified as attraction-coding at the ePN level, while two aversion-coding glomeruli (DL1, DL5) were not innervated at all (Knaden et al., 2012).

This analysis revealed that iPN innervation comprises a major portion of the AL, but nevertheless exhibits a high selectivity in targeting specific glomerular subsets, hinting at a relevant function for odor processing within the olfactory network.

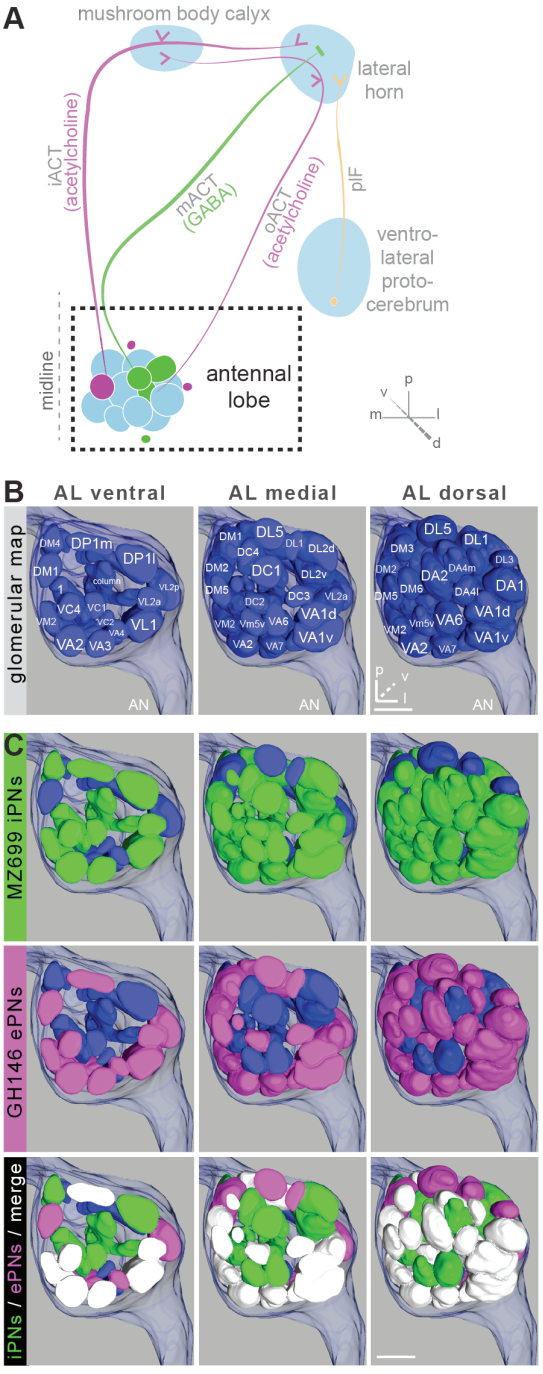

Figure 2. Detailed glomerular innervations of ePNs and iPNs in the AL3

(A) Schematic drawing of the olfactory circuitry (right hemisphere) with outlined input site (AL).

(B) Complete glomerular assignment of the AL neuropil (right AL), labeled with END1-2. Indicated are deep levels (ventral, medial) of the AL and a dorsal view onto the AL.

(C) Glomerular reconstructions of the innervation of both PN populations related to *in vivo* images in (Figure S3A). Depicted are the ventral level (~ -40 µm), the medial level (~ -20 µm) and the view from dorsal onto the AL. Color annotation: blue glomeruli are not innervated by one of the used GAL4-lines and only labeled by END1-2 (top and middle row), green glomeruli are innervated by MZ699 iPNs (top row) or magenta by GH46 ePNs (middle row), in the lowest panel: blue glomeruli are not innervated by both lines, green glomeruli are innervated by MZ699 iPNs exclusively or magenta by GH46 ePNs exclusively, white glomeruli are innervated by both PN types or enhancer trap lines. Scale bar, 20 µm.

LH calcium signals are odor-specific, stereotypic and spatially segregated in distinct response domains

Probabilistic synaptic density maps of GH146+ PNs (Jefferis et al., 2007) indicated regionalized neuronal activity in the LH. Do iPNs exhibit a comparable segregation of odor representation in the LH? We expressed the Ca^{2+} -sensitive reporter G-CaMP3.0 (Tian et al., 2009) in MZ699-GAL4 and performed functional imaging in the LH (Figure 3A, B). We initially tested if odors evoke Ca^{2+}-signals in general in the LH area and applied the following three odors: acetoin acetate, an attractive byproduct of the yeast fermentation process (Magee and Kosaric, 1987), balsamic vinegar, an attractive odor mixture, for which the OSN activity pattern is well investigated (Semmelhack and Wang, 2009) and benzaldehyde, a well-known fly repellant (Keene et al., 2004). Taking concentration dependency into account, high (1:1000), median (1:100) and low (1:10) concentrations were applied. We indeed observed odor evoked Ca^{2+}-activity in clearly separated regions of the LH (Figure 3C, Figure S3A). Acetoin acetate and balsamic vinegar evoked Ca^{2+}-activity in spatially similar regions. At higher concentrations, an additional region was recruited. Benzaldehyde elicited no response at very low concentrations. However, at median and high concentrations a third region, which is completely separated from the regions activated by acetoin acetate and balsamic vinegar, was activated with increasing signal-intensity. Thus, spatial patterns of Ca^{2+}-responses in the LH area are odor-specific. Moreover, observed patterns were clearly reproducible and stereotypic for individual odors and concentrations, as shown for the stimulation with 1-octen-3-ol, which evoked a pattern potentially comprising all regions activated by the other odors (Figure 3D). Hence, odor-specific spatial activity patterns and signal intensity in the LH are consistent across animals.

Due to the lack of morphological landmarks in the LH, functional data was analyzed using the pattern recognition algorithm Non-Negative Matrix Factorization (NNMF), which automatically extracts spatial areas possessing a common distinct time-course, further termed LH odor response domains (ORD). NNMF analysis extracted three clearly reproducible and spatially robust ORDs (Figure 3E). Remarkably, ORDs occupying common temporal kinetics (Figure S3C, C') exhibited a highly stereotypic spatial pattern. Corresponding to their anatomical positions, we termed the ORDs LH-PM (LH-posterior-medial), LH-AM (LH-anterior-medial) and LH-AL (LH-anterior-lateral).

To validate our observations and to get a more accurate insight into ORD-activity, we extended our stimulus battery to 11 additional odorants at three concentrations. Odorants were chosen according to chemical classes, hedonic valence and biological value. Hence, the odor set included acids, lactones, terpenes, aromatics, alcohols, esters, ketones and the natural blend balsamic vinegar. Some of these odors have been shown to be highly attractive, e.g. γ-butyrolactone, 2,3 butanedione, propionic acid, or strongly aversive, e.g. benzaldehyde and 1-octen-3-ol (Knaden et al., 2012). Notably, analyzing the complete odor set still revealed neuronal activity exclusively within the three described ORDs (Figure 3E). Median NNMF-extracted Ca^{2+} -activity traces with indicated statistical quartiles furthermore

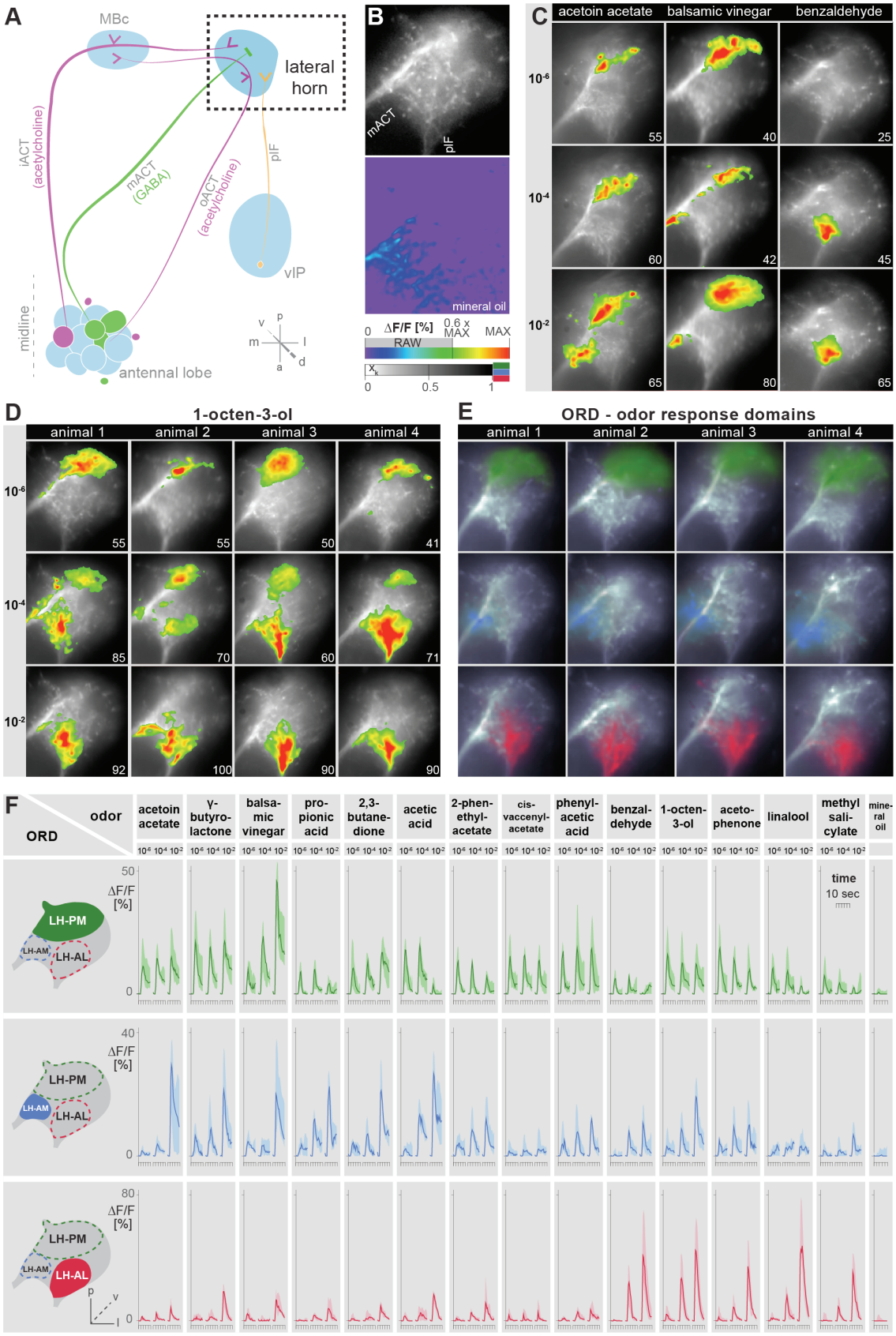
A
MBc
lateral horn
iACT (acetylcholine)
mACT (GABA)
oACT (acetylcholine)
pIF
vIP
midline
antennal lobe
B
mACT
pIF
mineral oil
ΔF/F [%]
0.6 x MAX
MAX
RAW
C
acetoin acetate
balsamic vinegar
benzaldehyde
D
1-octen-3-ol
animal 1
animal 2
animal 3
animal 4
E
ORD - odor response domains
F
ORD
odor
acetoin acetate
γ-butyro-lactone
balsa-mic vinegar
pro-pionic acid
2,3-butane-dione
acetic acid
2-phen-ethyl-acetate
cis-vaccenyl-acetate
phenyl-acetic acid
benzal-dehyde
1-octen-3-ol
aceto-phenone
linalool
methyl sali-cylate
mine-ral oil
time
10 sec
ΔF/F [%]
LH-PM
LH-AM
LH-AL

Figure 3. Odors evoke specific and stereotypic calcium responses in the LH subdivided into three distinct odor response domains

(A) Schematic drawing of the olfactory circuit (right hemisphere) with the investigated neuropil highlighted (iPN output site, LH).
(B) RAW image of the lateral horn (top picture) depicting the recorded area of figures (C) - (E) and the corresponding false color image (bottom picture) of the same region during the application of the solvent control. The ΔF/F scale bar applies for all false color coded pictures in (C)-(D) , the alpha-bar for the pixel participation x_k of the indicated colors applies for (E)-(F).
(C) Representative LH calcium responses (ΔF/F %) of acetoin acetate, balsamic vinegar and benzaldehyde at three concentrations. Spatial odor responses are distinct and distinguishable between different odorants. Numbers in the lower right corner of any image in (C) and (D) indicates the individual maximum.
(D) Reproducibility of odor-evoked spatial calcium responses (ΔF/F %) are exemplarily depicted for 1-octen-3ol-stimulated activity at three concentrations in four animals.
(E) NNMF-extracted LH ORDs of four representative animals: three LH ORDs were fully reproducible extracted throughout all measured animals. Domains classified as identical are similarly color-coded: the green response domain located in the posterior-medial region of the LH is termed LH-PM; blue, located anterior-medial: LH-AM and red in the anterior-lateral LH area: LH-AL. The alpha-bar for green, blue and red shades is placed in (B).
(F) Schematic outlines of the LH with indicated response domains (left). For filled domains in outlines, the corresponding median activity traces of all odors at three concentrations are depicted in the (right) main part of (F). Shadows represent lower and upper quartiles, respectively (n = 6-7 animals for each odor and concentration).

illustrated very low variability and high reproducibility of LH responses (Figure 3F). The global responsiveness within separated ORDs in the LH substantiates our anatomical results of a broad cholinergic AL input, which evidently converges into a highly ordered regionalized LH activity. In general, LH-AL and LH-PM showed the highest median activities. The LH-PM revealed chiefly constant odor-evoked activity across concentrations. In contrast, the LH-AM domain was mainly activated at very high odor concentrations, which was in particular manifested in the Ca^{2+} response patterns to acetoin acetate and acetic acid. A similar phenomenon was observed for the LH-AL domain but in response to different odorants.

In summary we demonstrate that neuronal activity in the LH is highly reproducible, stereotypic, and spatially separated into three distinct ORDs, exhibiting characteristic time courses.

iPNs innervating two large AL regions converge into two distinct odor response domains

The clearly separated odor representation within few ORDs implies that the separation might already be reflected in axonal terminations of neurons in the LH. We thus examined if already a physical segregation within the iPN population provided the neuronal substrate for the highly regionalized Ca^{2+} activity observed in the LH neuropil. Furthermore, investigating individual neurons allowed an insight into a possible segmentation of the glomerular input deriving from the AL, comparable to the ePN partition. To analyze iPNs at the single neuron level, we performed neural tracing by employing

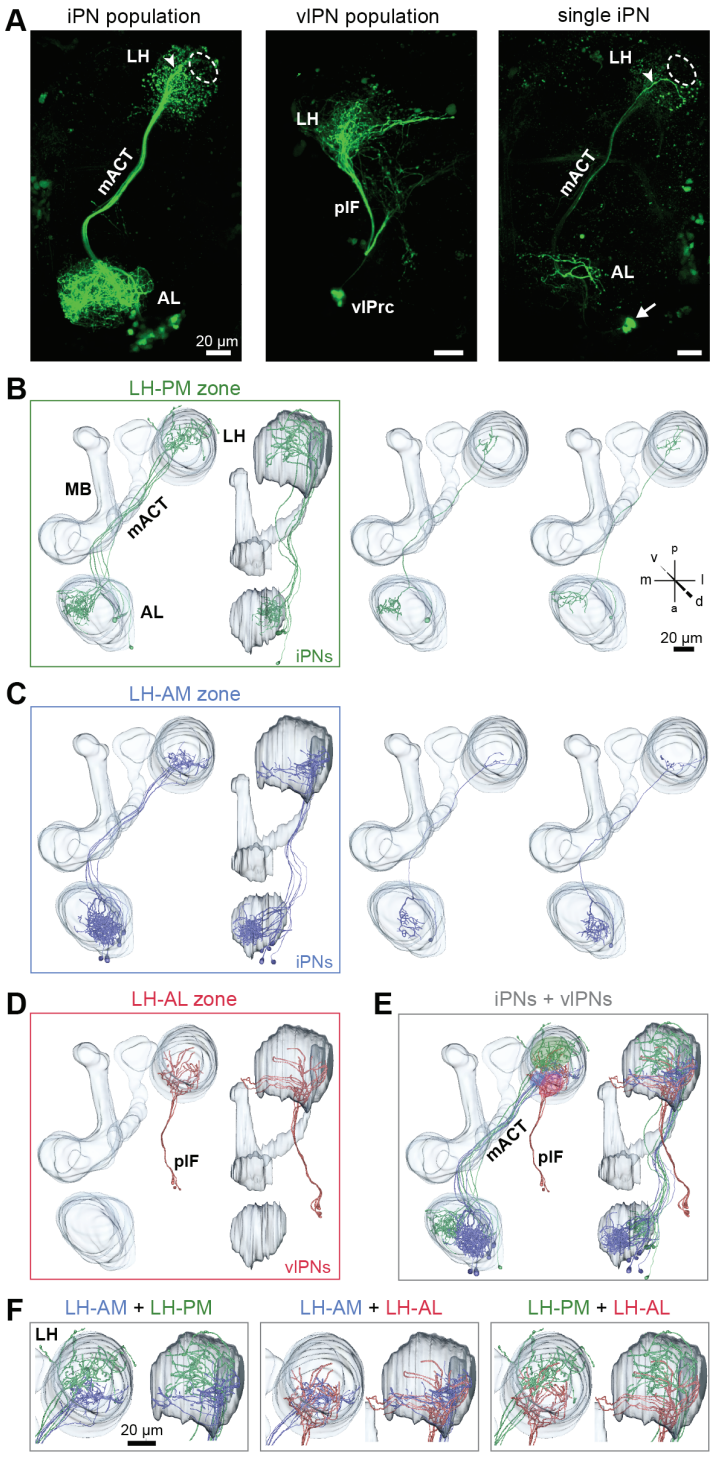

Figure 4. iPNs can be classified according to their projection pattern in three distinct LH zones

(A) Complete iPN population labeled with PA-GFP (left image), the circle indicates the posterior-lateral region and the arrowhead the final common projection point of iPN axons. Middle image: vlPNs projecting from the vlP to the LH via the plF. Right image: exemplary single iPN, labeled by photoconverting PA-GFP in a soma (arrow) located ventral to the AL. Scale bar, 20 µm.

(B) Framed images (left): all iPNs projecting to the LH-PM zone with outlined olfactory neuropils. View from dorsal (left) and lateral (right). Right part shows two exemplary registered individual iPNs.

(C) iPNs projecting into the LH-AM zone, images are arranged as in B.

(D) vlPNs projecting to the LH-AL zone with outlined olfactory neuropils. View from dorsal (left) and lateral (right).

(E) Combination of all registered neurons with outlined determined LH zones.

(F) Dual combinations of registered neurons.

photoactivatable GFP (PA-GFP) (Datta et al., 2008; Patterson and Lippincott-Schwartz, 2002; Ruta et al., 2010). Photoconvertion of all MZ699+ neurons leaving the AL confirmed the homogeneous distribution of iPN neurites in the LH and the sparse innervation of the posterior-lateral region as already mentioned above (Figure 4A, Figure S1A). After entering the LH neuropil at ~46µm below its

most dorsal point, mACT axons diverge from the center into almost the complete LH neuropil (Figure S1A).

Next we illuminated PA-GFP in single somata to trace individual iPNs. Diffusion of the photoconverted GFP molecule selectively labeled single neurons from the soma up to the furthermost axonal terminals. Individual iPNs were reconstructed and transformed into a reference brain using the segmentation software AMIRA (Figure 4B). The END1-2 background enabled an accurate alignment of neurons from different specimens into the reference brain architecture. Our results confirm the morphological stereotypy among iPNs as described by Lai et al. (Lai et al., 2008; data not shown). Interestingly, individual iPNs diverge from the LH center into two opposing regions of the neuropil (Figure 4C). As expected from the extracted ORDs, one group diverged to the posterior-medial LH zone (LH-PM), while a second group of neurons extended their axonal terminations exclusively within the anterior-medial zone of the LH (LH-AM). Illuminating a small fraction of the posterior lateral fascicle (plF), which consists of axons of 4-6 ventrolateral protocerebral neurons (vlPNs), revealed a bifurcation of these third-order neurons into the anterior-lateral zone (LH-AL). Dual combinations of all registered neuron types within the assigned zones revealed that iPNs of the LH-AM and vlPNs of the LH-AL clearly intermingle (Figure 4F).

Regarding the branching pattern in the AL, we did not observe any clear multi- or panglomerular innervations that span the entire AL, as has been observed for some LN populations (Chou et al., 2010; Seki et al., 2010). Instead, iPNs develop oligoglomerular patterns comprising only a small subset of 3-6 glomeruli, which are not necessarily in close proximity. Dendritic patterns of single neurons revealed a variety of shapes and densities and likewise glomerular ramifications spanned from very sparse to broad. Nevertheless, having classified all registered neurons according to their LH zones, we indeed observed a segregation of iPN dendritic fields in the AL. Whereas LH-PM iPNs extended dendrites merely into the ventromedial area of the AL, comprising e.g. the VM2 and DM4 glomerulus, iPNs targeting the LH-AM zone were mainly connected to glomeruli within a broader AL region ranging from dorsolateral to ventrocentral, comprising e.g. the glomeruli DA1 and DC3. Combination of all designated iPNs for both LH zones revealed a clear restriction of axonal terminal fields within the defined LH zones as well as a spatial subdivision of these neurons in the AL (Figure 4E, F).

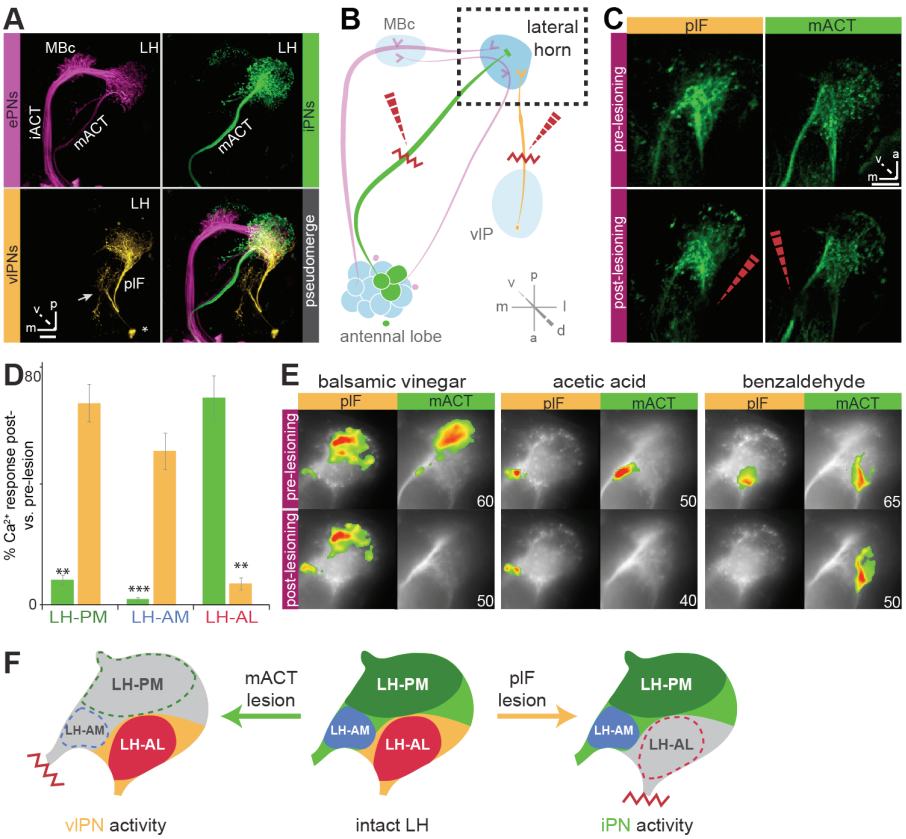

Figure 5. Distinct ORDs in the LH constitute neuronal activity of iPNs and third-order vlPNs

(A) PA-GFP labeled second- and third-order olfactory neurons of GH146-GAL4 and MZ699-GAL4. 75-85 uniglomerular ePNs (magenta) project via the iACT to the MBc and terminate in the LH, 4-6 iPNs project via the mACT directly to the LH. Approximately 45, mainly oligoglomerular, iPNs labeled by MZ699 (green) project via the mACT to the LH. Approximately four MZ699 labeled third-order vlPNs (yellow) project into the vlP and via the plF to the LH. The overlay image depicts a pseudo-merge image of the distinct labeled GAL4 driver lines to illustrate the connectivity relay in the LH region covered by MZ699 and GH146.

(B) Schematic outline of the olfactory circuit with integrated microlesion-layout. After simultaneous Ca^{2+}-imaging of bilateral LHs, the ipsilateral plF and contralateral mACT was ablated (dashed red arrow and zigzag line) using infrared light and subsequently the same odor set imaged post-lesion.

(C) Projection images of a 7 µm stack of the LH area prior and post photoablation. Left images plF severed, right image mACT severed. The ablated region is indicated by the tip of the dashed red arrowhead in the bottom image. Scale bar, 20 µm.

(D) Bar plot displaying the median percental change of ΔF/F (%) values for the indicated ORDs prior to post ablation of the mACT (green) and the plF (orange). For the percental change calculation within an ORD all odors were included, that evoked a response above 10% prior photoablation: LH-PM (n=4-8), LH-AM (n=6-12), LH-AL (n=5-10). Deviation of ORD Ca^{2+}-activity was tested with a paired Student's t test. (n=5-10) Error bars represent SEM.

(E) ORD activity of three odors in one exemplary animal in bilateral LHs before and after microlesion of the indicated neuronal tract. Left images show responses in the LH before (top) and after elimination (bottom) of vlPNs responses and right images before (top) and after (bottom) elimination of iPNs responses. ΔF/F scale bar for all images is placed in Figure 4B.

(F) Summarized cartoon of the neuron populations contributing to ORD activity prior and post microlesion of iPN or vlPN axons.

Overall, individual iPNs could be assigned to two morphological classes based on distinct areas of innervation at the input level, i.e. the AL, as well as at their output region, the LH. Additionally, we could designate a third LH zone (LH-AL) innervated by third-order neurons connecting the LH to downstream brain regions.

ORDs comprise activity of two distinct neuronal populations

To illustrate higher order connectivity, we labeled the three major neuron types targeting the LH within the olfactory circuitry using PA-GFP (Figure 5A). The LH is innervated by MZ699+ inhibitory, oligoglomerular iPNs and GH146+ excitatory, uniglomerular ePNs. Moreover, MZ699 labels vlPN neurons connecting the lateral region of the LH via the plF with the ventrolateral protocerebrum (vlP). Therefore Ca^{2+}-responses in the LH-AL region might reflect activity of vlPNs rather than iPNs. To dissect neuronal contributions to our observed Ca^{2+}-activity within each extracted ORD, we conducted microlesioning experiments using two-photon laser-mediated microdissection (Figure 5B). By severing the mACT, we abolished LH-responses deriving from iPNs, while interrupting the plF connection should eliminate potential odor-evoked vlPN activity. To achieve unambiguous and comparable results, functional imaging was performed in both brain hemispheres simultaneously. Immediately after imaging the intact brain areas, both tracts were selectively lesioned on each brain side, i.e. the plF ipsilaterally and the mACT contralaterally (Figure 5C), and the imaging procedure was repeated. We applied a reduced odor set comprising eight odors, which elicited activity in all ORDs, and subsequently performed NNMF for pre- and post-lesion recordings (Figure S4). Severing the mACT indeed reduced responses in the LH-PM and LH-AM significantly, whereas plF-lesion had no effect within these domains (Figure 5D). In contrast LH-AL responses were significantly decreased by plF-ablation, but unaffected by mACT-ablation. Hence, activity in the LH-PM and LH-AM zone can be clearly assigned to iPNs that project via the mACT from the AL to the LH. Remarkably, LH-AL activity is mainly evoked by vlPNs that project through the plF from the LH to the vlP (Figure 5A). Representative recordings of balsamic vinegar and acetic acid clearly demonstrated the lack of iPN responses within LH-AM and LH-PM after mACT-ablation and benzaldehyde demonstrated the elimination of vlPN responses within the LH-AL domain after plF-ablation (Figure 5E). In summary, these experiments demonstrate that ORD patterns can be subdivided into the second-order iPN population responsible for activation of medial ORDs and third-order vlPNs evoking LH-AL activity (Figure 5F).

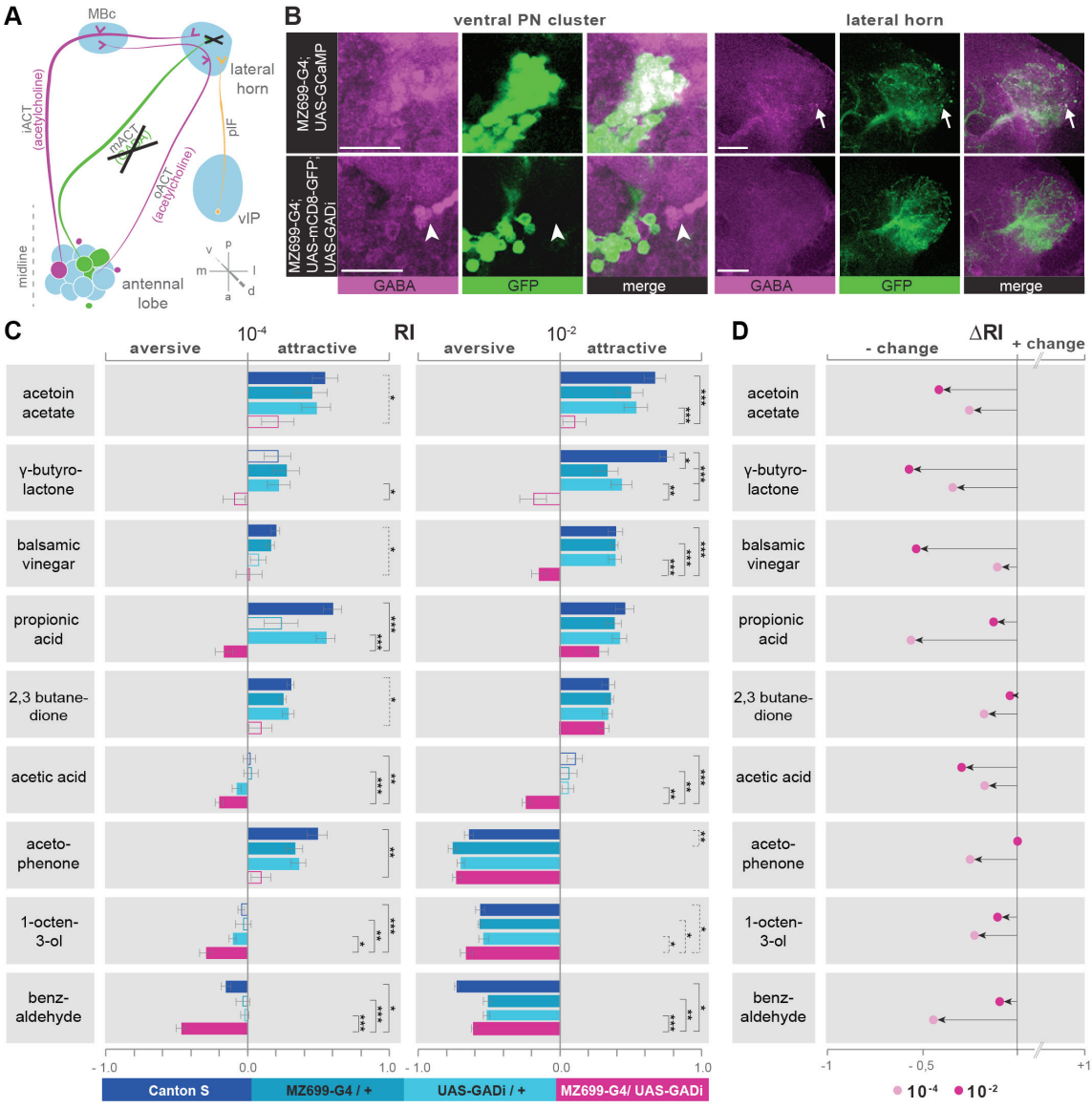

Figure 6. iPN GABA release in the LH mediates odor attraction behavior

(A) Experimental layout: iPN GABA production was selectively silenced via GADi expression. Second order iPN activity as well as third order vlPN activity remains unaffected.

(B) Immunostainings against GABA and GFP within AL somata (left) and LH neurites (right) of iPNs with intact (top images) and silenced GABA production (bottom images). GADi flies only show GABA expression in somata of iPNs labeled by GH146 (arrowhead). The arrow points on an exemplary GABA-positive bouton. Scale bar, 20 µm.

(C) Averaged response indices (RIs) for wild-type flies (dark blue), parental controls (light blue) and experimental animals (magenta) for nine odorants at two different concentrations. Empty boxes display no response (Wilcoxon signed-rank test to determine difference from zero). Deviation of the RI against controls was tested with Dunn's Multiple Comparison (solid line) or Dunn's selected Pairs (dashed line). Error bars represent SEM. RI of GADi flies are significantly reduced compared to control flies.

(D) RI differences between GADi flies and averaged parental controls. RI differences are negative for all but one odor indicating that GADi expression shifts odor-guided behavior towards aversion.

Inhibitory iPN activity in the LH mediates odor attraction behavior.

We next turned to determine the behavioral relevance of iPN activity in the LH for innate odor-guided behavior. To date it is assumed that the LH plays a crucial role for innate odor preference, in particular avoidance behavior (Séjourné et al., 2011; Wang et al., 2003b). However, direct functional evidence by experiments targeting LH neurons is still lacking. The sole study investigating PN function in the LH revealed impaired innate odor recognition after elimination of synaptic transmission in GH146+ ePNs (Heimbeck et al., 2001). Nevertheless, information conveyed by ePNs is still processed in the MB calyx. The iPN population investigated here is the only neuronal population mediating olfactory information from the AL directly to the LH and therefore could specifically shed light onto the still challenging question about the impact of the LH for odor-guided behavior.

We so far demonstrated that oligoglomerular iPNs collect sensory input over a broad range of glomeruli and integrate this information into segregated axonal terminal fields in the LH. Thus integration via iPN synaptic transmission across GABAergic terminals is arranged in a spatially discriminative manner in distinct ORDs (Figure 4). To precisely target iPN function, we employed an RNAi construct against glutamic acid decarboxylase 1 (GADi; Liu and Davis, 2009). Thereby, only GABA synthesis was interrupted and vital neuronal properties were unaffected. To realize the GABA knock-down selectively in iPNs, we expressed UAS-GADi in MZ699+ neurons. Immunostainings of flies expressing G-CaMP solely in comparison to flies expressing GADi revealed a clear reduction in GABA production (Figure 6B). To genetically verify the knock-down we performed quantitative RT-PCR (qPCR) (Figure S5).

Using wild-type flies (WT) and parental controls we then conducted T-maze assays (Chakraborty et al., 2009; Tully and Quinn, 1985) with nine of the odorants applied in functional imaging experiments at medium and high concentrations. Notably, flies with silenced iPN GABA production exhibited significantly reduced attraction behavior to almost all tested odorants if compared to control flies with full iPN GABA release in the LH (Figure 6C). In detail, odors like acetoin acetate or γ-butyrolactone, which evoked attraction behavior in control flies, evoked no attraction in flies with silenced GABA synthesis. Thus, attraction behavior was completely abolished towards these normally highly attractive odors. The behavioral preference to some odors, e.g. balsamic vinegar at 10^{-2} and propionic acid at 10^{-4}, was even reversed so that these odors became aversive. In addition, odorants normally evoking no response, as e.g. 1-octen-3-ol at 10^{-4} or acetic acid, induced an aversive behavior in GADi flies, while repellent odorants, as e.g. 1-octen-3-ol 10^{-2} and benzaldehyde, evoked an even stronger aversion. To compare the T-maze data more accurately, we calculated the average change of behavioral response indices (RIs) between GADi flies and parental controls (Figure 6D). Indeed, all responses changed in a negative direction indicating a crucial role of inhibitory iPN transmission to the LH in mediating odor attraction behavior. The sole exception was the most repulsive odor, acetophenone, at high concentration since this odor already induced maximum aversion. The strongest change in RI was

observed after stimulation with the attractive odorants γ-butyrolactone, balsamic vinegar at high concentration and propionic acid at low concentration, indicating that the effect was not concentration dependent. Nevertheless, for some odorants flies were able to distinguish between the two concentrations tested, manifested in distinct behavioral responses, e.g. to 1-octen-3ol. Interruption of iPN GABA-synthesis led to a similar response to both tested concentrations, indicating impeded intensity discrimination. Thus, iPNs potentially affect concentration coding as well.

Overall, these experiments reveal a crucial function of iPNs in mediating odor-intensity and odor-guided attraction behavior via GABA release in the LH.

iPNs integrate positive hedonic valence and odor intensity into separate LH domains

The global behavioral consequences of the selective iPN knock-down indicate that ORD activity patterns encode positive hedonic valences. Moreover odor intensity coding could be disturbed, which is less obvious from the behavioral experiments, since the valence-effect was striking over a range of different concentrations.

To analyze the complete ORD pattern array related to innate behavioral preference, we assigned additional RIs for all odors at median and high odor concentrations using again the T-maze assay (Figure 7A). Since extremely low concentrations rarely evoke any behavioral responses, we excluded the 10^{-6} concentration in this analysis. Plotting median odor-evoked activity in a three-dimensional space defined by the three ORDs, visualized a clear clustering of activity evoked by aversive odorants in the LH-AL domain, constituted by vlPNs (Figure 7B). Interestingly, attractive odors elicited no activity in the LH-AL domain, but almost exclusively activated LH-PM and LH-AM. Thus, activity in the LH-AL domain was almost exclusively induced by repulsive odors. The prevalence of attractive odor activation in the LH-PM and LH-AM domain, which implies iPN activity, supports our hypothesis of positive valence integration by iPNs, whereas vlPNs, which are assigned to LH-AL activity, encode a negative behavioral significance.

To further quantify this observation, we dissected the different LH domains and correlated ORD activity to odor valence for all ORDs separately. This evaluation also enabled us to analyze iPN and vlPN coding properties apart from each other (Figure 7C). As expected, the analysis revealed a significant correlation between positive valence coding and the LH-PM domain, whereas Ca^{2+}-activity in the LH-AL was strongly negatively correlated to hedonic valence. The LH-AM domain exhibited a positive, but not significant correlation for odor valence. Remarkably, activity within the LH-PM was totally independent of concentration, whereas activity in both anterior domains was significantly correlated to odor intensity (Figure 7D). Hence, iPNs integrate odor attraction information into the LH-PM domain independent of odor intensity, confirming behavioral experiments. Intensity coding is in turn conducted separately by distinct iPNs within the LH-AM domain. In contrast, third-order vlPN-

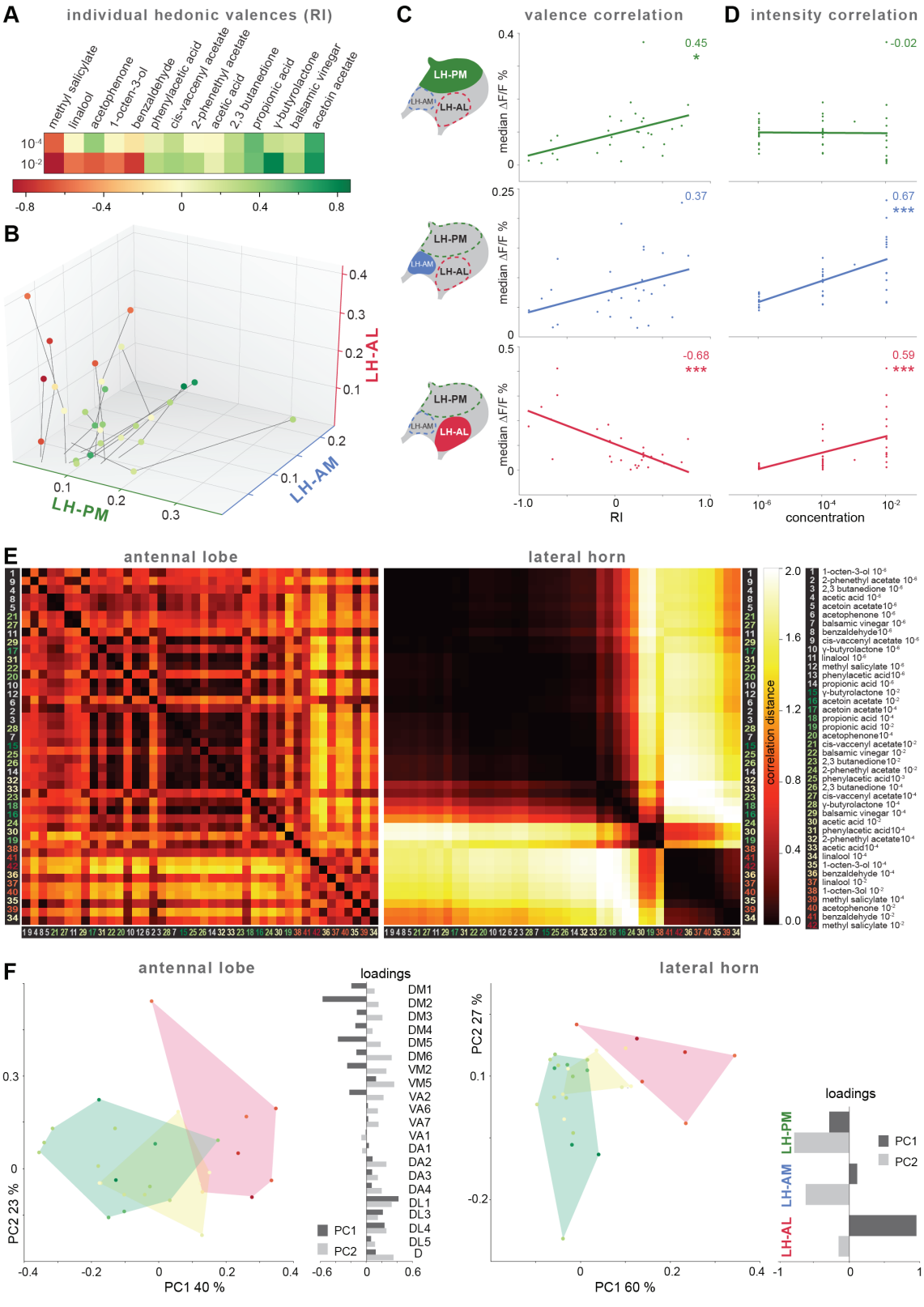
A
individual hedonic valences (RI)
methyl salicylate
linalool
acetophenone
1-octen-3-ol
benzaldehyde
phenylacetic acid
cis-vaccenyl acetate
2-phenethyl acetate
acetic acid
2,3 butanedione
propionic acid
γ-butyrolactone
balsamic vinegar
acetoin acetate
B
LH-PM
LH-AL
LH-AM
C
valence correlation
median ΔF/F %
0.45
*
0.37
-0.68
***
RI
D
intensity correlation
-0.02
0.67
***
0.59
***
concentration
E
antennal lobe
lateral horn
correlation distance
F
antennal lobe
loadings
PC2 23 %
PC1 40 %
PC1
PC2
lateral horn
PC2 27 %
PC1 60 %
loadings
PC1
PC2

62

Figure 7. Integration of hedonic valence and odor concentration into ORDs

(A) Response indices of wild type flies for all odors at median and high concentrations. Odors are sorted from highly aversive (-1, red) to highly attractive (+1, green).

(B) 3D-scatter plot of median Ca^{2+}-activity of all odors based on the three ORDs. Odors are labeled due to their behavioral RI shown in (A). Similar odors are connected with a line, the dot at the terminus depicts the 10^{-2} value, the centered dot 10^{-4}, and the end of the line give the response to 10^{-6}.

(C) Left, schematic LH outlines with colored ORDs corresponding to data on the right. Correlation score r (upper right corner) between median activity and measured RI in T-maze experiments, with significance denoted below (upper right corner); p-values: LH-PM: p = 0.016, LH-AM: p = 0.055, LH-AL: p = 0.000.

(D) r between median activity and odor concentration; p-values: LH-PM: p = 0.922, LH-AM: p = 0.000, LH-AL: p = 0.000.

(E) Complete correlation matrices for Ca^{2+}-activity patterns of OSNs in the AL and iPNs in the LH. The odors are arranged according to single linkage clustering in the LH ORD activity-space (Figure S7A). Heatmap color-code refers to the correlation distance scale bar indicated to the right. Odor letters are color-coded according to hedonic valence, 10^{-6} RI values are labeled in grey (complete list right hand). Clustering of red numbers indicates a separation of aversive and attractive response patterns in the LH.

(F) Median odor activity in the AL and LH in a PCA space. Respective loadings indicated to the right. Odors are grouped according to valence: RI for repulsive odors: -1 and -0.1, neutral odors: -0.1 to + 0.1 and attractive odors: 0.1 and +1. Calculation was performed with complete imaging data; 10^{-6} data points without cognate RI were excluded from the graph for perspicuity. Odors are clearly grouped due to valence in the LH, while a tendency is obvious at the AL level.

responses projecting from the LH-AL area code both hedonic valence and concentration of odors with negative behavioral significance.

Finally, we wondered how the odor-evoked topographic map in the AL is translated into the observed LH response domains. Is the evident valence-specific LH representation already reflected at the primary level of olfactory processing? To answer this question, we performed functional imaging of odor-evoked Ca^{2+}-dynamics in the AL. Since, dendritic calcium elevation in PNs is mainly evoked by Ca^{2+} influx through AChRs, but not voltage-gated calcium channels, it is much lower than observed presynaptic Ca^{2+} transients (Oertner et al., 2001). Therefore, oligoglomerular and very sparse dendrites of MZ699+ PNs within the AL did not provide sufficient Ca^{2+}-activity for a comprehensive analysis. However, dense AChR immunoreactivity (Figure 1C) in iPN dendrites indicated a straight forward transduction of cholinergic OSN responses. We therefore expressed G-CaMP 3.0 in OSNs using Orco-GAL4 (Larsson et al., 2004) to acquire Ca^{2+}-imaging data of the AL input to all odors. Furthermore, we generated a glomerular response pattern-array, analogous to the LH imaging data set (Figure S6). We next calculated correlation distances for all pair-wise combinations of odor-evoked response patterns (Figure S7A) and plotted these with respect to minimal pattern distances, i.e. maximal ORD pattern similarity in the LH (Figure 7E). As expected, odor representations in the LH clearly clustered within three separated parts of the matrix. However, this coding similarity could not predict AL activity patterns, which showed a scattered response pattern correlation. Notably, also within pattern correlation distances repulsive odorants cluster and are arranged in large distances to attractive

odorants. Hence, attractive or repulsive odor representations are highly similar to each other, respectively, whereas the repulsive and attractive representations are highly dissimilar (Figure S7A). To clearly visualize the separation of odor representations by hedonic valence, we reduced the dimensionality of the data set using principal component analysis (PCA). Clusters of attractive and aversive odor representations still overlap within the PCA space for AL responses, whereas the same odors are represented completely separately in the LH (Figure 7E). A tendency for separation due to odor valence is, however, already visible within the PCA space at the AL level, which is consistent with previous results (Knaden et al., 2012). Interestingly, the identical PCA space reveals no concentration-specific separation at the AL level, but a minor tendency for intensity dependent odor representation at the LH level, congruent with behavioral results (Figure S7B). This indicates a masking effect of the concentration-independent LH-PM domain over intensity-coding domains, which is ultimately reflected in the global behavioral effect on positive valence.

Inhibitory PNs evidently collect specific attraction coding odor traits from different glomerular subsets in the AL and transform this information into highly ordered response domains in the LH. Inhibitory PNs integrate the conveyed information in an inhibitory fashion into two domains of the LH relay, one region for encoding positive behavioral output, another region encoding intensity information. In addition, we discovered a distinct third-order vlPN domain, which responds to aversive odorants exclusively and which is not inhibited or biased by iPN input as shown in behavioral and microlesion experiments (Figure 5, 6).

DISCUSSION

We augment our present understanding of the *Drosophila* olfactory circuitry by elucidating a behaviorally relevant, parallel higher-order processing stream to the LH. Morphological, functional and behavioral approaches provide strong evidence for a functional subdivision of iPNs into neurons coding either odor-attraction or odor-intensity. Inhibitory properties of iPNs are necessary for innate odor-guided attraction and configure odor-intensity discrimination. We also reveal a third neural pathway coding odor repellence.

Two PN populations – two processing pathways

Higher olfactory processing centers decode important features of an odor stimulus from the primary AL activity map of PNs towards a final behavioral output. Uniglomerular ePNs innervate the entire AL and receive OSN-specific information, which leads to a complete transfer of the encoded olfactory information from the primary onto the secondary processing level, though with an optimized code (Sachse and Galizia, 2006; Vosshall and Stocker, 2007). Initially ePNs converge randomly onto third-order Kenyon cells of the MBc, the center for olfactory memory formation, and terminate in the LH, which is assumed to play a role for innate olfactory behavior (Heisenberg, 2003). In the LH ePNs retain the topographic AL code by shaping various stereotypic and glomerulus-specific axonal terminal fields. The invariant topography at the input and output level of ePNs provides an ideal strategy to maintain and relay odor-identity towards higher brain areas (Jefferis et al., 2007; Marin et al., 2002; Wong et al., 2002). We wondered which strategy is pursued by the olfactory network to extract odor features as e.g. intensity and hedonic value from the primary topographic code. Along the ePN pathway, the *Drosophila* olfactory network contains a spatially separated second-order pathway comprised of iPNs (Ito et al., 1997). Parallel pathways are a prominent strategy of sensory systems to process distinct features of encoded objects, as e.g. in the visual system, where features like form, color and motion are segregated into separate channels (Sanes and Zipursky, 2010). So far, the iPN pathway has only been partly investigated at the morphological level (Ito et al., 1997; Lai et al., 2008), while any functional evidence for its olfactory role is missing. Since iPNs target the LH exclusively and bypass the MBc, we expected this neuronal PN population to fulfill an important task regarding olfactory coding. Their oligoglomerular innervations and presumable inhibitory properties led us to propose that iPNs generate a parallel processing stream by extracting odor features from the primary olfactory code generated in the AL and by integrating this information into the LH.

Morphological prerequisites of iPNs enabling parallel processing

We initially investigated if iPNs fulfill anatomical qualifications to constitute a separate processing channel. These qualifications included verification of the presumable transmitter GABA, the neuronal polarity and the neurite distribution at their input and output regions. Selective labeling of post- and presynapses of both PN populations revealed that iPNs do, like its excitatory partners, receive cholinergic input in the AL. Confirming earlier synaptopHluorin expression we detected ACh-release sites of ePNs in higher brain areas, but, interestingly, also in the AL (Ng et al., 2002). Thus, ePNs likely fulfill a multimodal role in the network and serve also as modulators of the combinatorial glomerular code. In contrast, iPNs release its inhibitory neurotransmitter GABA in the LH exclusively. The strict unidirectional polarity implicates that iPNs do not exert a modulating effect in the AL. Hence, sensory activation of iPNs and the conducted direct feed-forward inhibition towards the LH indicates the main impact of iPNs in the higher brain.

A remarkable anatomical feature of iPNs is their glomerular innervation pattern. Whereas ePNs are uniglomerular (Vosshall and Stocker, 2007) and retain the topographic code in their axonal arrangement (Jefferis et al., 2007; Marin et al., 2002; Wong et al., 2002), most MZ699+ iPNs innervate three to six glomeruli. We therefore redefined iPNs as oligo- instead of multiglomerular neurons. The peculiar oligoglomerular dendritic pattern has the effect that individual iPNs can be activated by a set of OSN types, which therefore very likely disables the iPN population to carry precise odor-identity information. However, the divergence of iPNs in the AL into specific glomerular subsets, already pre-determines the iPN population to selectively extract common traits of distinct odors.

Three-dimensional reconstructions revealed that iPNs innervate more than two-thirds of the AL. Interestingly, Tanaka et al. described a complete AL coverage by iPNs (Tanaka et al., 2012). This discrepancy could be due to the unique iPN dendritic pattern since iPN dendrites encircle without innervating several glomeruli when picking their way to encounter presynaptic partners within other, more distant glomeruli. These projections across the AL convey the impression of glomerular innervations, although dendritic terminals are absent. Even none of the six GH146+ iPNs innervate the complete AL (Marin et al., 2002). This indicates that not the entire information encoded in the AL is read-out by iPNs, but promotes the hypothesis of a selective extraction of relevant odorant features.

We have previously shown that the AL map at the PN level already exhibits a spatial segregation of valence representation (Knaden et al., 2012). Certain glomeruli, e.g. the DL1 or DL5, which have been classified as aversion coding at the ePN level, are omitted by MZ699+ iPN, whereas some, but not all, glomeruli classified as attraction coding, e.g. DM2 or DM5, are particularly densely innervated. These results indicate that within the iPN population mainly positive odor traits are extracted, whereas odor information of negative valence is neglected. We furthermore demonstrated that the iPN population is

split into two groups diverging into distinct parts of the AL and even converging strictly into two discrete ORDs in the LH. These results reveal that the iPN level possesses, like the ePN level, some degree of spatial segregation in the AL, which is maintained within the LH.

The morphological properties of iPNs thus meet requirements to enable them to selectively extract odor information from specific glomerular subsets and integrate this information into two main LH zones.

iPNs and vlPNs constitute independent odor response domains in the LH

As mentioned, numerous functional studies target the combinatorial code of the AL to unravel encoding of specific olfactory objects or the olfactory space (Silbering and Galizia, 2007; Silbering et al., 2008; Wilson and Mainen, 2006). Even though these questions are not completely resolved, we focused on higher processing mechanisms decoding behaviorally relevant information. So far a handful neuroanatomical studies targeting ePNs deal with the question of how olfactory information is integrated and possibly read-out by higher brain structures, in particular the LH (Marin et al., 2002; Wong et al., 2002; Tanaka et al., 2004). In these studies, pheromone processing is always of outstanding interest, since it represents an innate behavioral trait. In the LH, a general separation of ePN representations of general and pheromone odors has been shown (Jefferis et al., 2007) and an elegant study by Ruta et al. completely dissected a segregated pheromone circuit, ranging from the sensory input to the ventral nerve cord output (Ruta et al., 2010). However, we did not examine sex pheromone information processing, since iPNs are negative for the sexually dimorphic transcription factor fruitless.

Pre- and postsynaptic markers indicate a major effect of iPNs in the LH area. Silencing MB function revealed that the LH alone is sufficient for basic olfactory behavior (De Belle JS, 1994; Connolly et al., 1996; Heimbeck et al., 2001). Moreover, a more general function of the LH is plausible, since it is targeted by all PNs, whereas the MBc is avoided by the entire iPN population. Based on plain morphology, the features relayed by iPNs should be ineligible for associations and sensory integration, whereas the universal distributed ePNs possess the capacity to encode odor-identity. For example, a highly concentrated odor that represents danger does not imply that *any* odor of high concentration predicts danger. Therefore contextualization of a stimulus feature alone, isolated of odor-identity might be inconvenient. In contrast, a common computation in the LH of ePN and iPN information is more likely since necessary and relevant information are reunited, potentially optimized for olfactory decision making. The oligoglomerular divergence of iPN dendrites onto glomerular subsets and the convergence onto two LH domains clearly possess coding capabilities to extract specific features of the primary AL code and to integrate this information into restricted LH zones, where coincidence with ePN innervation might occur (as shown by double *in vivo* labelings).

So far functional data of second-order neuronal activity in the *Drosophila* LH to substantiate the proposed LH function are missing. To unravel the coding properties of iPNs within the LH, we conducted the first Ca^{2+}-imaging study of LH PNs.

Our data analysis, employing the modified NNMF algorithm, extracted three ORDs displaying common temporal kinetics and highly stereotypic spatial patterns in numerous LH recordings. Two medial ORDs, termed LH-PM and LH-AM are formed by iPNs, while a lateral ORD, termed LH-AL, is formed by third-order vlPNs. Single neuron tracing of iPNs and vlPNs validated the LH segmentation into MZ699+ iPNs and vlPNs and revealed that the neural substrate for the ORDs is formed by different axonal (iPN) or dendritic (vlPN) terminal fields of individual neurons. In line with our results are the morphological studies on ePNs and third-order LH neurons that revealed a comparable tight constriction into three zones within the LH (Tanaka et al., 2004). Nevertheless, a more accurate expansion of these observations via MARCM led to a higher number of ePN target zones (i.e. five zones), whereas third-order vlPNs were highly restricted within one zone (Jefferis et al., 2007).

Since we observed some intermingling of the vlPN zone and the LH-AM iPN zone, we conducted microlesioning experiments to decipher neuronal contributions to defined ORDs. These confirmed the independence of the vlPN associated LH-AL ORD of iPN activity, since severing the mACT did not trigger increased LH-AL Ca^{2+}-activity. We therefore conclude that third-order vlPNs are not inhibited by iPNs. Immunostaining with the AChR-marker Dα7-mcherry indicated that these vlPNs receive cholinergic input in the LH, while the presynaptic marker syt:HA revealed the vlP as their major output region (data not shown). The vlP is supposedly also a target of visual neurons from the optic lobe (Tanaka et al., 2004), implying a certain integration of different sensory inputs to take place at this central processing relay.

Jefferis et al. calculated synaptic densities of GH146+ neurons and vlPNs to assess probabilistic synaptic connectivity. This map predicted that vlPNs establish synapses with the few GH146+ iPNs. However, functional data confirming this prediction is missing and MZ699+ iPNs were not included in their analysis. Nevertheless, the positive AChR staining of vlPNs indicates rather a cholinergic than a GABAergic input onto vlPNs as produced by the six GH146+ iPNs. A clear candidate for the cholinergic innervation of vlPNs would be the ePN population.

The iPN population can be split into two neuronal groups innervating distinct AL and LH regions. This implies a topographic large-scale partition of the AL for iPN mediated feature-extraction of odor stimuli, as e.g. shown for hedonic valence (Knaden et al., 2012).

iPNs decode odor features and configure olfactory decision making

Selective silencing of inhibitory iPNs by interrupting GABA synthesis severely reduced odor attraction behavior of flies to almost the complete odor set tested. Also odor intensity discrimination was diminished in cases where animals were capable to distinguish between different concentrations under normal conditions (i.e. with different behavioral preferences). It has to be noted that GABA negative vlPNs are not affected by this manipulation. Though, the valence effect clearly dominates over the concentration effect, our results suggest that oligoglomerular iPNs are indeed capable of extracting both features from the combinatorial AL-code. Notably, when we correlated the innate valences of all odors with the corresponding Ca^{2+} dynamics of the ORDs, we found that the functional properties of the LH-PM domain are in fact completely concentration independent, but strongly correlated with positive hedonic valence. This coincides with the aversion-shift of manipulated flies in the behavioral experiments. Moreover, activity in the second iPN domain, LH-AM, is valence independent, but correlates significantly with odor-intensity, explaining the disturbed intensity discrimination of flies with silenced inhibitory iPN activity.

Odor-evoked Ca^{2+}-signals of the iPN-independent LH-AL domain correlate strikingly to negative hedonic valences as well as odor-intensity. We thus detected three zones in the LH seemingly extracting different features of the olfactory stimulus. One iPN group decodes odor attraction, independent of odor-identity and intensity, since even repulsive odors become even more repulsive after silencing these neurons. A second iPN group decodes odor-intensity, and a small vlPN group in the LH most likely exclusively receives and transfers information regarding odors of negative valence information. Unfortunately, immunostaining for diverse transmitters and peptides have been negative in vlPNs so far (data not shown), which prevented us from selectively silencing vlPN function in order to confirm their involvement in negative olfactory behavior.

Since we detected immnuostaing signals for AChRs in vlPNs in the LH, the hypothesis emerges that negative valence might be conveyed via a direct and selective ePN input onto vlPNs. However, how such a mechanism might be accomplished remains to be elucidated in future studies.

A behavioral study revealed that silencing MBc neurons impairs odor attraction, but not repulsion (Wang et al., 2003b). Silencing MBc neurons with *shibire* showed that repulsive, high concentration odors remained as repulsive, whereas lower concentration attractive odorants became less attractive. The authors drew the conclusion that the LH is rather involved in mediating innate repulsion than attraction. These results are not necessarily contradictory to ours. As already proposed, some ePNs might activate the LH-AL domain exclusively (i.e. vlPNs). On the other hand, Wang et al. did not include highly concentrated attractive odors. Therefore it is possible that the odor detection threshold is simply reduced, so that only the high concentrated odors, which induced odor aversion in their study, can be distinguished. Our behavioral results in contrast revealed a constant influence of the

MZ699+ iPNs in mediating attraction for usually attractive as well as aversive odorants over a range of concentrations, implying a general attraction-mediating function of these neurons within the LH. Wang's assay displayed a tendency towards a null response for low concentration attractive odorants, possibly indicating that odors at this concentration are neutral or cannot be detected.

Jefferis et al. provided evidence for a separated representation of pheromone and fruit odors in the LH and therefore hypothesized that the LH is organized on the basis of odorants' biological values (Jefferis et al., 2007). Within our functional imaging screen the fly pheromone cis-vaccenyl-acetate activated the attraction coding LH-PM region in a strikingly constant fashion, providing evidence that even in the case of the attractive fly pheromone, iPNs extract the specific trait selectively and integrate this information into a common domain with distinct odorant information (Bartelt et al., 1985; Kurtovic et al., 2007). This further reveals the independency of the iPN-processing stream from the ePN channel, since iPNs obviously transfer odor valence completely detached from odor-identity.

Feature extraction of the primary topographic code

We provide functional and behavioral evidence regarding integration of odor attraction and intensity by iPNs in the LH. Upstream, at the input level, we demonstrated excitatory input and a subdivision of the iPN population into two separate AL areas. How might iPNs extract the respective features? Direct functional investigation of dendritic iPN Ca^{2+}-dynamics could not be conducted due to insufficient signal-to-noise ratios of the Ca^{2+} signals in the AL. Nevertheless, to gain insight if the highly reduced arrangement of activity-encoding features is already reflected topographically at the AL level, we indirectly investigated the input and recorded OSN activity patterns to the same odor set as tested for the LH activation. Correlation distances of all pair-wise combinations of odor-evoked response patterns in the LH clearly cluster within three separate ORDs and moreover patterns elicited by attractive and aversive odors are highly dissimilar. However, the strict LH arrangement does not predict coding similarity at the AL input level. Furthermore, plotting neuronal activity of the LH ORDs and the AL glomeruli using PCA confirmed that the separate representation of valence in the LH is not reflected in specific spatial sensory activity patterns in the AL. In contrast, odor intensity cannot be predicted from activity patterns in any of the two processing centers. A selective feature extraction by oligoglomerular iPNs of various glomerular activity patterns is thus very likely.

Besides extraction of odor features from spatial patterns, temporal aspects might play an important role in decoding odor features (Wilson et al., 2004) and would presumably be worth investigating. For example, in the locust oscillation- and phase-coding of identity and intensity have been shown (Stopfer et al., 2003). Though, it has to be pointed out that PNs of locusts are exclusively multiglomerular, therefore coding strategies realized in locusts cannot directly be mirrored onto other

insects as the fly. Generally, details of how the iPN subgroups selectively extract features from the primary sensory code remain to be investigated.

Another intriguing aspect emerging from our study are the potential target neurons of iPNs. It is obvious that the inhibitory effect within the ORDs contributes to the configuration of a decisive behavioral output. This can be accomplished via presynaptically inhibiting ePN terminal groups to sharpen the input towards third-order afferents or to re-integrate the respective odor feature with odor-identity coded by ePNs. The identity-code transmitted by ePNs might thereby have been modulated already by association taking place within the MBc. Alternatively, iPNs could directly inhibit third-order neurons, possibly in conjunction with ePN input to create the right balance for a quality decoding behavioral output. Our data indicate that iPNs do not exert their effect on vlPNs, which moreover might constitute LH output neurons transferring negative behavioral output provided by ePNs. Another comparatively large group of third-order output neurons, that would be promising candidates are middle superiormedial protocerebral neurons (Séjourné et al., 2011; Tanaka et al., 2004). Nevertheless, a large screening of GAL4 lines for all possible candidates is beyond the scope of our study, but needs to be elucidated in the near future.

Our study provides a first step in exploring and unraveling higher olfactory processing encoding odor features crucial for an adaptive behavioral output in *Drosophila*. We postulate a circuit of at least two secondary parallel processing streams; an excitatory and an inhibitory stream extracting odor-identity or distinct features of diverse AL patterns and integrating these in constricted zones of the LH. Moreover, we provide functional evidence for a feature based spatial arrangement of the LH into distinct ORDs, decoding opposing hedonic valences and odor intensity. The role of the LH as a center for integrating biological values towards innate decisions by (re-)computing conveyed information of two processing streams is thus expanded

.

METHODS

Drosophila stocks

All fly stocks were maintained on conventional cornmeal-agar-molasses medium under L:D 12:12, RH = 70% and 25°C. For wild-type controls *D. melanogaster* of the Canton-S strain has been used. Transgenic *D. melanogaster* were obtained from the Bloomington *Drosophila* Stock Center (http://flystocks.bio.indiana.edu/) and the Vienna RNAi stock center (http://www.vdrc.at). Other Fly stocks were kindly provided by: P[MZ699-GAL4]: Kei Ito; P[UAS-Dα7::mcherry]: Stefan Sigrist; P[UAS-Syt::HA], P[UAS-mCD8::GFP]: Hiromu Tanimoto and UAS-C3PA: Maria Luisa Vasconcelos.

Generation of transgenic constructs

Generating P[END1-2] (elav n-synaptobrevin-DsRed 1-2) has been performed using a modified pCaST-elav-Gal4AD vector (plasmid 15307, addgene, USA). The GAD domain present in the original vector was excised using NotI and FspAI enzymes, withthe FspAI recognition site located within the DsRed coding sequence. A DNA oligonucleotide containing a modified n-synaptobrevin-coding ORF (n-syb)(DiAntonio et al., 1993), upstream to a sequence identical to the excised DsRed-fragment, as well as a *Drosophila* Kozak site (caaaATG) and recognition sites for NotI and FspAI were synthesized and inserted into the vector. The n-syb contains one silent mutation at position (C168T) to eliminate a FspAI-recognition site within the fragment. Excision, synthesis and ligation have been performed by MWG Eurofins (Germany). The resulting plasmid was amplified in *E. coli* (One Shot® Top10 *E. coli*, Invitrogen, Eugene, OR) and purified using a Qiagen midi-prep kit (Qiagen, Germany). *E*mbryo transformation to generate transgenic lines was performed by Aktogen (Cambridge, UK).

qRT-PCR

RNA from heads of 50 female flies (4-10 days old) for each sample was isolated with the RNA Mini Kit (Analytik Jena). cDNA synthesis was performed with SuperScript® First-Strand Synthesis System (Invitrogen). The acquired cDNA was subjected to quantitative RT-PCR performed with a Rotor-Gene Q and the Rotor-Gene SYBR Green PCR Kit (both Qiagen) following the manuals. Each sample was run as a triplicate and cycles have been replicated 4 times. Average values were normalized to the control gene, rp49. Final quantification has been performed after the ΔΔCt method (Livak and Schmittgen, 2001). Primer sequences: RP49 (69 bp): for CCAGTCGGATCGATATGCTA; rev

TCTGTTGTCGATACCCTTGG. GAD1 (139bp): for CCGCAGAACCCATTTAGTCCAT; rev TTGAGCTTAATTGACTCCGGGC.

Optical imaging

Fly preparation and functional imaging of odor-induced glomerular activity was conducted as previously described (Stökl et al., 2010; Strutz et al., 2012). LH imaging was conducted similar, except for the higher resolution achieved with a 60x water immersion objective (LUMPlanFl 60x / 0.90 W, Zeiss, Germany). The optical plane was ~30µm below the most dorsal point and chosen according to a maximal variety of signals, i.e. more than 5µm below or above the chosen level, signals blurred and could not be categorized appropriately. The binning on the CCD-camera chip produced a resolution of 1 pixel = 0.4 x 0.4µm. For bilateral LH imaging prior and post microlesion a 20x water immersion objective (NA 0.95, XLUM Plan FI, Olympus) was employed. To receive a comparable resolution binning was decreased by 50%. All recordings had a duration of 10 s with an acquisition rate of 4 Hz. Odors included acids (propionic acid, acetic acid), lactones (γ-butyrolactone), terpenes (linalool), aromatics (acetophenone, methyl salicylate, benzaldehyde, phenylacetic acid), alcohols (1-octen-3-ol), esters (acetoin acetate, cis-vaccenyl acetate, 2-phenethyl acetate), ketones (2,3 butanedione) and balsamic vinegar diluted in mineral oil. Odors were applied during frame 8–14 (i.e. after 2 s, lasting for 2 s). Flies were imaged for up to one hour, with a minimum inter-stimulus interval of one minute.

We have selected conventional widefield Ca^{2+}-imaging as the method of choice, since we were able to obtain single bouton resolution with this technique (Figure 3B). Nevertheless, the z-range collected significantly more Ca^{2+}-signals due to light scattering than compared to multi-photon imaging (depth reachable about ~35 µm, Strutz et al., 2012). Furthermore, the LH does not offer anatomical and functional landmarks (as visible for the AL glomeruli), thus we orientated us at the entrance point of the mACT, which is ~45 µm below the most dorsal point of the arborizations of MZ699+ neurons in the LH. At this level and below, Ca^{2+}-signals blurred and hardly yielded distinguishable domains (data not shown). Similarly, a blur to one large signal occurred from ~15 µm above the mACT entrance point. An optical plane of ~5 µm above the mACT entrance point yielded sharp recordings as well as the most comprehensive set of different regions. Therefore, we assumed that signals above and below the imaging level simply reflected broadened signals of ORDs detected with our method and we chose to image the optical plane covering all existing domains labeled by MZ699-GAL4. Moreover, widefield-imaging is capable of recording signals of ~35 µm depth. Since we are able to obtain even single bouton resolution, we do believe that we have recorded the maximal variety of signals in the LH evoked by MZ699+ neurons.

OSN Ca^{2+}-imaging data analysis

False color coded images of LH Ca^{2+}-imaging (Figure 4B-D , Figure 5D-D'' and Supplemental Figure 4A,B) were obtained with a custom written IDL software (ITT Visual Information Solutions, www.ittvis.com) provided by Mathias Ditzen. Ca^{2+}-imaging data of the AL shown in Supplemental Figure 6A-C have been analyzed as previously described (Stökl et al., 2010; Strutz et al., 2012).

LH Ca^{2+}-imaging data analysis

To ensure high reliability of extracted domain information recordings of any odor at any concentration was repeated 2-3 times within measurements. Only if response properties of replicates are identical within an animal, the recording for the analyzed odor was rated as valid and taken into account for the final analysis (Supplemental Figure 3C, C''). To execute NNMF analysis (see below), at least six to seven valid measurements, i.e. animals with repeated identical recordings, were collected for each odor and employed for the analysis. The comprehensive set of odorants (altogether 14 odorants, applied in three concentrations, at least repeated twice, resulting in 84 necessary recordings) faced us with evident physiological restrictions and we consequently split the analysis into four groups. Fortunately, the strong reproducibility of recordings yielded measurements coherent enough throughout animals (Figure 3B, C, Supplemental Figure 3C, C') so that the outcome of the NNMF analysis was unimpaired.

LH data pre-processing

Individual odor measurements of each animal were concatenated to construct a complete recording series, which was further aligned using ImageJ (Fiji) to correct movement artifacts ('rigid body' transformation and 'image stabilizer' plugins). Fluorescence changes ($\Delta F/F$) for each odor were calculated in relation to the background fluorescence taking frames 0-6 (i.e. 2- 0.5 s before odor application). A Gaussian low-pass filter (σ=1px) was applied to compensate remaining movement artifacts and pixel noise. To reduce the computational load the frame rate was averaged by two consecutive frames and recordings were spatially down-sampled by a factor of two. The resulting concatenated time-series of the recordings is denoted as measurement matrix $\mathbf{Y}$ with element $\mathbf{Y}_{t,p}$ being the t^{th} observed value of pixel p.

NNMF - Non Negative Matrix Factorization

In contrast to the AL, which consists of highly ordered glomerular subunits, LH comprises a mainly homogenous neuropil which does not provide spatial or functional landmarks enabling the clear assignment of Calcium dynamics to well-known areas. Therefore, we used the novel automatic method NNMF to extract Calcium signals owing common spatial or temporal features.

The NNMF initially decomposed the measurement matrix **Y** into its main k components,

$$\mathbf{Y}=\sum_k \mathbf{x}_k * \mathbf{a}_k^T + \mathbf{R}.$$

Each represented time-course a_k contains a common underlying time-courses of all pixel and each pixel participation x_k declares for each pixel how strong it participates in this time-course. The residual matrix **R** contains the unexplained data. For the decomposition we choose the Non Negative Matrix Factorization (NNMF) approach as it is known to achieve a parts-based representation rather than the more holistic results of Principal Component Analysis or Independent Component Analysis (Lee and Seung, 1999; Lee et al., 2001). NNMF constrains both the extracted time-courses and pixel participations to be positive. Positive pixel participations enable a straightforward physiological interpretation, reading the participation values as contribution strength of an underlying physiological domain. The restriction to positive time-courses reflects that we did not observe any significant decrease of fluorescence in response to an odor. In order to perform NNMF, we implemented the HALS algorithm in Python including a spatial smoothness constraint (a_{sm} = 0.1) (Cichocki and Phan, 2009) and an additional spatial decorrelation constraint (a_{de} = 0.1) (Chen and Cichocki, 2005).

Decomposition was performed for each animal into k=5 components, therefore the residual matrix **R** contained no additional domains (residual movement artifacts induced only tiny additional structures). Of the five components extracted by NNMF three of them stood out: first they exhibited highly reproducible responses to stimuli repetitions, i.e. they have a high trial-to-trial correlation. Second they were extracted in all animals at defined anatomical positions and third they exhibited characteristic response spectra across animals. Besides those three ORDs, every factorization contained two additional components. Though we cannot completely rule out that these are ORDs of their own, there are several indications that they are not. They either exhibit a low trial-to-trial correlation or are extracted at the same anatomical position only in a small fraction of animals. Instead of independent ORDs, these might rather convey fluorescence change independent of odor stimulation or an overlap region of two of the reliable ORDs. To validate the reliability of our data analysis, we have employed another imaging analysis algorithm. Spatial Independent Component Analysis (sICA) yielded very similar results (data not shown)(Reidl et al., 2007). Particular the three reliable ORDs from NNMF were reproduced with sICA. Hence, we conclude, that the LH area comprised by MZ699+ neurons constitutes of three ORDs. Components were labeled according to anatomical position of pixel

participation within the LH and subsequently regionally assigned including coinciding reproducible Ca^{2+}-signals in all animals.

Statistical analysis of Ca^{2+}-imaging data

To determine coding properties of extracted odor response domains (ORDs) we calculated the mean response of each animal within a time window of 1- 4 s after stimulus onset. Hence, median responses over all animals defined the standard stimulated response of an ORD. Initially, regions were evaluated individually and correlations were calculated between standard response spectra and the behavioral response index (RI), or odor concentration, respectively, using the "linregress" function of the Python *scipy.stat* module. Pattern representations were analyzed in twofold directions. First, pattern correlations quantified pattern similarity independent of signal intensity. To visualize the correlation matrix in a comprehensible way, we then arranged odors according to the single linkage clustering of the Python *scipy.cluster.hierachy* module. Second, a 2-dimensional PCA representation (Python *scikit-learn* module) reduces visual complexity and depicts pattern separation comprising response strength.

Immunohistochemistry

Wholemount (wm) and vibratome (vt) dissection and staining procedure: Immunofluorescence staining was carried out essentially as described (Laissue et al., 1999; Vosshall et al., 2000). Initially brains were dissected in Ringer's solution (130 mM NaCl, 5 mM KCl, 2 mM MgCl(x $6H_2O$), 2 mM $CaCl_2$(x $2H_2O$), 36 mM Saccharose, 5 mM Hepes, [pH 7.3]) and fixed in 4% PFA in PBS-T (PBS, 0,2-1% Triton-X) for at least 30 minutes on ice. After washing three times with PBS-T (wm) or PBS (vt) they were blocked for two hours with PBS-T, 2% bovine serum albumin (BSA) or PBS-T, 5% normal goat serum (NGS). Vt-sections were blocked using 5% NGS and 5% normal donkey serum (NDS). Wash and blocking steps were constantly repeated after each incubation step. Primary antibodies were diluted in blocking solution or PBS-T and incubated at 4°C for 2 - 3 days (vt), respectively. Secondary antibody incubation lasted 1-2 days. After final wash for 20 minutes, brains were mounted in VectaShield™ (Vector Laboratories) on object slides. The following primary antibodies have been used: rabbit α-GABA (1:500) (Sigma), mouse α-GFP (1:500) or chicken α-GFP (1:1000) or rabbit α-GFP (1:500) (all Invitrogen), mouse monoclonal α-ChAT (1:500) (DSHB), mouse α-Nc82 (1:30) (DSHB) or rabbit α-Nc82 and guinea pig α-Nc82 (1:500), kindly provided by Stefan Sigrist, rabbit α-RFP (1:500) and mouse α-HA (1:1000) (both Abcam). The following secondary antibodies have been used: Alexa Fluor® 488, goat anti-mouse IgG (1:500); Alexa Fluor® 488, goat anti-rabbit (1:500); Alexa Fluor® 546, goat anti-rabbit (1:500); Alexa Fluor® 633, goat anti-mouse

(1:200), Fluor® 594 chicken anti mouse (1:200), Alexa Fluor® 488 donkey anti-chicken 1:200 (all IgG Invitrogen, Eugene, OR).

2-Photon photoactivation of C3PA labeled single neurons

For *in vivo* photoactivation experiments 1-6 day old flies (Genotype: END1-2,UAS-C3PA;MZ699-GAL4) were dissected similar to imaging experiments with the exception that tracts of the salivary glands were cut to prevent movement. Single somata were defined as regions of interest with an average diameter of ~40nm. Photoactivation was accomplished via continuous illumination with 760 nm for 15-25 min. After a 5 minute break to permit full diffusion of the photoconverted molecules, 925nm z-stacks of the whole brain were acquired and subsequently used for 3D-reconstruction of the labeled neuron.

2-Photon mediated photoablation

Microdissections of either the plF tract or the mACT have been conducted in one brain hemisphere, each of the same fly. The target area has been monitored with 925 nm and chosen close to the LH but distant enough not to affect neurites ramifying in the LH neuropil. For both tracts, lesioned areas had an average size of 34µm and were illuminated with short pulses of 710 nm every 40 ms for 250 ms in 60 (plF) – 80 (mACT) cycles. Overall the two simultaneous ablation procedures did last ~60 s. After a fast z-stack with 925nm to confirm the complete lesion, a 5 minute neuronal recovery interval followed before continuing the imaging procedure. Data were analyzed using NNMF as described above. For bar plot calculation of each ORD, only odors which evoked a response within the respective domain above 10% (ΔF/F) were included.

Image acquisition

Photoactivation and photoablation procedures as well as image acquisition following immunohistochemistry was accomplished with a 2-Photon Confocal Laser Scanning Microscope (2PCLSM, Zeiss LSM 710 meta NLO) equipped with a 40x (W Plan-Apochromat 40x/1.0 DIC M27) or 20x (W N-Achroplan 20x/0.5 M27). The 2PCLSM was placed on a Smart Table UT2 (Newport Corporation, Irvine, CA) and equipped with an infrared Chameleon Ultra™ Diode-pumped Laser (Coherent, Santa Clara, CA). Z-stacks were performed with Argon 488 nm and HeliumNeon 543 nm Laser or the Chameleon Laser 925 nm (BP500-550 for G-CaMP and LP555 for DsRed/Tomato) and had a resolution of 1024 or 512 square pixels. The maximum step size for immuno-preparations or single neuron projections was 1 µm and for AL reconstructions 2 µm.

3-D reconstructions and image processing

For all 3D reconstructions the segmentation software AMIRA 5.3.3 or 4.1 (Mercury Computer Systems, Berlin, Germany) has been used. Individual glomeruli of complete AL reconstructions were generated by segmentation of each spherical structure around its center in three focal planes. Subsequently, every third slice was three dimensionally interpolated employing the wrap interpolation tool of Amira. Visualization of AL reconstructions was simplified with the *SurfaceGen* modul to around 100,000 faces and further finished with the *SmoothSurface* modul. Single neurons reconstructions were performed with the *skeleton* module of AMIRA. Embedding of neurons of distinct specimen into the reference brain has been performed using a labelfield registration as previously described by (Rybak et al., 2010). Briefly, segmented labels of brain neuropils (MB, LH) were registered onto a reference brain image using affine registration followed by elastic warping. In a second step the calculated transformation matrix was applied to the respective neuron morphology that was then aligned to the reference brain image.

Figures have been edited in ImageJ (Fiji) or Adobe Photoshop CS4 (Adobe Systems, Inc.) and compiled with Adobe Illustrator CS4 without further modification of brightness or contrast.

Behavioral Assay

Flies carrying P[GAD1-RNAi];P[MZ699-GAL4] were crossed just before the experiment to prevent dosage compensation effects. T-maze experiments have been essentially performed as described (Stensmyr et al., 2012). WT, parental controls (P[GAD1-RNAi] or P[MZ699-GAL4]) and test flies carrying both insertions have been tested separately under identical conditions. The response index (RI) was calculated as (O-C)/T, where O is the number of flies in the odor arm, C is the number of flies in the control arm, and T is the total number of flies used in the trial (= 30). Hence, the RI ranges from -1 (complete avoidance) to 1 (complete attraction). A value of 0 characterizes no response, i.e. the odor is not detected or is neutral. Each experiment was repeated twelve times and the RIs of flies were compared with the Dunn's Multiple Comparison or Dunn's Selected Pairs and tested against 0 (no response) by the Wilcoxon-rank-sum test.

ACKNOWLEDGMENTS

We thank Silke Trautheim, Regina Stieber, Linda Gummlich and Sascha Bucks for excellent technical assistance; Ewald Grosse-Wilde and Christopher König for assistance with the qPCR and Stefan Sigrist for providing the Da7:mcherry strain and antibodies. This work was supported by the BMBF (Federal Ministry of Research and Education) and the Max Planck Society.

SUPPLEMENTAL MATERIAL

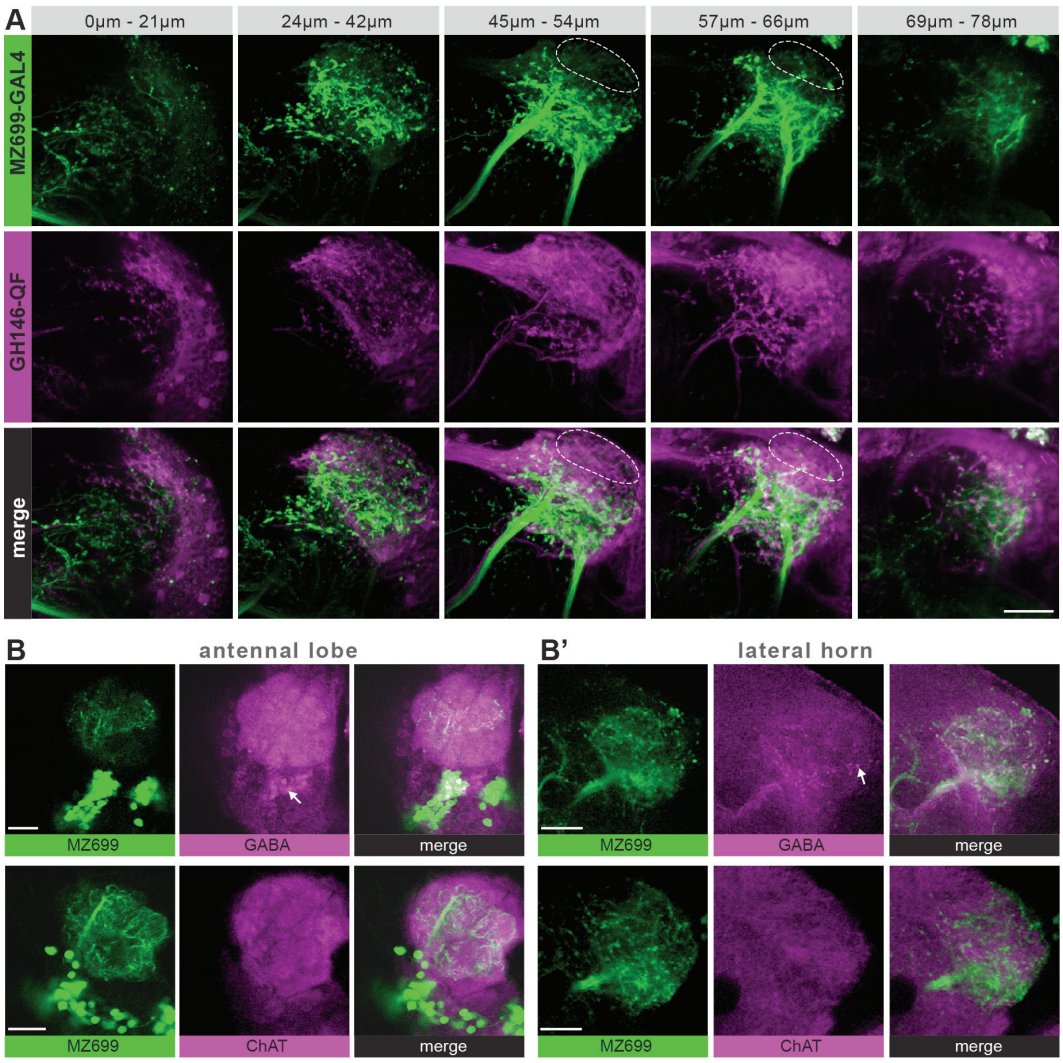

Figure S1 (related to Figure1).

(A) Overlap of ePNs (QUAS-Tomato) and iPNs (UAS-GCaMP3.0) in the LH area, the circle indicates the posterior lateral region, which is sparsely innervated by iPNs and dominated by ePN axonal terminal fields.
(B) GABA vs. ChAT Immuno in the AL and LH (B'). Somata and LH neurites of MZ699 iPNs are GABA-positive and ACh-negative. Scale bar, 20 µm.

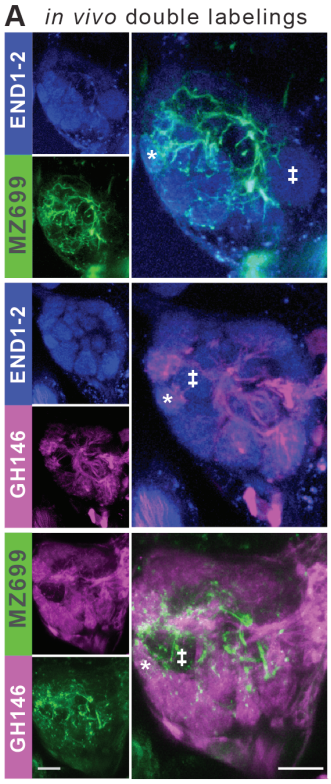

B

glomerulus	MZ699	GH146	merge
"column"			
"arm"			
D			X
DA1			X
DA2			X
DA3			X
DA4l			X
DA4m			
DC1			
DC2			X
DC3			X
DC4			
DL1			
DL2d			
DL2v			
DL3			
DL4			
DL5			
DM1			
DM2			X
DM3			X
DM4			
DM5			X
DM6			X
DP1l			
DP1m			X
V			
VA1d			X
VA1v			X
VA2			X
VA3			X
VA4			
VA5			X
VA6			
VA7l			X
VA7m			
VC1			
VC2			
VC3			
VC4			X
VC5			
VL1			X
VL2p			
VL2a			X
VM1			
VM2			X
VM3			X
VM4			
VM5d			
VM5v			
VM6			
VM7			
1			
53	**40**	**31**	**23**
	75.47 %	**58.49 %**	**43.40 %**

Figure S2 (Table related to Figure 2).

(A) Representative in vivo images for all reconstructions (right AL). MZ699 and GH146 have been reconstructed with END1-2 background (two upper planes) and dual labeling with the Q-system and the GAL4-UAS expression system (lowest plane). Scale bar, 20 µm

(B) Detailed glomerular AL innervation. Green filled cells indicate innervation by MZ699-GAL4, magenta GH146-GAL4 innervation, respectively and grey, no innervation by the indicated line. Bottom rows, total number of innervated glomeruli with percentage share indicated below. Merge column: white filled with "x" indicates glomeruli innervated by both lines, grey only one line. Blue filled rows are glomeruli labeled by none of the enhancer trap lines.

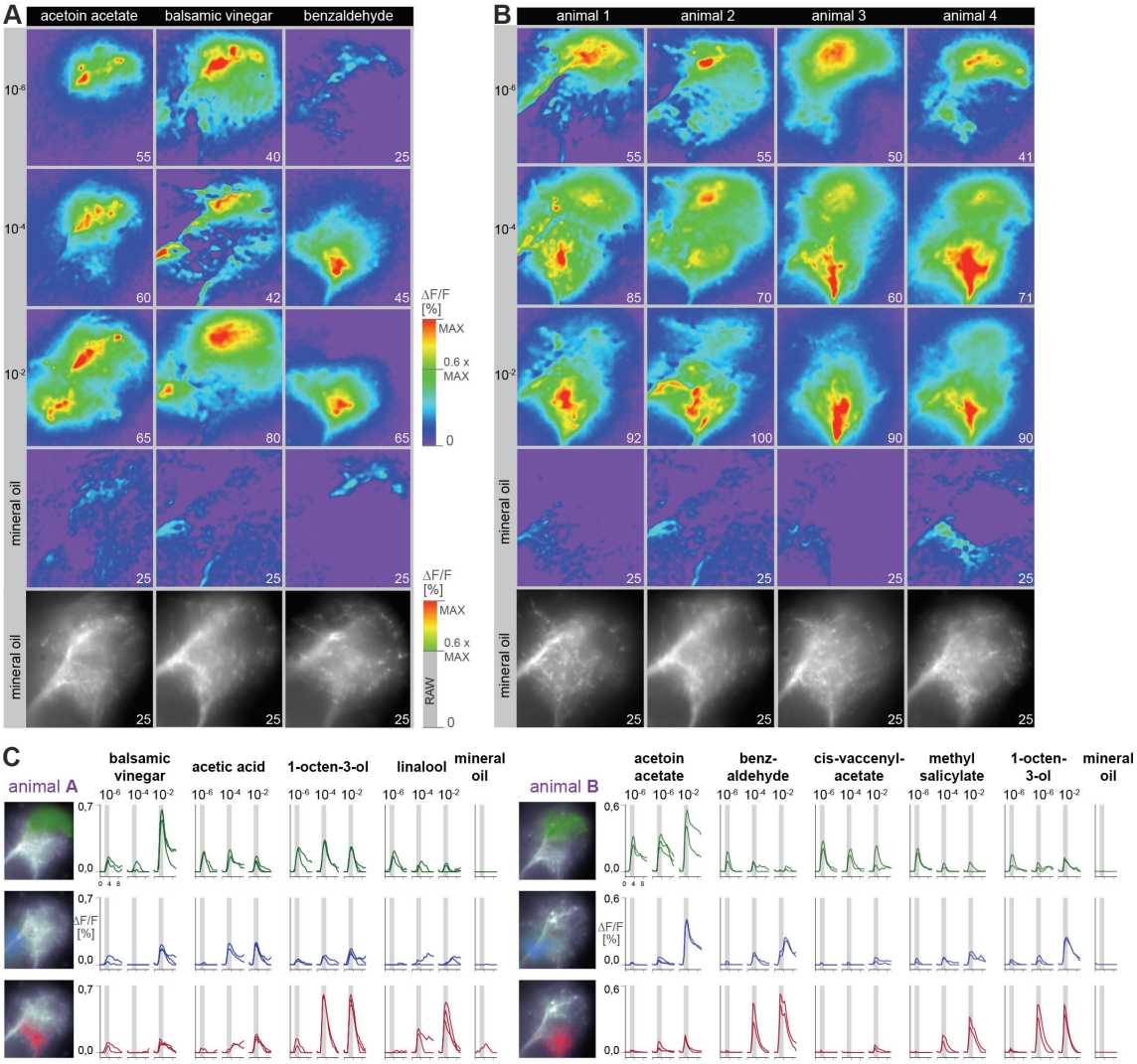

Figure S3 (related to Figure 3).

(A) Full false-color coded images of data shown in Figure 3 C plus mineral oil control measurement. The control measurement is also shown with cut off as in Figure 3C. The top scale bar applies for all full false-color coded pictures in (A) and (B), the bottom scale bar for the mineral oil recordings.
(B) Full false-color coded images of data shown in Figure 3 D plus mineral oil control measurement.
(C) NNMF-extracted LH odor response domains of two representative animals (color scale for pixel participation xk in Figure 3) and cognate time courses (ΔF/F %). Measurements have been repeated 2 - 3 times and show a clear reproducibility.

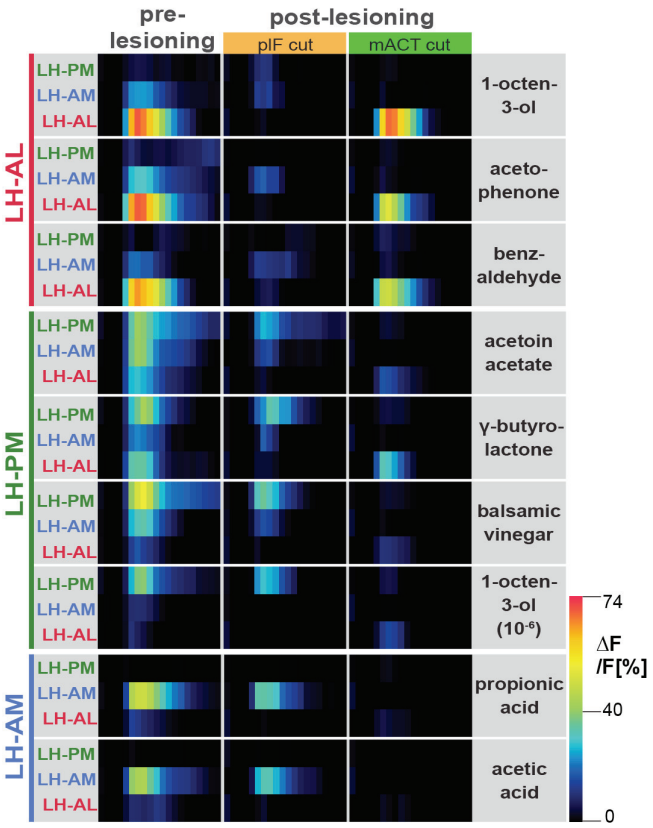

Figure S4. (related to Figure 5).

Median time traces (color coded as indicated in the scale bar right) for all odorants used in the microlesioning experiments. Odorants had a high concentration (10^{-2}), except 1-octen-3-ol, which was applied at 10^{-6} and 10^{-2}. ORDs to the very left (vertically typed) display the arrangement of the odorants in the figure, i.e. the affected domain by any of the two lesionings in the respective odorant. Indiviual ORDs are shown from top to bottom for every odor. First row is always LH-PM, second LH-AM and last LH-AL. The three columns reveal the results for the pre- and post lesioning recording. Lesioning the plF abolished LH-AL responses to mostly zero (ΔF/F [%]) and lesioning the mACT eliminates Calcium activity in the LH-PM and LH-AM.

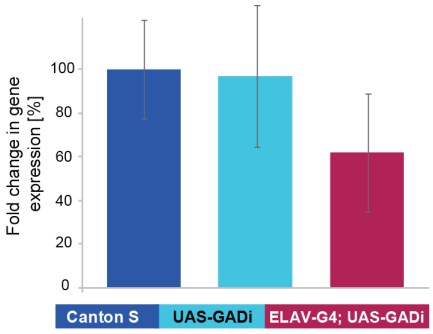

Figure S5 (related to Figure 6).

Q-PCR showing ~ 40% decrease of GAD1 mRNA in heterozygot ELAV-GAL4, GADi flies.

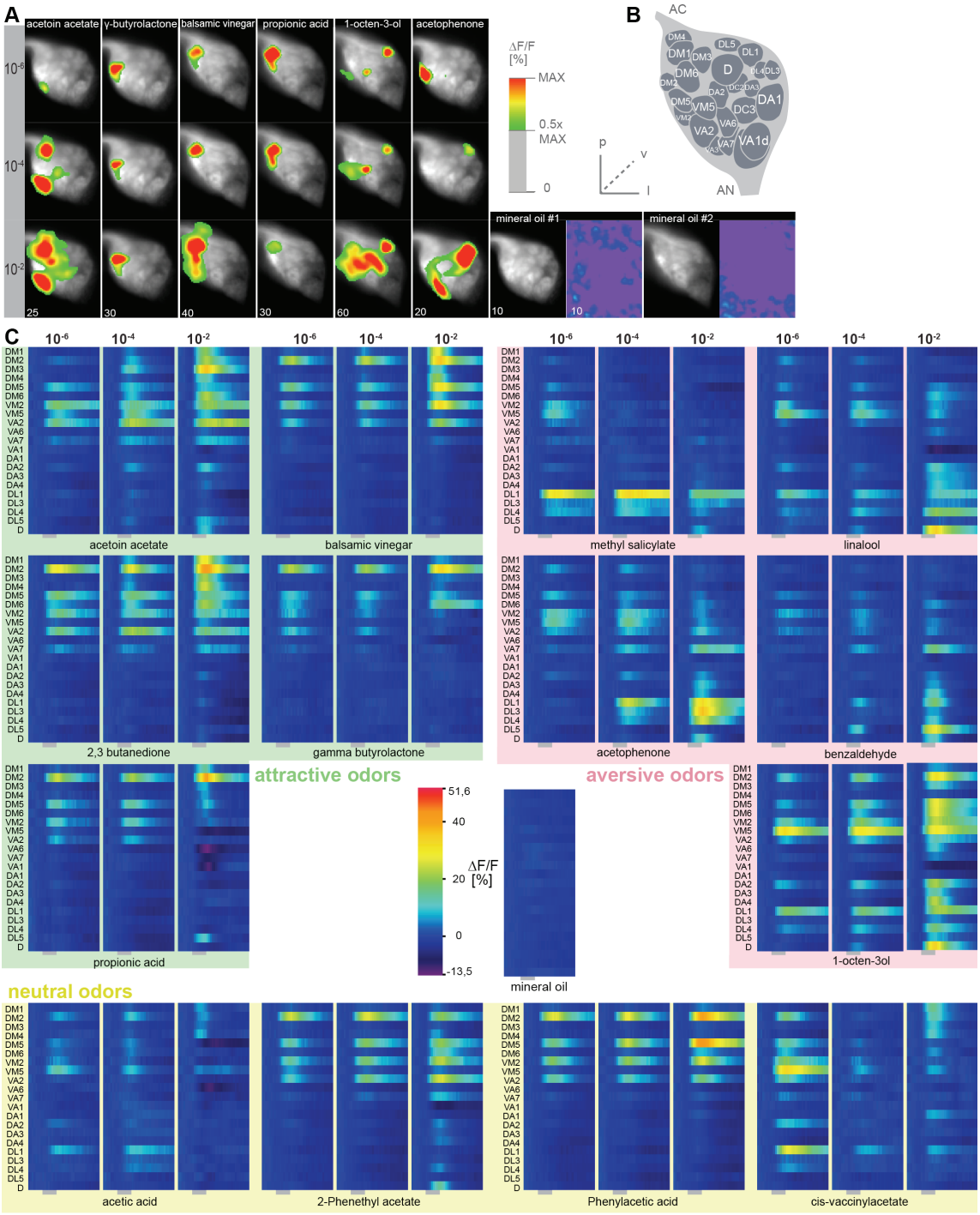

Figure S6 (related to Figure 7).

(A) Representative glomerular Ca^{2+}-responses for a subset of used odorants at three concentrations. Scale bar to the right. Control (mineral oil) recordings are shown additionally as full false-color coded images.

(B) Glomerular AL atlas.

(C) Median Ca^{2+}-activity traces of all glomeruli for all odorants at the three indicated concentrations. Scale bar and control measurement in the center. Odor application is indicated by the grey bar below the heatmaps (n=6-7).

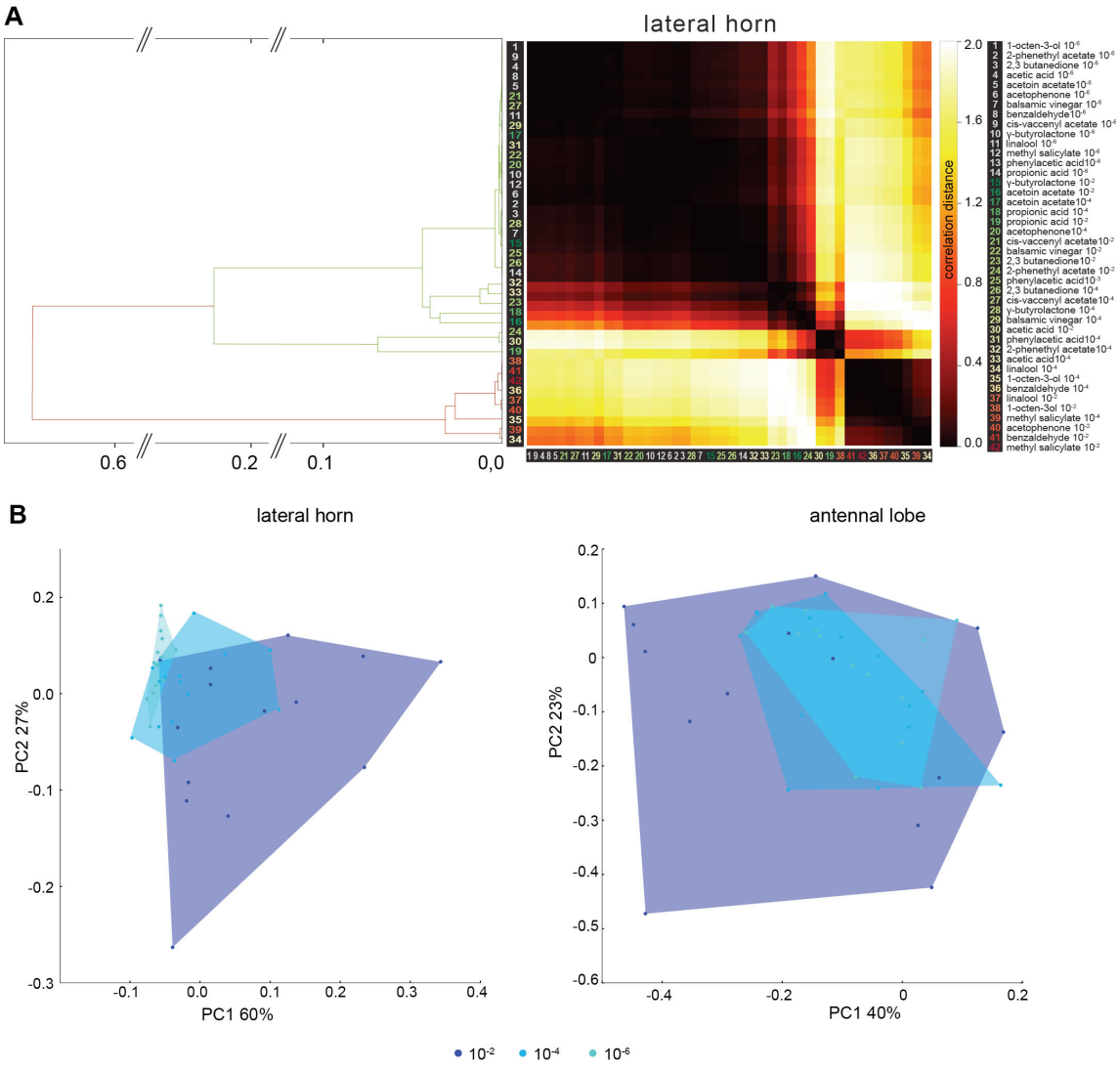

Figure S7 (related to Figure 7).

(A) Correlation distance dendrogramm of odor-evoked response patterns in the LH (left) and analogous matrix (right). For clarity dendrogramm arms were colored green and red: repulsive and attractive odorants are clearly not correlated, as indicated by a correlation distance > 0.6.

(B) Median odor activity in the AL and LH in a PCA space (identical to Figure 7D). Odors are grouped according to concentration: dark blue = 10^{-2} , median blue = 10^{-4} and light blue = 10^{-6}. In the AL odor representations clearly overlap for all concentrations. Similary in the LH, odor representations of all concentrations partly overlap, but do display a slight tendency to segregate.

General discussion

□ ithin its en□ironment an animal is sub□ected to an enormous number o□ di□□erent odorants. Some o□ these odorants might deri□e □rom □ood or mating □artners, and, hence, might mean something good to the recei□er. □thers might deri□e □rom a □redator or s□oiled □ood, and, there□ore, might be regarded as negati□e cues. Howe□er, the □ast amount o□ com□ounds might deri□e □rom sources that do not ha□e any meaning to the animal, and there□ore might be neutral. The main task of an animal's system is there□ore, to e□tract relati□e in□ormation □rom the otherwise con□using ol□actory background.

□he work □resented in my thesis deals with the □uestion, under which situation the □inegar □ly *Drosophila melanogaster* regards s□eci□ic odorants as attracti□e or re□ellent, and how attracti□e and re□ellent odorants are sensed and processed by the fly's olfactory system.

Single vs. combinatorial nature of odor coding

□dor□guided beha□ior is triggered by odor detection □ia □S□s e□□ressing di□□erent kinds o□ odorant rece□tors and the resulting acti□ation o□ a □articular neuronal circuit. □he ma□ority o□ odors are □rocessed by a combinatorial code, i.e., each odorant can acti□ate more than one rece□tor and each rece□tor can be acti□ated by more than one odorant. □hus, e□en indi□idual odorants acti□ate a com□rehensi□e neuronal circuit that □inally go□erns the beha□ioral out□ut. □ hat might be the ad□antage o□ this combinatorial code□ □t might be economically meaning□ul when an □S□ that e□□resses a single odorant rece□tor res□onds to more than one odor. As there are thousands o□ odorants □resent in the fly's environment, by detecting only one odorant □er □S□ ty□e, the □ly would need a □ery large number □S□ ty□es. Howe□er by a reduced number o□□S□ ty□es that each are rather uns□eci□ic, i.e., they res□ond to a subset o□ odorants with some odorants yielding higher res□onses than others, the □ly can co□e with only □ew □S□s and a com□arati□ely small brain. □nly in those cases, where the stimulus is ecologically □ery im□ortant for a fly's survival, the stimulus might target only a single highly s□eci□ic rece□tor. □n these cases there is only one rece□tor that detects a gi□en stimulus and acti□ates a segregated straight circuit □or a robust beha□ior□one e□am□le is □□□, which is □roduced by stressed □lies. Furthermore □rolonged e□□osure to high concentrations can cause unconsciousness and death. □here□ore this com□ound acts as a strong re□ellent □or other □lies (Suh et al., □□□□. □n □lies, the □□□ circuit there□ore □orms a □unctionally segregated labeled line □athway that mediates innate a□oidance (Suh et al., □□□□. □□□ is not detected by □Rs

but by a □air o□s□ecialized and conser□ed chemorece□tors nested within the insect gustatory rece□tor □amily (Jones et al., □□□□; Kwon et al., □□□□).

□his kind o□□rocessing □ia a so□called labeled line is a rare case and seems to be restricted to com□ounds o□signi□icance im□act to the fly's sur□i□al. □t was, there□ore, astonishing that we □ound another com□ound that is □rocessed as straight □orward as □□□.

Geosmin signals for toxic molds and bacteria modulate and override innate odor-guided behavior

Geosmin indicates to□ic microbes that can cause illness or death. □t belongs to the large ter□enoid class o□ chemicals, and is hence similar to many other members o□ this grou□ □resent in the habitat o□ the □ly. □ontrary to more than □□□□ other com□ounds tested, geosmin targets □R □□a and triggers a single, □unctionally segregated □athway that mediates innate a□oidance in the □inegar □ly. □ e could show that this rece□tor is conser□ed in many *Drosophila* s□ecies. □here□ore the circuit dedicated to the □rocessing o□ geosmin seems to be an ancestral □eature o□ the ol□actory system o□ the genus *Drosophila*. □ e could □urthermore show that the message contained within this circuit is trans□erred unaltered □rom the □eri□hery to higher brain centers. Hence, like □□□, geosmin is □rocessed along a labeled line. □ hat is the ecological signi□icance behind geosmin that could e□□lain the □ormation o□ a labeled line□ Geosmin is a true signal signi□ying to□ic microbes to the □ly. Although abundant in nature, it is only □roduced by a narrow range o□ microbes that are to□ic to *Drosophila* but settle on the flies' main □ood source – o□erri□e □ruits. □here□ore by smelling and a□oiding geosmin, □lies are able to a□oid s□oiled □ood and to o□i□osit on sources that would be detrimental to lar□al de□elo□ment. □nly one close relati□e o□ *Drosophila melanogaster* has e□ol□ed a com□letely di□□erent □ood re□erence (*D. elegans,* which nectar □eeds in □lowers). □nterestingly this s□ecies lacks the geosmin s□eci□ic □athway. □he lack o□ a geosmin detection system in *D. elegans* would accordingly be a conse□uence o□ the low susce□tibility to mold growth in □resh □lowers (□oshida et al., □□□□).

Geosmin is not only a re□ellent by itsel□. Addition o□ geosmin to □inegar signi□icantly reduced □ositi□e chemota□is by □lies towards this innately attracti□e odor. □he ability to modulate a su□□osedly innate beha□ior is □uite e□traordinary. □n the light o□ the □hysiology □indings, the cause o□ the reduced attracti□eness o□ the geosmin□□inegar mi□ should stem e□clusi□ely □rom the acti□ation o□ the □A□ glomerulus. Acti□ation o□□A□ conse□uently seems to ha□e an o□□erriding ca□acity, ca□able o□ modulating e□en an innately □ositi□e beha□ior (Stensmyr et

al., □□□□.□□□□loiting these ty□es o□a□ersi□e s□eci□ic circuits that o□erride attraction to □ood sources could be an e□icient method □or mani□ulating the beha□ior o□insects□disease □ectors as well as agricultural □ests.

How hunger changes the perception and the responsiveness towards odors?

□ hile com□ounds that are sensed □ia a labeled line usually □ro□oke a stereoty□ic res□onse, other stimuli like e.g. □ood odors might change their meaning to an animal de□ending on the internal □in this case □eeding□state. A well□□ed animal should rather ignore in□ormation about □oodand should □ocus e.g. on cues leading to o□i□osition. Accordingly sensory □erce□tion o□ some odors has been shown to de□end on the □hysiological status o□an animal and is in□luenced by changes at di□□erent le□els o□the neural circuit. Root et al. found that the flies' beha□ior towards a single □ood odorant changes u□on star□ation and that this change is go□erned □ia a □athway including neuronal in□ormation trans□er □ia short neuro□e□tide F □s□□F□. Based on these □indings □asked, whether this star□ation e□□ect is restricted to □ood odorants and to sensory neurons e□□ressing s□□F or its corres□onding rece□tor. □sing beha□ioral bioassays □could show that □lies e□hibit increased attraction to ethyl acetate a□ter star□ation. Star□ation did not increase the res□onse to this odorant only but also to another □oododor and e□en to a re□ellent □benzaldehyde□and a □heromone □cVA□□conclude that the star□ation e□□ect is not restricted to a small subset o□□ood odorants □Farhan et al. in □ress□. □ ne□t □er□ormed single sensillum recordings to e□amine whether □ood de□ri□ation causes increased sensiti□ity at the le□el o□□S□s. □ndeed, we □ound increased sensiti□ities in all □S□ ty□es tested. □ur □indings are su□□orted with results showing that star□ation increased □eri□heral sensiti□ity in *Spodoptera littoralis* □Martel et. al., □□□□□. □ur □indings are in accordance with studies showing that host seeking beha□ior by □emale mos□uitoes *Aedes aegypti* is de□ressed □ollowing a blood meal, suggesting a □ossible link between □eeding and rece□tor sensiti□ity. □a□is □□□□□□in his study in□estigated the e□□ect o□blood □eeding on sensory neurons that are s□eci□ic to lactic acid □i.e. one o□the main attractants in host odor□ and □ound that stimulus□induced s□ike re□uency in □emales decreased u□on blood □eeding. □nterestingly the sensiti□ity towards lactic acid returns to normal when a □ed □emale was allowed to o□i□osit. □n a se□arate study, Bernays and □ha□man □□□□□□ re□orted that a substance □rom the cor□ora cardiaca o□recently □ed *Locusta migratoria* directly acts on a sensillum o□the ma□illary □al□. □t □resumably causes the closure o□terminal □ores o□the sensilla, and, thereby, reduces the sensiti□ity o□the neurons □ollowing □eeding. □ e also made similar obser□ations when we shortly □ed □lies a□ter a □rolonged □eriod o□star□ation. □he

sensitivity towards food odorants fell within a short time after feeding both in the behavioral and physiological experiments. It will be interesting to test, whether the reduction of the starvation effect is governed via gustatory input (i.e. gustatory sensory neurons that become activated by tasting e.g. sugar), or via feedback from the digestive system.

When Root et al., (2011) observed an increased physiological responsiveness in starved flies, they did so by measuring the activity of olfactory glomeruli in the antennal lobe via calcium imaging. We reasoned that an increased behavioral sensitivity of starved flies could also be mediated by an increased physiological sensitivity already in the periheral sensory neurons housed in the fly's sensilla. Our electrophysiological recordings support this hypothesis, since we found increased responses already at this level in starved flies. However, we cannot rule out that additional effects within the antennal lobe or higher brain structures play a role governing the starvation effect. Indeed Root et al. described an elegant mechanism by which insulin signaling modulates the expression of sNPF, leading to presynaptic enhancement of odor responses selectively in the starved state (Root, 2011). This, in turn, increased food-seeking behavior in starved animals. As some of these PNs do not express neither sNPF nor its receptor sNPFR (Wilson et al., 2003; Carlsson et al., 2010), next investigated, which other molecular players could be involved in the starvation effect and, therefore, performed microarray analyses with isolated antennae and isolated brains from starved and fed flies. The resulting gene expression analysis revealed several genes whose expression levels were affected by the flies' physiological status. While most of these genes belonged to gene classes involved in nutrient metabolism, others were uncharacterized and were probably not related to feeding or behavior. The relative ease of conducting RNAi knockdown experiments with some the identified genes coupled with a quantitative olfactory assay opened the door to identify novel regulators of a feeding-state-dependent modulation of odor-guided behavior. By doing so we identified AstA-Hamide as another molecular player that is involved in governing the starvation effect. As some of these PNs express neither sNPF nor its receptor sNPFR (Wilson et al., 2003; Carlsson et al., 2010), next investigated, which other molecular players could be involved in the starvation effect. We focused on some of the up-regulated genes that are known to be involved in the synthesis of neuropeptides (allatostatine) or of neuropeptide receptors (sNPFR and AlstR). Found the differential role of these molecules according to their localization in sensilla. When we tested the behavior of starved flies to ethyl acetate, silencing allatostatine and its corresponding receptor, or the sNPF receptor did not affect the starvation effect. Only silencing the AstA-Hamide-receptor resulted in an

abolished starvation effect, suggesting a major role of DH44-Hamide-2 or its corresponding receptor in starvation-induced modulation in PR-to-PN processing OSNs. Which we further confirmed by DH44-Hamide-2 mutant study.

This study shows that the fly's antennal OSNs seem to be constantly tuned to current needs. By increasing the sensitivity of many OSN populations not only those that are involved in detecting food odors, starved flies might improve their ability not only to detect food sources, but also to judge their quality. Future investigation will tell, whether starvation effects can be foundalso in neuronal population other than OSNs, like e.g. interneurons or projection neurons. Furthermore it would be interesting to test, whether the response to stimuli like CO2 or geosmin that are processed by labeled lines also becomes affected by starvation.

Which part in the brain controls innate odor-guided behavior?

As discussed above, whether or not a fly becomes attracted to an odor source depends not only on the odorant's identity, but also on the internal state of the fly. When investigating the starvation effect we already observed that in addition to the internal state the concentration of an odorant strongly affects its valence for a fly. In most cases, even regarding food odorants flies are attracted to low or medium concentrations but become repelled by highly concentrated odorants. Therefore, the olfactory system of the fly does not only need to identify an odorant's identity, but also has to inform about its concentration. We, therefore, asked the question, which part of the brain is involved in processing odorant identity and concentration. It has been shown, that particular glomeruli are involved in the processing of innately attractive and repellent odorants (Semmelhack and Wang, a et al., 2014Ai M et al., 2010Min S et al., 2013). It seems that glomeruli situated in the lateral part of the antennal lobe are mainly activated by repellent odorants, while glomeruli in the medial part more strongly respond to attractive odorants (Knaden et al., 2012). From the antennal lobe, however, olfactory information is transferred via excitatory projection neurons (PNs) to the mushroom body and the lateral horn. As the experimental exclusion of the mushroom body does not affect the behavior of naive flies towards innately attractive or repellent odorants (Heisenberg, 2003), this part of the olfactory circuit seems to be mainly or even exclusively involved in associative olfactory learning (Heisenberg, 2003Hebelle, 2015). A recent study (Caron et al., 2013) showed that each Kenyon cell in the mushroom body integrates information from a random set of glomeruli. Having no stereotyped connection, the pattern of Kenyon cell activity probably does not represent innate olfactory valence but rather informs

about learned associations o an odorant and a good or bad e erience. e, there ore, ocused on the role o the lateral horn on the rocessing o innate ol actory res onses. Recent indings suggest that the segregated re resentation o attracti e and re ellent odorants that was ound in the antennal lobe Knaden et al., is maintained rom the antennal lobe to the lateral horn Min et al., as s emerging rom glomeruli that rocess re ellent stimuli like or acids ro ect to the medial anterior region o the lateral horn H, while those carrying in ormation about attracti e amines ro ect to the lateral osterior region. his segregation at the lateral horn was, howe er, deduced rom only a ew traced lines, and did not include a sub o ulation o inhibitory ro ection neurons i s. So ar, the i athway is only artly in estigated at the mor hological le el to et al., ai et al., i s target the H e clusi ely and by ass the MBc. By using a s eci ic dri er line M we were able to in estigate the im act o this inhibitory athway on ol actory rocessing within the H. e were able to identi y two s atially and unctionally segregated grou s o i s o which one e tracts ositi e hedonic alence i.e. mainly rocesses attracti e odorants and the other intensity in ormation. haracterizing the mor hological structure o these i s re ealed that they e hibit an oligoglomerular dendritic attern, and hence di er rom e s that ha e been shown to be uniglomerular Vosshall and Stocker, herefore, indi idual i s can be acti ated by a subset o S s. nterestingly those glomeruli that had been shown to be in ol ed in rocessing attracti e alence Knaden et al., were articularly densely inner ated, while glomeruli rocessing negati e alence were rather omitted by i s.

o these i s decode odor eatures and go ern decision making By selecti ely silencing i s ia interru ting GABA synthesis we were able to reduce the lies' attraction to almost all attracti e odorants. As mentioned be ore, whether a ly becomes attracted by an odorant or not does not only de end on the odorants identity but also intensity. nterestingly, silencing the i s did not only reduce the odorants' overall attractiveness, but resulted also in lies that were less able to discriminate between di erent odorant concentrations. hough the alence e ect clearly dominates o er the concentration e ect, our results suggest that i s are indeed ca able o e tracting both modalities rom the combinatorial A code.

hen we er ormed calcium imaging e eriments to study the ol actory dri en acti ation attern within the lateral horn, we ound three domains with di erent highly stereoty ic res onse atterns. he so called lateral horn osterior medial domain H M domain was strongly acti ated by innately attracti e odorants, while the anterior lateral domain was

mainly activated by repellent odorants. Interestingly the activation of the third domain, the anterior medial domain (mAH AM domain) was valence independent and mainly coded for odorant intensity.

To internally reflect the sensory environment, animals create neural maps encoding the raw information of the external stimulus space. From that primary neural code relevant information has to be extracted for accurate navigation. Our findings suggest that the spatial representation of odorant valence, which is formed within the antennal lobe, still exists at the level of the lateral horn but becomes further complemented by a segregated representation of stimulus intensity.

Jefferis et al. already provided evidence for a separated representation of pheromone and fruit odors in the mAH and therefore hypothesized that the mAH is organized on the basis of the biological values of odorants (Jefferis et al., 2007). Within our functional imaging screen the fly pheromone cis-vaccenyl acetate activated the attraction coding mAH-mM region in a strikingly constant fashion, providing evidence that even in the case of this attractive fly pheromone (Bartelt et al., 1985; Kurtovic et al., 2007) iPNs collect the specific trait selectively and integrate this information into a common domain with distinct information about odorants. This additionally reveals the independence of the iPN processing stream from the ePN channel, since iPNs obviously transfer the odor modalities completely detached of the initial odor identity.

Conclusion

This thesis extends our current knowledge regarding odor-guided behavior in Drosophila by revealing strategies of olfactory coding and of modulations of the olfactory circuit. It describes a segregated neuronal pathway to detect toxic microbes by the signature odor geosmin. Being so specific this pathway displays an exception from the general combinatorial coding strategy. Furthermore, this thesis elucidates how hunger can change the flys physiological perception of odors and the attraction to these odors. Finally the thesis highlights the role of inhibitory projection neurons in odor coding at a higher brain centre and their role in odor-guided behavior. In conclusion, the findings within my thesis reveal general rules of how olfactory valence is processed in the Drosophila brain and how the valence is affected by the inner state of the fly.

Summary

The aim of this dissertation thesis is to unravel the strategies for odor-guided behavior and its modulation mechanism. To investigate we employed the fruit fly *Drosophila melanogaster* as model system. Using an odor set of versatile ecological relevance we studied modulation at several processing stages, including at the periphery (the antennae), the primary olfactory center (the antennal lobe) and the higher brain centers. The methods we applied were the Y-maze assay for behavior, single sensillum recording for electrophysiology and Ca2+ imaging of distinct neuronal types contributing to the olfactory network. In addition to all these techniques we also used the *Drosophila* genetics toolbox for manipulation of desired proteins to neuronal pathways.

The fly detects odor by different physiological types of sensory neurons, each one expressing only one specific olfactory receptor. To detect a very large number of volatiles, most of the olfactory receptors have multiple affinities to different odorants and form the combinatorial patterns. Also there are only a few olfactory receptors which have specific affinity to one odorant and form the segregated pathway. This thesis elucidates one exceptional case with highly conserved evolutionarily principles. A *labeled line* circuit of fundamental significance for the animal's survival could be discovered: the geosmin pathway is exclusively tuned to the repellent product of toxic microorganisms and therefore displays an exception from the general combinatorial coding strategy.

Modulation and plasticity are key functions for all organisms to adapt to stress and a changing environment. Examples of this include blood-feeding insects, which after a blood meal switch their olfactory preference from host odors to odors specific for oviposition sites. We investigated whether the feeding status modulates the flies' physiological and behavioral responses to odors. We first started with behavior trials for different odorants. Also to know if these modulations are peripheral or central we included an electrophysiological study. Starved flies exhibited a decreased behavioral threshold to odorants, while the sensitivity of OSNs was increased after starvation. The change in behavioral and physiological modulations was not restricted to food odors only, but was also found for non-food odors and pheromones. Furthermore we did microarray analysis to get the hint for molecular players. We dissected out the role of biogenic amines by using the TASTRNAi and GAL4 silencing tool. It revealed neuropeptides play a role at the level of olfactory sensory neurons. Hence, flies seem to be

tuned to locate potential food sources from long distance, as well as to evaluate food quality and the presence of conspecifics efficiently, depending on their feeding status.

Depending on the receptor expressed, sensory neurons send their axons to the antennal lobe and target functional and morphological subunits, termed as glomeruli. In the antennal lobe, local interneurons can modulate olfactory information by interconnecting glomeruli. Projection neurons, which are the output neurons from the antennal lobe, receive modified olfactory information, which they convey to higher brain regions, including the mushroom body and the lateral horn. The mushroom body calyx is mainly involved in the formation of olfactory memories while the lateral horn is thought to be responsible for innate behaviors, therefore these have been a major focus of this thesis. Projection neurons appear as two types. One type is uniglomerular, which is excitatory and innervates all antennal lobe glomeruli as well as both higher brain regions. The second is oligoglomerular, which is inhibitory and targets the lateral horn exclusively. The modulatory interneurons transform the primary odor code towards a code containing information about the hedonic valence of odors. Since excitatory projection neurons are dedicated to single glomeruli, they extract odor identity and hedonic valence from the combinatorial code in the antennal lobe. Moreover we were able to show that inhibitory projection neurons constitute a segregated parallel processing stream to the higher brain and indeed perform a *decoding* of odor features from the antennal lobe. Since the lateral horn is innervated by all projection neurons, these processing streams are reunited in this area and valence and intensity specific information can be computed to configure the ultimate behavioral output.

In conclusion, the findings within my thesis indicate a general rule for innate odor-guided behavior as well as a mechanism modulating or underlying innate odor-guided behavior. I suggest that these modulatory mechanisms might also be a general feature of olfactory systems in other species ranging from invertebrates to mammals to maximize their chance of fitness for survival.

Zusammenfassung

Diese Dissertation behandelt die Strategien und modulatorischen Mechanismen des duftgesteuerten Verhaltens am Modell der Fruchtfliege *Drosophila melanogaster*. Anhand ökologisch relevanter Düfte habe ich untersucht, wie duftgesteuertes Verhalten von verschiedenen Verrechnungsebenen des duftsensorischen Systems moduliert und gesteuert wird. Dabei habe ich sowohl die Detektion der Düfte in der sensorischen Peripherie (d.h auf der Antenne), als auch die neuronale Verarbeitung im ersten Duftverrrechnungszentrum (dem Antennallobus) und in höheren Gehirnzentren (dem lateralen Horn) berücksichtigt. Die Methoden meiner Arbeit umfassen Verhaltensexperimente, bei denen die Fliegen in einem T-förmigen Rohr sich für oder gegen einen Duft entscheiden müssen. Weiterhin wurden Einzelsensillenableitungen und Ca^{2+}-Imaging Experimente durchgeführt, um Aussagen über die olfaktorische Sensitivität der Fliegen und die Art der neuronalen Verrechnung im Gehirn treffen zu können. Bei all diesen Experimente konnte ich mich zusätzlich der ausgefeilten genetischen Werkzeuge bedienen, die für *Drosophila* etabliert worden sind.

Die Fruchtfliege nimmt Duft über physiologisch unterschiedliche Typen von sensorischen Neuronen wahr, von denen jeder Typ einen spezifischen Duftrezeptor exprimiert. Um die Vielzahl der Umweltdüfte wahrnehmen zu können, sind die meisten Rezeptoren nicht sehr spezifisch, sondern reagieren mit verschiedenen Duftmolekülen. Anhand der sogenannten kombinatorischen Kodierung, d.h. der Verrechnung gleichzeitiger Aktivierungen verschiedener Neuronentypen, ist die Fliege dennoch in der Lage, einzelne Düfte oder Duftgemische zu erkennen. Zusätzlich verfügt *Drosophila* jedoch über einige wenige Neuronentypen mit hochspezifischen Rezeptoren, die nur auf einzelne, ökologisch besonders relevante, Düfte reagieren, und die diese Information nahezu unprozessiert an höhere Hirnzentren weiterleiten. Einer dieser seltenen Fälle, die hochspezialisierte Detektion von Geosmin, einem Signaturduft verdorbener Nahrung, wird in dieser Arbeit vorgestellt.

Modulation und Plastizität sensorischer Systeme sind Schlüsselfunktionen, die es einem Tier erlauben, auf Stresssituation, eine sich verändernde Umwelt, oder neue Anforderungen im Verlauf des Lebenszyklusses zu reagieren. Beispielsweise ändern

blutsaugende Mücken, die normalerweise von C□2 und Körperdüften angezogen werden, nach einem Blutmahl ihre Präferenz hin zu Düften, die spezisch für mögliche Eiablageplätze sind. Diese geänderte Verhaltenspräferenz geht einher mit einer geänderten physiologischen Sensitivität für die involvierten Düfte. In meiner Arbeit untersuche ich, abermals anhand des Modellorganismus *Drosophila*, inwieweit ausgedehnte Hungerperioden die olfaktorische Sensitivität und Präferenz der Tiere beeinflussen. Gehungerte Fliegen wurden in Verhaltensexperimenten generell stärker von Düften angezogen. Diese Verhaltensänderung ging einher mit einer erhöhten Sensitivität der olfaktorischen sensorischen Neurone (□SNs). Interessanterweise beschränkte sich sowohl die Modulation des Verhaltens als auch die der Sensorik nicht auf Futterdüfte, sondern zeigte sich auch bei Düften aus anderen Kontexten, wie z.B. Pheromonen. Anhand einer Genexpressionsanalyse, konnte ich einige Gene identifizieren, die bei hungrigen Fliegen stärker exprimiert wurden. Da für biogene Amine gezeigt wurde, dass sie oft an der Modulation von neuronalen Prozessen beteiligt sind, habe ich die Amine, deren Expression (bzw. die Expression der zugehörigen Rezeptoren) durch Hunger hochreguliert war, näher untersucht. Anhand des genetischen UAS-*RNAi* und GAL□ Werkzeugs, war ich in der Lage die Expression einzelner Gene zu unterbinden (bzw. stark abzuschwächen) und mit den so manipulierten Fliegen die Hungerexperimente zu wiederholen. Es zeigte sich, dass nicht nur der schon beschriebene *Short neuropeptide F* Rezeptor, sondern auch der Rezeptor für CCHamide □ eine modulierende Rolle bei der Sensitisierung gehungerter Fliegen spielt. Meine Ergebnise deuten darauf hin, dass der olfaktorisch sensorische Apparat gehungerter Fliegen gezielt darauf abgestimmt wird, nicht nur Futter schon von gro□er Entfernung wahrzunehmen (durch die Sensitisierung von auf Futterdüfte spezialisierten □SNs). Durch die globale Sensitisierung aller □SNs sollten die Fliegen auch auch besser in der Lage sein, die □ualität des Futters und die Anwesenheit weiterer Fliegen.

Während die letztgenannte Studie sich u.a. mit der Detektion der Düfte durch □SNs beschäftigte, ging es in der letzten Studie um die Verrechnung und Bewertung von Düften im Gehirn. □e nachdem, welchen Rezeptor ein □SN exprimiert, innerviert dieses eine bestimmte morphologische Untereinheit im Antennallobus, den sogenannten Glomerulus. Nach einer gewissen Prozessierung durch Interneurone, die die verschiedenen Glomeruli miteinander verbinden, wird die Information von Projektionsneuronen (PNs) weiter an die höheren Hinzentren Pilzkörper und laterales Horn geleitet. Da die Rolle des Pilzkörpers schon umfangreich untersucht wurde (er ist in

das assoziative Lernen von Düften involviert), habe ich mich mit der Rolle des lateralen Horns befasst. Das laterale Horn steht im Verdacht, hauptsächlich das angeborene duftgesteuerte Verhalten der Fliege zu generieren. Es wird von zwei verschiedenen Typen von Projektionsneuronen innerviert, den exzitatorischen und den inhibitorischen PNs. Ich konnte zeigen, dass die inhibitorischen PNs, im Gegensatz zu den besser untersuchten exzitorischen PNs, welche ihre Information jeweils nur von einem Glomerulus beziehen, oligoglomerular verschalten sind, d.h. Informationen von mehreren Glomeruli bekommen. Weiterhin konnte ich zeigen, dass diese Neuronen nicht nur Informationen bezüglich der Wertigkeit der Düfte (d.h., ob ein Duft attraktiv oder abschreckend ist) prozessieren, sondern eine Subpopulation dieser PNs auch die für das Verhalten der Fliege ebenfalls entscheidende Konzentration der Düfte verarbeitet. Interessanterweise innervieren die verschiedenen PN Populationen drei unterschiedliche Regionen im lateralen Horn, von der eine hauptsächlich durch attraktive und die zweite durch abschreckende Düfte angeregt wird, während die dritte Region die Duftkonzentration verarbeitet.

Zusammenfassend deuten die Ergebnisse meiner Arbeit auf generelle Regeln für die Modulation und das Auslösen duftgesteuerten Verhaltens hin. Aufgrund des sehr ähnlichen Aufbaus der olfaktorischen Systeme in Insekten und Wirbeltieren, vermute ich, dass die von mir beobachteten Eigenschaften des olfaktorischen Systems auch bei anderen Tieren eine überlebenswichtige Rolle spielen.

References

Ai M, Min S, Grosjean □, Leblanc C, Bell R, Benton R, Suh GSB (2□□□). Acid sensing by the *Drosophila* olfactory system. Nature *468*□□□□-U□□2.

Arndt, C., Cruz, M.C., Cardenas, M.E., and Heitman, □ (□□□□). Secretion of FK□□□FK□2□ and rapamycin by Streptomyces inhibits the growth of competing *Saccharomyces cerevisiae* and *Cryptococcus neoformans*. Micro-biology *145*, □□□□-2□□□.

Asahina, K., Pavlenkovich, V., and Vosshall, L.B. (2□□□). The survival advantage of olfaction in a competitive environment. Curr Biol *18*, □□□-□□□□

Axel, R. (□□□□). The Molecular Logic of Smell. Sci. Am. *273*, □□-□□□□.

Barrows, W. M. (□□□□). The reactions of the Pomace fly, *Drosophila ampelophila loew*, to odorous substances. □. Exp. Zool. *4*□□ □-□□□□.

Bartelt, R.□, Schaner, A.M., and □ackson, L.L. (□□□□). Cis-vaccenyl acetate as an aggregation pheromone in *Drosophila melanogaster*. □Chem Ecol *11*, □□□-□□□□.

Baumberger, □ (□□□□). Solid media for rearing *Drosophila*. Am. Nat. *51*(□□□,)□□□-□□□.

Bausenwein, B., Dittrich, a P., and Fischbach, K.F. (□□□2). The optic lobe of *Drosophila melanogaster*. II. Sorting of retinotopic pathways in the medulla. Cell Tissue Res *267*, □□-2□.

Becher, P.G., Bengtsson, M., Hansson, B.S. and Witzgall, P. (2□□□). Flying the fly□Long-range flight behavior of *Drosophila melanogaster* to attractive odors. □ Chem. Ecol. *36*, □□□□-□□.

Benton, R. (2□□□). Chemical sensing in *Drosophila*. Curr □pin Neurobiol *18*□□□□-□□.

Benton, R., Vannice, K.S., Gomez-Diaz, C., and Vosshall, L.B (2□□□). Variant ionotropic glutamate receptors as chemosensory receptors in *Drosophila*. Cell *136*, □□□-□□2.

Bernays, E.A., Blaney, W.M. □ Chapman, R.F. (□□□2). Changes in chemoreceptor sensilla on the maxillary palps of *Locustamigratoria* in relation to feeding. □exp.Biol.*57*, □□-□□□□.

Bhandawat, V., □lsen, S.R., Gouwens, N.W., Schlief, M.L., and Wilson, R.I.(2□□□). Sensory processing in the *Drosophila* antennal lobe increases reliability and separability of ensemble odor representations. Nat. Neurosci. *10*, □□□□-□□□□2.

Bowen, M.F., Davis, E.E., Haggart, D.A.(□□□□). A behavioural and sensory analysis of host-seeking behaviour in the diapausing mos□uito *Culex pipiens*. □ Insect Physiol. *34*, □□-□□□□.

C. □ Denotter, T. Tchicaya, A. M. Schutte (□□□□) Effects of age, sex and hunger on the antennal olfactory sensitivity of tsetse flies. Physiol. Entomol. *16*□□ □-□□2.

Carlson, R. (). lfaction in *Drosophila* From odor to behavior. TIG *12*, -.

Carlsson, M.A., Diesner, M., Schachtner, , Nässel, D.R. (2) Multiple neuropeptides in the *Drosophila* antennal lobe suggest complex modulatory circuits. Comp. Neurol. *518*() --.

Caron, S., Ruta, V., Abbott, L.F., and Axel, R. (2). Random convergence of olfactory inputs in the *Drosophila* mushroom body. Nature *497*, –.

Carvalho GB, Kapahi P, Anderson D, Benzer S (2). Allocrine modulation of feeding behavior by the sex peptide of *Drosophila*. Curr Biol *16* 2– .

Castillo, M.-A., Moya, P., Cantín, A., Miranda, M.A., Primo, , Hernández, E., and Primo-u fera, E. (). Insecticidal, antijuvenile hormone, and fungicidal activities of organic extracts from different *Penicillium* species and their isolated active components. Agric. Food Chem. *47*, 2–2–2.

Chakraborty, T.S., Goswami, S.P., and Siddi i, . (2). Sensory correlates of imaginal conditioning in *Drosophila melanogaster*. neurogenet. *23*, 2- 2.

Chen, Z., and Cichocki, A. (2). Nonnegative Matrix Factorization with Temporal Smoothness and or Spatial Decorrelation Constraints. Signal Processing (preprint).

Chou, .-H., Spletter, M.L., aksi, E., Leong, C.S., Wilson, R.I., and Luo, L. (2). Diversity and wiring variability of olfactory local interneurons in the *Drosophila* antennal lobe. Nat. Neurosci *13*, –.

Cichocki, A., and Phan, A. (2). Fast Local Algorithms for Large Scale Nonnegative Matrix and Tensor Factorizations. IEICE Trans. *E92-A*, -.

Connolly, B., Roberts, I. H., Armstrong, D., Kaiser, K., Forte, M., Tully, T., and Kane, C. . (). Associative Learning Disrupted by Impaired Gs Signaling in *Drosophila* Mushroom Bodies. Science *274*, 2–2.

Couto, A., Alenius, M., and Dickson, B. (2). Molecular, anatomical, and functional organization of the *Drosophila* olfactory system. Curr. Biol. *15*, –.

Datta, S.R., Vasconcelos, M.L., Ruta, V., Luo, S., Wong, A., Demir, E., Flores, , Balonze, K., Dickson, B., and Axel, R. (2). The *Drosophila* pheromone *c*VA activates a sexually dimorphic neural circuit. Nature *452*, –.

Davis, E.E. (). Regulation of sensitivity in the peripheral chemoreceptor systems for host-seeking behaviour by a haemolymph-borne factor in *Aedes aegypti*. Insect Physiol. *30*, –.

Davis, R.L. (2). Traces of *Drosophila* memory. Neuron *70*, -.

De Belle S, H.M. (). Associative dor Learning in *Drosophila* Abolished by Chemical Ablation of Mushroom Bodies. Science *263*, 2-2.

de Bruyne M, Foster K, Carlson R (2□□□). □dor coding in the *Drosophila* antenna. Neuron *30*, □□□ □□2.

de Bruyne, M., Clyne, P.□, and Carlson, □R. (□□□□). □dor coding in a model olfactory organ□The *Drosophila* maxillary palp. □ Neurosci. *19*, □□2-□□□2.

Debelle □S, Heisenberg M. (□□□□). Associative odor learning in *Drosophila* abolished by chemical ablation of mushroom bodies. Science *263*□□□2-□□□.

Denotter, C.□, Tchicaya, T., and Schutte, A.M. (□□□□). Effects of age, sex and hunger on the antennal olfactory sensitivity of tsetse flies. Physiol. Entomol. *16*, □□-□□□2.

Devaud □M, Acebes A, Ramaswami M, Ferrus A (2□□□). Structural and functional changes in the olfactory pathway of adult *Drosophila* take place at a critical age. □Neurobiol. *56*□□□–2□.

DiAntonio, A., Schwarzl, T.L., Burgess, W., Scheller, H., Chin, C., and Deitcher, I.D.L. (□□□□)Identification and Characterization of *Drosophila* Genes for Synaptic Vesicle Proteins. □ Neurosci. *73*, □□2–□□□□.

Fishilevich, E., and Vosshall, L.B. (2□□□). Genetic and functional subdivision of the *Drosophila* antennal lobe. Curr. Biol. *15*, □□□–□□□□.

Galizia, C.G., and Rössler, W. (2□□□). Parallel olfactory systems in insects□anatomy and function. Annu. Rev. Entomol. *55*, □□-□□2□.

Gao, F.B., Kohwi, M., Brenman, □E., □an, L.□., □an, □.N. (2□□□). Control of dendritic field formation in *Drosophila*□the roles of flamingo and competition between homologous neurons. Neuron *28*(□)□□□--□□□.

Gerber, N. N. and Lechevalier, H. A. (□□□□). Geosmin, an earthy-smelling substance isolated from *actinoycetes*. Appl. Microbiol. *13*, □□-□□□□.

Giurfa, M. (2□□□). Behavioral and neural analysis of associative learning in the honeybee□a taste from the magic well. □ Comp. Physiol. A *193*, □□-□□2□.

Gong, Z. (2□□2). Innate preference in *Drosophila melanogaster*. Sci. China Life sci. *55*, □-□□.

Guo, S., and Kim, □ (2□□□). Molecular evolution of *Drosophila* odorant receptor genes. Mol. Biol. Evol. *24*, □□□□–□2□□.

Gust, B., Challis, G.L., Fowler, K., Kieser, T., and Chater, K.F. (2□□□). PCR- targeted *Streptomyces* gene replacement identifies a protein domain needed for biosynthesis of the ses□uiterpene soil odor geosmin. Proc. Natl. Acad. Sci. USA *100*, □□□□–□□□□.

Hallem, E.A., and Carlson, □R. (2□□□). Coding of odors by a receptor repertoire. Cell *125*, □□□□-□□.

Hallem, E.A., Ho, M.G., and Carlson, R.(2). The molecular basis of odor coding in the *Drosophila* antenna. Cell *117*, .

Hamada, F.N., Rosenzweig, M., Kang, K., Pulver, S.R., Ghezzi, A., egla, T., and Garrity, P.A. (2). An internal thermal sensor controlling temperature preference in *Drosophila*. Nature *454*, 2.

Hansson, B.S., and Stensmyr, M.C. (2). Evolution of insect olfaction. Neuron *72*, .

Hansson, B.S., Knaden, M., Sachse, S., Stensmyr, M.C., and Wicher, D. (2). Towards plant-odor-related olfactory neuroethology in *Drosophila*. Chemoecology *20*, .

Harris, A., Petersen, R.S., and Diamond, M.E. (2). The Cortical Distribution of Sensory Memories. Neuron *30*, .

Heimbeck, G., Bugnon, V., Gendre, N., Keller, a, and Stocker, R.F. (2). A central neural circuit for experience-independent olfactory and courtship behavior in *Drosophila melanogaster*. Proc. Natl. Acad. Sci. USA *98*, .

Heisenberg M, Borst A, Wagner S, Byers D (). *Drosophila* mushroom body mutants are deficient in olfactory learning. neurogenet. *2*.

Heisenberg, M. (2). Mushroom body memoir from maps to models. Nat. Rev. Neurosci. *4*, 2.

Hildebrand, G., and Shepherd, G.M. (). Mechanisms of olfactory discrimination converging evidence for common principles across phyla. Annu. Rev. Neurosci. *20*, .

Ito, K., Sass, H., Urban, , Hofbauer, A., and Schneuwly, S. (). Regular articles GAL-responsive UAS-tau as a tool for studying the anatomy and development of the *Drosophila* central nervous system. Cell Tissue Res. *290*, .

Iyengar, A., Chakraborty, T.S., Goswami, S.P., Wu, C.F., and Siddi i, . (2). Post-eclosion odor experience modifies olfactory receptor neuron coding in *Drosophila*. Proc. Natl. Acad. Sci. USA *107*, .

a, W.W., Carvalho, G.B., Mak, E.M., de la Rosa, N.N., Fang, A., Liong, C., Brummel, T., and Benzer, S. (2). Prandiology of *Drosophila* and the CAFE assay. Proc. Natl. Acad. Sci. USA *104*, 2.

efferis, G.S.E., Marin, E.C., Stocker, R.F., and Luo, L. (2). Target neuron prespecification in the olfactory map of *Drosophila*. Nature *414*, 2.

efferis, G.S.E., Potter, C., Chan, A.M., Marin, E.C., Rohlfing, T., Maurer, C.R., and Luo, L. (2). Comprehensive maps of *Drosophila* higher olfactory centers spatially segregated fruit and pheromone representation. Cell *128*, 2.

□ones, P. Cayirlioglu, I.G. Kadow, L.B. Vosshall (2□□□). Two chemosensory receptors together mediate carbon dioxide detection in *Drosophila*. Nature *445* pp. □□-□□

□ones, P.L., Pask, G.M., Rinker, D.C., and Zwiebel, L.□ (2□□□). Functional agonism of insect odorant receptor ion channels. Proc. Natl. Acad. Sci. USA *108*, □□2□-□□2□.

□uttner, F., and Watson, S.B. (2□□□). Biochemical and ecological control of geosmin and 2-methylisoborneol in source waters. Appl. Environ. Microbiol. *73*, □□□□-□□□□.

Karlson, P., and Lu□scher, M. (□□□□). Pheromones□a new term for a class of biologically active substances. Nature *183*, □□-□□.

Keene, A.C., Stratmann, M., Keller, A., Perrat, P.N., Vosshall, L.B., and Waddell, S. (2□□□). Diverse odor-conditioned memories re□uire uni□uely timed dorsal paired medial neuron output. Neuron *44*, □2□-□□□□.

Kitamoto, T. (2□□□). Conditional modification of behavior in *Drosophila* by targeted expression of a temperature-sensitive shibire allele in defined neurons. □ Neurobiol. *47*, □□-□2.

Klowden, M.□ (□□□□). Endogenous regulation of the attraction of *Aedes aegypti* mos□uitoes. □ Am. Mos. Control Assoc. *10*, □2□-□□2.

Klowden, M.□, Lea, A.□. (□□□□). Abdominal distention terminates subse□uent hostseeking behaviour of *Aedes aegypti* following a blood meal. □ Insect Physiol. *25*, □□□-□□□.

Klowden, M.□, Lea, □.A. (□□□□). Blood meal size as a factor affecting continued hostseeking by *Aedes aegypti*. Am. □ Trop. Med. Hyg. *27*, □2□-□□□.

Knaden, M., Strutz, A., Ahsan, □, Sachse, S. and Hansson, B.S. (2□□2). Spatial representation of odorant valence in an insect brain. Cell Rep. *1*, □□2-□□□.

Kreher, S.A., Mathew, D., Kim, □, and Carlson, □R. (2□□□). Translation of sensory input into behavioral output via an olfactory system. Neuron *59*, □□-□2□.

Kurtovic, A., Widmer, A., and Dickson, B.□ (2□□□). A single class of olfactory neurons mediates behavioural responses to a *Drosophila* sex pheromone. Nature *446*, □□2-□□□.

Kwon, □□., Dahanukar, A., Weiss, L.A., Carlson, □R. (2□□□). The molecular basis of C□2 reception in *Drosophila*. Proc. Natl. Acad. Sci. U.S.A. *104*(□)□□□□-□□□□.

Lai, S.-L., Awasaki, T., Ito, K., and Lee, T. (2□□□). Clonal analysis of *Drosophila* antennal lobe neurons□ diverse neuronal architectures in the lateral neuroblast lineage. Development *135*, 2□□-2□□□.

Laissue, P.P., Reiter, C., Hiesinger, P.R., Halter, S., Fischbach, K.F., Stocker, R.F. (□□□□). Three-dimensional reconstruction of the antennal lobe in *Drosophila melanogaster*. □ Comp. Neurol.*405*, □□-□□2.

Larsson, M.C., Domingos, A.I., □ones, W.D., Chiappe, M.E., Amrein, H., and Vosshall, L.B. (2□□). □r□□b Encodes a Broadly Expressed □dorant Receptor Essential for *Drosophila* □lfaction. Neuron *43*, □□-□□□□.

Lee, D.D., and Seung, H.S. (□□□□). Learning the parts of objects by non-negative matrix factorization. Nature *401*, □□-□□□□.

Lee, D.D., Laboratories, B., Hill, M., and □, H.S.S. (2□□□). Algorithms for Non-negative Matrix Factorization. Adv. Neural Inf. Process. Sys. *13*, □□-□□□2.

Liu, □., and Davis, R.L. (2□□□). The GABAergic anterior paired lateral neuron suppresses and is suppressed by olfactory learning. Nature Neurosci. *12*, □□-□□.

Livak, K.□, and Schmittgen, T.D. (2□□□). Analysis of relative gene expression data using real-time □uantitative PCR and the 2(-Delta Delta C(T)) Method. Methods *25*, □□2–□□□.

Livingstone, M., and Hubel, D. (1988). Segregation of Form, Color, Movement, and Depth : Anatomy , Physiology , and Perception. Science *240*, □□-□□□□.

Manni, E., and Petrosini, L. (2□□□). A century of cerebellar somatotopy□a debated representation. Nat. Rev. Neurosci. *5*, □-□

Marin, E.C., □efferis, G.S.□.E., Komiyama, T., Zhu, H., and Luo, L. (2□□2). Representation of the glomerular olfactory map in the *Drosophila* brain. Cell *109*, 2□□-2□□.

Martel V, Anderson P, Hansson BS and Schlyter F (2□□□). Peripheral modulation of olfaction by physiological state in the Egyptian leaf worm *Spodoptera littoralis* (Lepidoptera□Noctuidae)□□Insect Physiol. *55*(□)□□□-□□.

Mattheis, □P., and Roberts. R.G. (□□□2). Identification of geosmin as a volatile metabolite of *Penicillium expansum*. Appl. Environ. Microbiol. *58*□□□□-□□□□2.

Min S, Ai M, Shin SA, Suh GSB (2□□□). Dedicated olfactory neurons mediating attraction behavior to ammonia and amines in *Drosophila.* Proc. Natl. Acad. Sci. USA *110*.

Nässel, D.R., Enell, L.E., Santos, □G., Wegener, C., □ohard, H.A. (2□□□). A large population of diverse neurons in the *Drosophila* central nervous system expresses short neuropeptide F, suggesting multiple distributed peptide functions. BMC Neurosci. *9*□□□.

Ng, M., Roorda, R.D., Lima, S.□., Zemelman, B. V, Morcillo, P., and Miesenböck, G. (2□□2). Transmission of olfactory information between three populations of neurons in the antennal lobe of the fly. Neuron *36*, □□-□□□.

□kada, R., Awasaki, T., and Ito, K. (2□□□). Gamma-aminobutyric acid (GABA)-mediated neural connections in the *Drosophila* antennal lobe. □ Com. Neurol. *514*, □□-□□.

□lsen SR, Wilson RI (2□□□). Lateral presynaptic inhibition mediates gain control in an olfactory circuit. Nature *452*□□□□–□□□.

Pasternak, T., and Greenlee, M.W. (2□□□). Working memory in primate sensory systems. Nat. Rev. Neurosci. *6*, □□–□□□.

Petro-Turza, M. (□□□□). Flavor of tomato and tomato products. Food Rev. Int.*2*, □□□–□□□.

□iu, □.T., van Loon, □.□A., Takken, W.,Meijerink, □, Smid, H.M., (2□□□). □lfactory coding in antennal neurons of the malaria mos□uito, *Anopheles gambiae*. Chem. Senses *31*, □□–□□□.

R.F. Stocker, M.C. Lienhard, A. Borst, K.F. Fischbach (□□□□). Neuronal architecture of the antennal lobe in *Drosophila melanogaster* Cell Tissue Res., *262* (□□□), pp. □–□□.

Robertson HM, Warr CG, Carlson □R (2□□□). Molecular evolution of the insect chemoreceptor gene superfamily in *Drosophila melanogaster*. Proc. Natl. Acad. Sci. USA *100* Suppl 2□□□□□–□□□□2.

Robinson, I.M., Ranjan, R., and Schwarz, T.L. (2□□2). Synaptotagmins I and IV promote transmitter release independently of Ca(2+) binding in the C(2)A domain. Nature *418*, □□–□□□.

Root CM, Ko KI, □afari A, Wang □W (2□□□). Presynaptic facilitation by neuropeptide signaling mediates odor-driven food search. Cell *145*□□□–□□□.

Russo, C.A.M., Takezaki, N., and Nei, M. (□□□□). Molecular phylogeny and divergence times of drosophilid species. Mol. Biol. Evol. *12*, □□□–□□□.

Ruta, V., Datta, S.R., Vasconcelos, M.L., Freeland, □, Looger, L.L., and Axel, R. (2□□□). A dimorphic pheromone circuit in *Drosophila* from sensory input to descending output. Nature *468*, □□–□□□.

Rybak, □, Ku□, A., Lamecker, H., Zachow, S., Hege, H.-C., Lienhard, M., Singer, □, Neubert, K., and Menzel, R. (2□□□). The Digital Bee Brain□ Integrating and Managing Neurons in a Common □D Reference System. Front. Sys. Neurosci. *4*, □–□□.

Sachse, S., and Galizia, C.G. (2□□□). Topography and Dynamics of the □lfactory System. Microcircuits□the Interface Between Neurons and Global Brain Fu Nction. Dahlem Wo Rkshop Report □□ (ed. by S Grillner) MIT Press, Cambridge, MA, USA. 2□□–2□□.

Sachse, S., Rueckert, E., Keller, A., □kada, R., Tanaka, N.K., Ito, K., and Vosshall, L.B (2□□). Activity-dependent plasticity in an olfactory circuit. Neuron *56,* □□□–□□□.

Sandeep Robert Datta, Maria Luisa Vasconcelos, Vanessa Ruta, Sean Luo, Allan Wong, Ebru Demir, □orge Flores, Karen Balonze, Barry □ Dickson □ Richard Axel (2□□□).

The *Drosophila* pheromone *c*VA activates a sexually dimorphic neural circuit. Nature *452*, □□□□-□□.

Sanes, □R., and Zipursky, S.L. (2□□□). Design principles of insect and vertebrate visual systems. Neuron *66*, □□-□□.

V. Sargsyan, M.N. Getahun, S. Lavista Llanos, S.B. □lsson, B.S. Hansson, D. Wicher (2□□). Phosphorylation via PKC regulates the function of the *Drosophila* odorant coreceptor. Front. Cell Neurosci. p. □

Saveer, A.M., Kromann, S.H., Birgersson, G., Bengtsson, M., Lindblom, T., Balkenius, A., Hansson, B.S., Witzgall, P., Becher, P.G., and Ignell, R. (2□□2). Floral to green□ mating switches moth olfactory coding and preference. Proc. R. Society B *279*, 2□□□-2□22.

Schlief, M.L., and Wilson, R.I. (2□□□). □lfactory processing and behavior downstream from highly selective receptor neurons. Nat. Neurosci. *10*,□2□-□□□□.

S□journ□, □., Pla□ais, P.-□., Aso, □., Siwanowicz, I., Trannoy, S., Thoma, V., Tedjakumala, S.R., Rubin, G.M., Tch□nio, P., Ito, K., et al. (2□□□). Mushroom body efferent neurons responsible for aversive olfactory memory retrieval in *Drosophila*. Nat. Neurosci. *14*, □□-□□□□.

Seki, □., Rybak, □, Wicher, D., Sachse, S., and Hansson, B.S. (2□□□). Physiological and morphological characterization of local interneurons in the *Drosophila* antennal lobe. □ Neurophysiol. *104*, □□□-□□□□□.

Semmelhack, □L., and Wang, □W. (2□□□). Select *Drosophila* glomeruli mediate innate olfactory attraction and aversion. Nature *459*, 2□□-22□

Shanbhag, S.R., Müller, B. □ Steinbrecht, R.A. (□□□□). Atlas of olfactory organs of *Drosophila melanogaster* □.Types, externalorganization, innervation and distribution of olfactory sensilla. *Int.* □ Insect Morphol. Embryol. *28*, □□-□□□□.

Shang, □., Claridge-Chang, A., Sjulson, L., Pypaert, M., and Miesenböck, G. (2□□□). Excitatory local circuits and their implications for olfactory processing in the fly antennal lobe. Cell *128*, □□□-□□2.

Shier, D., Butler, □ and Lewis, R. (2□□□). Hole's Human Anatomy □ Physiology, Boston□ McGraw Hill.

Siddi□i, □. (□□□□). Neurogenetics of olfaction in *Drosophila melanogaster*. TIG, *3*□, □□□-□□2.

Siju, K. P., Hill, S. R., Hansson, B., □ Ignell, R. (2□□□) Influence of blood meal on the responsiveness of olfactory receptor neurons in antennal sensilla trichodea of the yellow fever mos□uito, *Aedes aegypti*. □ Insect Physiol. *56*, □□-□□□□.

Silbering, A.F., and Galizia, C.G. (2□□□). Processing of odor mixtures in the *Drosophila* antennal lobe reveals both global inhibition and glomerulus-specific interactions. □ Neurosci. *27*, □□□□–□□□□□.

Silbering, A.F., □kada, R., Ito, K., and Galizia, C.G. (2□□□). □lfactory information processing in the *Drosophila* antennal lobe□anything goes□ □ Neurosci. *28*, □□□□□–□□□□□.

Singh, R.N., Singh, K. (□□□□). Fine structure of the sensory organs of *Drosophila melanogaster* Meigen larva(Diptera□Drosophilidae). Int. □ Insect Morphol. Embryol. *13*(□)□2□–2□.

Steck, K., Veit, D., Grandy, R., Badia, S.B., Mathews, Z., Verschure, P., Hansson, B.S., and Knaden, M. (2□□2). A high-throughput behavioral para- digm for *Drosophila* olfaction - The Flywalk. Sci. Rep. *2*, □□□.

Stensmyr, M.C., Dweck, H.K.M., Farhan, A., Ibba, I., Strutz, A., Mukunda, L., Linz, □, Grabe, V., Steck, K., Lavista-Llanos, S., et al. (2□□2). A Conserved Dedicated □lfactory Circuit for Detecting Harmful Microbes in *Drosophila*. Cell *151*, □□□□–□□□□.

Stocker, R.F., (□□□□). The organization of the chemosensory system in *Drosophila melanogaster*□a review. Cell Tissue Res. *275*, □–2□.

Stocker, R.F., Heimbeck, G., Gendre, N., and De Belle, □S. (□□□□). Neuroblast ablation in *Drosophila* P□GAL□□lines reveals origins of olfactory interneurons. □ Neurobiol. *32*, □□–□□□□.

Stocker, R.F., Lienhard, M.C., Borst, A., and Fischbach, K. (□□□□). Neuronal architecture of the antennal lobe in *Drosophila melanogaster*. Cell Tissue Res. *262*, □– □□.

Stökl, □, Strutz, A., Dafni, A., Svatos, A., Doubsky, □, Knaden, M., Sachse, S., Hansson, B.S., and Stensmyr, M.C. (2□□□). A deceptive pollination system targeting drosophilids through olfactory mimicry of yeast. Curr. Biol. *20*, □□□–□□2.

Stopfer, M., □ayaraman, V., and Laurent, G. (2□□□). Intensity versus identity coding in an olfactory system. Neuron *39*, □□–□□□□.

Strutz, A., Völler, T., Riemensperger, T., Fiala, A., and Sachse, S. (2□□2). Genetically Encoded Functional Indicators. Genetically Encoded Functional Indicators, Neuromethods, Springer Protocols *72*, □□–□□.

Suh, G.S.B., Wong, A.M., Hergarden, A.C., Wang, □W., Simon, A.F., Benzer, S., Axel, R., and Anderson, D.□ (2□□□). A single population of olfactory sensory neurons mediates an innate avoidance behaviour in *Drosophila*. Nature *431*, □□–□□□.

Takken, W., van Loon, □□, Adam, W. (2□□□). Inhibition of host-seeking response and olfactory responsiveness in *Anopheles gambiae* following blood-feeding. □ Insect Physiol. *47*, □□–□□□.

Tanaka, N.K., Awasaki, T., Shimada, T., and Ito, K. (2□□□). Integration of Chemosensory Pathways in the *Drosophila* Second-□rder □lfactory Centers. Curr. Biol. *14*, □□□–□□□.

Tanaka, N.K., Endo, K., and Ito, K. (2□□2). □rganization of antennal lobe-associated neurons in adult *Drosophila melanogaster* brain. □. Comp. Neurol. *520*, □□□–□□□□.

Thorpe, W. (□□□□). Further studies on pre imaginal olfactory conditioning in insects. Proc. R. Soc. Lond. (Biol)., *127*, □2–□□□.

Tian, L., Hires, S.A., Mao, T., Huber, D., Chiappe, M.E., Chalasani, S.H., Petreanu, L., Akerboom, □, McKinney, S. a, Schreiter, E.R., et al. (2□□□). Imaging neural activity in worms, flies and mice with improved GCaMP calcium indicators. Nat. Methods *6*, □□–□□□.

Tinbergen, N. (□□□□). The Study of Instinct. □xford□The Clarendon Press.

Tully, T., and □uinn, W.G. (□□□□). Classical conditioning and retention in normal and mutant *Drosophila* melanogaster. □. Comp. Physiol. A *157*, 2□□–2□□.

van der Goes van Naters, W., and Carlson, □R. (2□□□). Receptors and neurons for fly odors in *Drosophila*. Curr. Biol. *17*, □□□–□□2.

Vosshall, L.B., Amrein, H., Morozov, P.S., Rzhetsky, a, and Axel, R. (□□□□). A spatial map of olfactory receptor expression in the *Drosophila* antenna. Cell *96*, □2□–□□□.

Vosshall, L.B., and Stocker, R.F. (2□□□). Molecular architecture of smell and taste in *Drosophila*. Annu. Rev. Neurosci. *30*, □□–□□□□.

Vosshall, L.B., Wong, a M., and Axel, R. (2□□□). An olfactory sensory map in the fly brain. Cell *102*, □□–□□□□.

Wang, □W., Wong, A.M., Flores, □, Vosshall, L.B., and Axel, R. (2□□□). Two-photon calcium imaging reveals an odor-evoked map of activity in the fly brain. Cell *112*, 2□□–2□2.

Wang, L.M., and Anderson, D.□ (2□□□). Identification of an aggression-promoting pheromone and its receptor neurons in *Drosophila*. Nature *463*, 22□–U□□□.

Wang, □., Chiang, A.-S., □ia, S., Kitamoto, T., Tully, T., and Zhong, □. (2□□□). Blockade of Neurotransmission in *Drosophila* Mushroom Bodies Impairs □dor Attraction, but Not Repulsion. Curr. Biol. *13*, □□□–□□□□.

Wicher, D., Schäfer, R., Bauernfeind, R., Stensmyr, M.C., Heller, R., Heine- mann, S.H., and Hansson, B.S. (2□□□). *Drosophila* odorant receptors are both ligand-gated and cyclic-nucleotide-activated cation channels. Nature *452*, □□□–□□□□.

Wilson RI, Laurent G (2□□□). Role of GABAergic Inhibition in Shaping □dor-Evoked Spatiotemporal Patterns in the *Drosophila* Antennal Lobe. □ Neurosci. *25*, □□□□–□□□□.

Wilson, R.I. (2□□□). Neural and behavioral mechanisms of olfactory perception. Curr. □pin. Neurobiol. *18*, □□–□□2.

Wilson, R.I., and Laurent, G. (2□□□). Role of GABAergic inhibition in shaping odor-evoked spatiotemporal patterns in the *Drosophila* antennal lobe. □ Neurosci. *25*, □□□–□□□□.

Wilson, R.I., and Mainen, Z.F. (2□□□). Early events in olfactory processing. Annu. Rev. Neurosci *29*, □□–2□□.

Wilson, R.I., Turner, G.C., and Laurent, G. (2□□□). Transformation of olfactory representations in the *Drosophila* antennal lobe. Science *303*, □□□–□□□.

Wong, A.M., Wang, □.W., and Axel, R. (2□□2). Spatial representation of the glomerular map in the *Drosophila* protocerebrum. Cell *109*, 22□–2□□.

□ang, Z.H. (□□□□). PAML□a program package for phylogenetic analysis by maximum likelihood. Comput. Appl. Biosci. *13*, □□□–□□□.

□ao, C.A., Ignell, R., Carlson, □.R. (2□□□). Chemosensory coding by neurons in the coeloconic sensilla of the *Drosophila* antenna. □ Neurosci. *25*(□□)□□□□□--□□□□.

□asuyama, K., Meinertzhagen, I. a, and Schürmann, F.W. (2□□□). Synaptic connections of cholinergic antennal lobe relay neurons innervating the lateral horn neuropile in the brain of *Drosophila melanogaster*. □ Comp. Neurol. *466*, 2□□–□□□.

□oshida, T., Chen, H.W., Toda, M.□, Kimura, M.T., and Davis, A.□ (2□□□). New host plants and host plant use for *Drosophila elegans* Bock and Wheeler, □□□2. Drosoph. Inf. Serv. *83*, □□–2□.

□oung, W.F., Horth, H., Crane, R., □gden, T., and Arnott, M. (□□□□). Taste and odour threshold concentrations of potential potable water contaminants. Water Res. *30*, □□–□□□□.

Declaration of independent assignment

I declare in accordance with the conferral of the degree of doctor from the School of Biology and Pharmacy of Friedrich Schiller University □ena that the submitted thesis was written only with the assistance and literature cited in the text. People who assisted in experiments, data analysis and writing of the manuscripts are listed as coauthors of the respective manuscripts. I was not assisted by a consultant for doctorate theses. The thesis has not been previously submitted whether to the Friedrich Schiller University, □ena or to any other university.

Abu Farhan
□ena, Dec □□, 2□□□

Acknowledgements

My first thanks goes to my boss, Professor Bill S. Hansson, for giving me the opportunity to obtain my Ph.D. in his well e□uipped department, as well as the opportunity to gain and improve my talent and knowledge. In addition to his excellent scientific profile, he is also very generous, kind, and so much filled with humanity and always providing motivation. He is atop of my list of people whom I came across in my life, as epitome. I feel lucky to have him in my life and I was, am and will be proud to be part of the □Hanssons□. Second I would like to thank Late Professor □baid Siddi□i for lighting my brain with his simple but effective ideas and talks and for teaching me olfaction basics and olfactory assays. I would also like to thank my first guide Professor N. Sakthivel for nurturing me through his visions and experiences. I want to thank my supervisor Dr. Markus Knaden, who taught me a lot about practicality of science, how to purse and prevail. I thank him for his intensive discussions and extensive supervision. Also I would like to thank Dr. Marcus Stensmyr for collaborating with me on his projects and teaching me the basics and advances of paper writing and figure making. Also I thank the other group leaders Deiter, Ewald, Silke, □urgen, Shanon for teaching their specialties and for discussions.

I would like to say that Marid made my stay wonderful. He has always been on my side and made my way easy by his mature advice. Also I have my gratitude to Hany, my brother, for supporting and motivating me always. I thank both of them for long and fre□uent scientific discussions and all the fun. I would also like to thanks □oichi, □ksana, Sofia, Federica and Ian for nice discussions.

I would like to thank Anna, □eanine, Regina and Linda (my senior in Ph.D) for all the experiences they shared and spontaneous help when it was needed. I want to thank Antonia for the nice collaboration. I am very thankful for her support and hopefully we will be rewarded soon. Also I would like to thank Sonja, Christine, Christian, Katharina, Veit, Cornelia, Michael, Latha, Christopher, Alex, Fabio, Katrin, Amelie, Shimaa, Kerstin, and Elisa. I want to also thank all former and present members of the □Hanssons□ family. I like to thanks my other college and friends in □ena.

A very big □Thank you□goes to Silke T., the soul of the fly lab, for her helping nature and for preparing a lot of basic needs for our experiments. Thanks to Swetlana Laubrich for the kind assistance with contracts, visa, conference trips and lately all the organizational

issues for my thesis. I would like to thank the IT department as well, and I thank the Max Planck Gesellschaft for funding my research.

I would like to state my appreciation for my father Mohd. Arif for his supports especially in my struggles and for encouraging me always. It is easy that you can love anyone but it is very difficult that you make people to love you. Such people are very rare who loves you from soul and I lost one, my sweet sister Zeba Arif, is heavenly soul now. I owed her a lot and she is the one who taught me how to prevail over the impossible. I love to thank the love of my life, my wife Afreen Farhan, for her love care and for giving me the best gift ever, our baby Zeba Farhan. I will be biased if I failed to show my gratitude to my other family members, friends and relatives for everything, for their love, appreciation, care, support and even criticism.

Curriculum vitae

Personal details

Date of Birth: 02-12-1983	Male, married, Indian
Address of communication	Department of Evolutionary Neuroethology
Phone: +49 (0)3641 57 1456	Max Planch Institute for Chemical Ecology
Fax: +49 (0)3641 57 1402	Hans-Knöll-Straße 8, 07745 Jena, Germany
E-mail : afarhan@ice.mpg.de	Educational Status: Pursuing Ph.D.

Education

B.Sc.	V.B.S. Purvanchal University, 1999-2003.
M.Sc. Biotechnology	Pondicherry University, 2004 -2006.

Research Experiences

Ph.D. Title: Odor guided behavior and its modulation in the fruit fly *Drosophila melanogaster*.
Duration: Sept 2009 – till date, Supervisor: Prof. B.S. Hansson, Dr. M. Knaden,

Max Planch Institute for Chemical Ecology, Department of Evolutionary Neuroethology, Hans-Knöll-Straße 8, 07745 Jena, Germany.

Junior Research Fellow (JRF)

Title: Differential analysis of continuous vs. discontinuous conditioning in term of memory consolidation and decay with due course of time in *Drosophila* with the help of behaviour assays, electrophysiology and microscopy.

Duration: July 2007–July 2009, Supervisor: Prof. Obaid siddiqi.

M.Sc Research Project

Title: Characterization of 2,4-Diacetylphloroglucinol-producing species of *fluorescent pseudomonads.*

Duration: July 2005- May 2006, Supervisor: Prof.N.Sakthivel.

Department of Biotechnology, Pondicherry University, Pondicherry.

Summer Research Training

Title: *In vitro* studies on *Hybanthus enneaspermus* L. *Mull.*, a medicinally important herb.

Duration: May 2005-July 2005, Supervisor: Dr. V. Ravi Sankar Rai

Dept. of Applied Botany, Seed Technology and Biotechnology, University of Mysore, India.

Honours, Awards, Fellowships

- ECRO Ph.D. travel award to attend ESITO conference, Italy, 2013.
- Qualified: CSIR-UGC Test for JRF & LS (NET) (Council of Scientific and Industrial Research) June- 2007.
- Cleared ICMR-JRF (Indian council of medical research-Junior Research Fellowship) category-A list -2008.
- Cleared DBT-JRF (Department of Biotechnology-Junior Research Fellowship) 2007.
- Cleared GATE (97.5 percentile approx) All India Rank-261, 2007.
- Qualified All India Combined Entrance Examination conducted by JNU-New Delhi, on behalf of DBT-Govt. of India got scholarship for M.Sc. studies 2004-2006.

Publications

1. Stensmyr , M. C*., Dweck, H.*, Farhan, A*., Ibba, I.*, Strutz, A., Mukunda, L., Linz, J., Grabe, V., Steck, K., Lavista Llanos, S., Wicher, D., Sachse, S., Knaden, M., Becher, P. G., Seki, Y., Hansson, B. (2012). A conserved dedicated olfactory circuit for detecting harmful microbes in *Drosophila*. *Cell, 151*(6), 1345-1357. *equally contributed first author.

2. Abu Farhan, Jyotasana Gulati, Ewald Große-Wilde, Heiko Vogel, Bill S. Hansson * and Markus Knaden* (2013) The CCHamide 1 receptor modulates sensory perception and olfactory behavior in starved Drosophila. *Scientific Reports*, Accepted September 4.*These authors contributed equally to the work.

3. Antonia Strutz, Jan Soelter, Amelie Baschwitz, Abu Farhan, Veit Grabe, Jürgen Rybak, Michael Schmucker, Markus Knaden, Bill S. Hansson & Silke Sachse (2013) Decoding Odor Attraction and Intensity in the Drosophila brain. Under review in *Neuron*.

Oral Presentations

Farhan A. Olfactory modulations in starved and fed fruit fly Drosophila. NeuroDoWo 2013 - 24th Neurobiology doctoral students workshop, Max Planck Institute of Experimental Medicine, Göttingen, DE, Jul 2013.

Farhan A. Feeding status modulates peripheral olfactory sensitivity and behavior in Drosophila. 12th European Symposium for Insect Taste and Olfaction (ESITO), St. Petersburg, RU, Sep 2011.

Farhan A. Feeding status modulates peripheral olfactory sensitivity and behavior in Drosophila. Neuro DoWo (22nd Neurobiology PhD Student Workshop), Universtität Bonn, Bonn, DE, Jul 2011.

Farhan A. Starvation and Olfactory modulation at periphery in *Drosophila melanogaster*. 10th IMPRS Symposium, MPI for Chemical Ecology, Dornburg, DE, Feb 2011.

Farhan A. Effects of starvation on olfactory sensitivity in *Drosophila melanogaster*. Chemical Ecology 2010 Mini-Symposium, Jena, DE, Sep 2010.

Poster Presentations

Dweck H., Farhan A., Knaden M., Stensmyr M.C., Hansson B.S. Functional Dissection of the olfactory sensory neurons on the maxillary palp of the vinegar fly. 33rd Blankenese Conference - Nutrient Sensing: From Brain to Gut, Hamburg, DE, May 2013

Strutz A., Soelter J., Baschwitz A., Grabe V., Farhan A., Rybak J., Knaden M., Schmuker M., Hansson B.S., Sachse S. Inhibitory projection neurons bias odor attraction behaviour in lateral horn area of *Drosophila melanogaster*. 10th Göttingen Meeting of the German Neuroscience Society, Göttingen, DE, Mar 2013

Farhan A., Knaden M., Hansson B.S. Behavioral and sensory modulation of olfactory responses in starved Drosophila. XVI International Symposium on Olfaction and Taste (ISOT), Stockholm, SE, Jun 2012

Strutz A., Soelter J., Grabe V., Baschwitz A., Farhan A., Rybak J., Knaden M., Schmuker M., Hansson B.S., Sachse S. Inhibitory projection neurons bias the evaluation of behaviorally relevant odors in the lateral horn area of *Drosophila melanogaster*. XVI International Symposium on Olfaction and Taste (ISOT), Stockholm, SE, Jun 2012

Strutz A., Soelter J., Grabe V., Baschwitz A., Farhan A., Rybak J., Knaden M., Schmuker M., Hansson B.S., Sachse S. Odor attraction behavior of *Drosophila melanogaster* is biased via inhibitory projection neuron activity in the lateral horn area. 34th annual meeting of the Association for Chemoreception Sciences (AChemS), Huntington Beach, US, Apr 2012

Farhan A. Behavioral and sensory modulation of olfactory responses in starved Drosophila. 11th IMPRS Symposium, MPI for Chemical Ecology, Dornburg, DE, Feb 2012

Farhan A., Knaden M., Hansson B.S. Olfactory Sensitivity: Modification by physiological status in Drosophila. 9th Göttingen Meeting of the German Neuroscience Society, Göttingen, DE, Mar 2011

Farhan A. Effects of starvation on olfactory sensitivity in *Drosophila melanogaster*. SAB Meeting 2010, MPI for Chemical Ecology, Jena, DE, Oct 2010

Farhan A. Starvation effects on olfactory sensitivity in Drosophila. 9th IMPRS Symposium, MPI for Chemical Ecology, Dornburg, DE, Feb 2010.

20 September, 2013